

ISSN 1023-9855



胸腔醫學

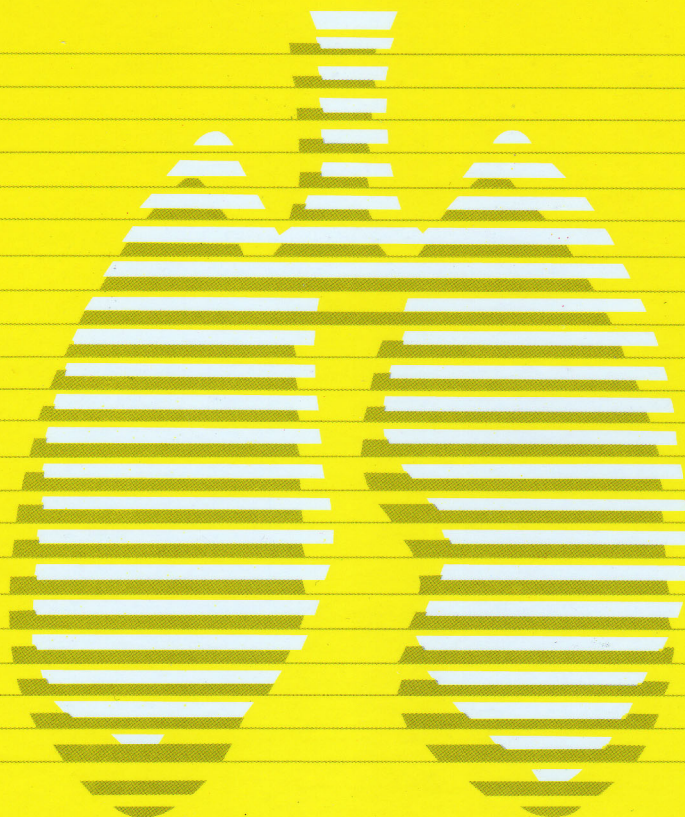
Thoracic Medicine

The Official Journal of Taiwan Society of
Pulmonary and Critical Care Medicine

Vol.30 No.4 August 2015

第三十卷 第四期

中華民國一〇四年八月



台灣胸腔暨重症加護醫學會

10048 台北市常德街 1 號

No. 1, Changde St., Jhongjheng Dist.,

Taipei City 10048, Taiwan



ISSN 1023-9855



Vol.30 No.4 August 2015

胸腔醫學

Thoracic Medicine

The Official Journal of Taiwan Society
of Pulmonary and Critical Care Medicine

原著

- 友復（UFT）對於Stage IB非小細胞肺癌病患術後的生存益處評估 191~200
吳青峰，傅瑞英，王志偉，劉永恆，謝明儒，吳青陽，吳怡成，劉會平
- 糖尿病患者有較高活動性結核病的風險－以全國人口為對象之研究 201~209
沈文偉，林恆毅，陳衛洲

病例報告

- 兩個同時發現的原發性肺癌合併對側自發性氣胸 210~216
黃柏年，黃維立，陳奕仁，林明憲，李世瑜
- 有PVL毒素之社區型methicillin抗藥性金黃色葡萄球菌在健康成年人引起的肺炎與菌血症
病例報告 217~223
郭家維，郭書辰，許正園，傅彬貴
- 異形腺瘤性增生與肺腺癌的迷思 224~231
黎書亮，林賜恩，曾明雄，李凱靈，蕭世欣，鍾啟禮
- 胸壁漿細胞瘤合併大量的骨髓瘤性肋膜積液 232~238
黃國良，蘇文麟，周紹庭，林志恭，彭萬誠
- 創傷後左主支氣管狹窄－病例報告 239~246
張凱惟，顏亦廷，曾堯麟，賴吾為
- 腦室腹膜分流管異位導致大量右側肋膜積液：病例報告 247~252
陳彥甫，陳志偉，謝俊民，柯獻欽
- 嗜伊紅性白血球超增多症候群（Hypereosinophilic syndrome）合併肝臟侵犯－
晚期肺癌的罕見表現 253~260
胡釋文，蔡子修，施金元



Vol.30 No.4 August 2015

胸腔醫學

Thoracic Medicine

The Official Journal of Taiwan Society
of Pulmonary and Critical Care Medicine

Original Articles

- Survival Benefit of Uracil-Tegafur (UFT) for AJCC 7th Pathologic Stage IB Non-Small Cell Lung Cancer Patients: A Propensity Score Matching Study..... 191~200
Ching-Feng Wu, Jui-Ying Fu, Chi-Wei Wang, Yun-Hen Liu, Ming-Ju Hsieh, Ching-Yang Wu, Yi-Cheng Wu, Hui-Ping Liu
- Increased Risk of Active Tuberculosis in Diabetic Patients: A Nationwide Population-Based Study 201~209
Wen-Wei Shen, Hen-I Lin, Wei-Chou Chen

Case Reports

- Double Primary Lung Cancer with Contralateral Spontaneous Pneumothorax – A Case Report .. 210~216
Bo-Nian Huang, Wei-Li Huang, Yi-Jen Chen, Ming-Shian Lin, Shih-Yu Lee
- Pneumonia and Bacteremia Due to Community-Acquired *Staphylococcus aureus* in a Healthy Adult Carrying the Panton-Valentine Leukocidin Gene – A Case Report 217~223
Chia-Wei Kuo, Shu-Chen Kuo, Jeng-Yuan Hsu, Pin-Kuei Fu
- Proper Diagnostic Differentiation of Atypical Adenomatous Hyperplasia and Pulmonary Adenocarcinoma..... 224~231
Kevin S. Lai, Sey-En Lin, Ming-Syong Zeng, Kai-Ling Lee, Shih-Hsin Hsiao, Chi-Li Chung
- Chest Wall Extramedullary Plasmacytoma with Myelomatous Pleural Effusion..... 232~238
Kuo-Liang Huang, Wen-Lin Su, Shao-Ting Chou, Chih-kung Lin, Wann-Cherng Perng
- Post-Traumatic Left Main Bronchus Stenosis: Case Report 239~246
Kai-Wei Chang, Yi-Ting Yen, Yau-Lin Tseng, Wu-Wei Lai
- Ventriculoperitoneal Shunt Catheter Dislocation Causing Massive Right-Side Pleural Effusion: A Case Report 247~252
Yen-Fu Chen, Chih-Wei Chen, Jiunn-Min Shieh, Shian-Chin Ko
- Hypereosinophilic Syndrome with Liver Involvement in Advanced Lung Cancer 253~260
Shih-Wen Hu, Tzu-Hsiu Tsai, Jin-Yuan Shih

Survival Benefit of Uracil-Tegafur (UFT) for AJCC 7th Pathologic Stage IB Non-Small Cell Lung Cancer Patients: A Propensity Score Matching Study

Ching-Feng Wu, Jui-Ying Fu*, Chi-Wei Wang**, Yun-Hen Liu, Ming-Ju Hsieh, Ching-Yang Wu, Yi-Cheng Wu, Hui-Ping Liu***

Purpose: Adjuvant chemotherapy with uracil-tegafur (UFT) is widely used for pathologic stage IB (pIB) non-small cell lung cancer (NSCLC) in Taiwan and Japan. The aim of this study was to identify the survival benefit for patients with and without UFT treatment.

Methods: We performed a retrospective review of 220 patients with stage pIB disease (using the 6th American Joint Committee on Cancer (AJCC 6th) Cancer Staging Manual) who underwent lung resection from January 2005 to July 2012. All patients were reclassified using the AJCC 7th cancer staging system, and 130 matched subjects were included. Using a propensity score matching method (1:4 match), patients with stage pIB disease were divided into 2 groups (UFT: 26, Non-UFT: 104). The oral dose of UFT was 400 mg/body. Multiple risk factors were analyzed, including age, gender, surgical method, cell type, visceral pleural invasion, and angiolymphatic invasion. The 2 study groups were well matched with respect to age, gender, surgical method (video-assisted thoracoscopic surgery or open thoracotomy), and pathological parameters, including cell type, visceral pleural invasion, and angiolymphatic invasion.

Results: A tumor diameter greater than 3 cm was a poor prognostic factor for overall survival of patients with stage pIB NSCLC. The survival rate was significantly higher in the UFT group than in the surgery-alone group. Multivariate analyses revealed that a tumor diameter >3 cm (odds ratio=3.496; 95% confidence interval, 1.49-8.20) and use of UFT (odds ratio=0.180; 95% confidence interval, 0.049-0.660) were predictive of overall survival. The overall survival of patients with a tumor diameter >3 cm who were treated with UFT was better than the overall survival of those not treated with UFT. ($p=0.041$)

Conclusion: In conclusion, UFT treatment was shown to prolong the overall survival of patients with newly diagnosed stage pIB NSCLC in our study. In addition, patients with a tumor diameter >3 cm had poor overall survival, but could obtain a survival benefit after completing 2 years of UFT treatment. (*Thorac Med* 2015; 30: 191-200)

Key words: non-small cell lung cancer, stage IB, uracil-tegafur, chemotherapy

Division of Thoracic and Cardiovascular Surgery, Department of Surgery, Chang Gung Memorial Hospital, Taiwan;
 *Division of Pulmonary and Critical Care, Department of Internal Medicine, Chang Gung Memorial Hospital, Taiwan;
 Division of Pathology, Chang Gung Memorial Hospital, Taiwan; *Division of Thoracic Surgery, New Journey Cancer Hospital, Beijing

Address reprint requests to: Dr. Ching-Yang Wu, Division of Thoracic and Cardiovascular Surgery, Department of Surgery, Chang Gung Memorial Hospital, 5 Fushing Street, Kweishan, Taoyuan, Taiwan 333, R.O.C.

Introduction

Lung cancer is the leading cause of cancer-related mortality worldwide [1]. Surgical resection constitutes the primary therapeutic option for the management of early-stage non-small cell lung cancer (NSCLC). According to several landmark studies and meta-analyses, the standard of care for patients with stage II-IIIa NSCLC is adjuvant cisplatin-based doublet chemotherapy performed after appropriate surgical resection [2-4]. However, patients in a poor general condition cannot tolerate the toxicity of chemotherapy. Ichinose Y *et al* also reported that uracil-tegafur (UFT) plus cisplatin and concurrent radiotherapy [5] had a treatment result similar to other cisplatin-combination chemotherapy [6]. The West Japan Study Group for Lung Cancer Surgery showed significantly longer survival for patients assigned to adjuvant treatment with UFT than for patients assigned to observation alone after complete resection of stage I, II, or III NSCLC [7]. The 5-year survival rate was 64% in the UFT group and 49% in the control group ($p=0.02$). In addition, Keto H *et al* reported postoperative adjuvant UFT therapy increased the 5-year survival of patients with stage IB adenocarcinoma by 11% [8]. However, according to the forthcoming edition of the staging classification for lung cancer by the 7th American Joint Committee on Cancer (AJCC 7th) Cancer Staging Manual, cancers previously classified as pathologic stage IB (pIB) disease in the AJCC 6th Cancer Staging Manual will be re-classified as pIB, pIIA, or pIIB according to the maximal diameter of the tumor. As the stage classification is being revised, a review of previous evidence is necessary.

Materials and Methods

Patients

We performed a retrospective review of 220 patients who underwent lung resection for stage IB NSCLC (AJCC 6th) from January 2005 to July 2012. Forty-seven patients received UFT postoperatively. The preoperative workup included chest radiography, bronchoscopy, chest computed tomography (CT), spirometry, bone scanning, and a thorough search for distant metastases, including the use of positron emission tomography (PET) imaging in recent years. Only those patients with stage pIB disease (AJCC 7th) were included and investigated in this study. The exclusion criteria included incomplete medical records, lost to follow-up, and discontinuation of adjuvant chemotherapy due to adverse events. A flowchart detailing patient selection is presented in Figure 1.

Surgical technique

All patients were Taiwanese and underwent surgical lobectomy for NSCLC. The primary determinant for the surgical procedure was the preoperative forced expiratory volume in 1 s value or the pulmonary perfusion scan result. Complete resections (R0) were achieved in all cases.

UFT therapy

UFT was administered orally twice daily before meals, excluding weekends, for 2 years beginning in the 4th postoperative week. The dose was rounded to the nearest 100 mg. Most patients received 2 capsules of UFT (200 mg of tegafur and 448 mg of uracil) twice daily. At each follow-up visit, treatment compliance and drug-related adverse events were evaluated. UFT treatment was discontinued if early relapse

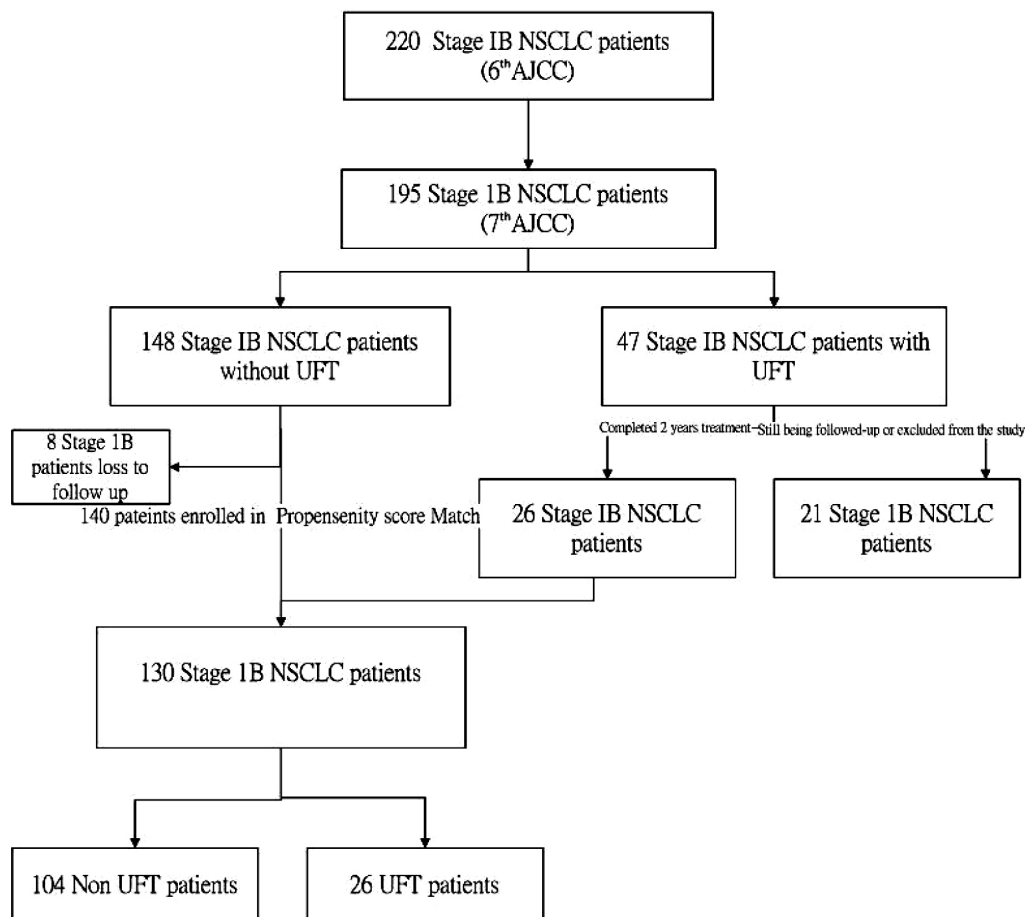


Fig. 1. Patient Selection Flow Chart — below, use “propensity score matching”

was noted during the follow-up examinations, if death occurred for any reason, or after the completion of 2 years of therapy [8].

Pathological evaluation

All patients were classified as having stage pIB NSCLC (AJCC 7th) [1]. The pathologically recorded variables included tumor size, tumor differential grade, visceral pleural invasion [9-10], angiolymphatic invasion [11-13], and tumor histology.

Follow-up examination

Patients were examined on an outpatient

basis at 3-month intervals for the first 5 years and at 6-month intervals thereafter. The follow-up evaluation included physical examination, chest radiography or chest CT, brain magnetic resonance imaging (MRI), and 18F-fluorodeoxyglucose PET. Recurrent NSCLC was diagnosed on the basis of physical examination and diagnostic imaging of lesions consistent with recurrent lung cancer. Follow-up examinations were continued until July 30, 2012.

Statistical analysis

Statistical analysis was performed using SPSS (V17.0, SPSS, Inc, Chicago, IL). SPSS

module PSM was used for propensity score matching and covariate imbalance testing [14]. All comparisons were 2-tailed. Categorical variables were compared using the χ^2 test. Continuous variables were compared using the *t*-test. Overall survival was defined as the time from surgery to death or to the last follow-up visit. Overall survival curves were estimated using the Kaplan-Meier method. Significance was assessed using the log rank test. A *p* value of <0.05 was considered to indicate statistical significance.

Results

Of the 130 patients with pIB NSCLC, 65 were female and 65 were male, with a mean age

of 60.82 years (range: 30-80 years). The average tumor size was 3.12 cm (range: 1.10-5.0 cm). Angiolymphatic invasion was observed in 95 patients (73%), and visceral pleural invasion was noted in 56 patients (43%) (Table 1). The mean survival time was 1271 days (range: 14-2663 days), and the median survival time was 1085 days.

In our control group (Non-UFT group), the 5-year survival rate was 62.5%. Adjuvant chemotherapy with UFT did improve the overall survival of patients with stage pIB disease (*p*=0.046, Figure 2A) We examined survival risk factors for stage pIB disease, including age, gender, method of operation, maximal tumor diameter, cell type, tumor cell differential grade, visceral pleural invasion, and angiolymphatic

Table 1. Patient Demographics and Characteristics

	UFT	Non-UFT	<i>p</i> value
Age (mean)	57	61	0.890
Gender (M/F)	11/15	54/50	0.380
Operation: VATS/Open*	6/20	38/66	0.194
Operation method: Lobectomy	26	104	
Lobectomy site:			
Left upper lobe	6	9	
Left lower lobe	8	27	
Right upper lobe	2	19	
Right middle lobe	3	9	
Right lower lobe	7	39	
Tumor diameter (mean)	3.09 cm	3.13 cm	0.480
Cell type			0.939
Adenocarcinoma	21	80	
Squamous cell	3	19	
Clear cell	2	5	
Angiolymphatic invasion (+/-)	19/7	76/28	1.00
Visceral pleural invasion (+/-)	9/17	47/57	0.330
Lymph node dissection number	23	19	0.067

*VATS: Video-assisted thoracoscopic surgery; Open: Open thoracotomy

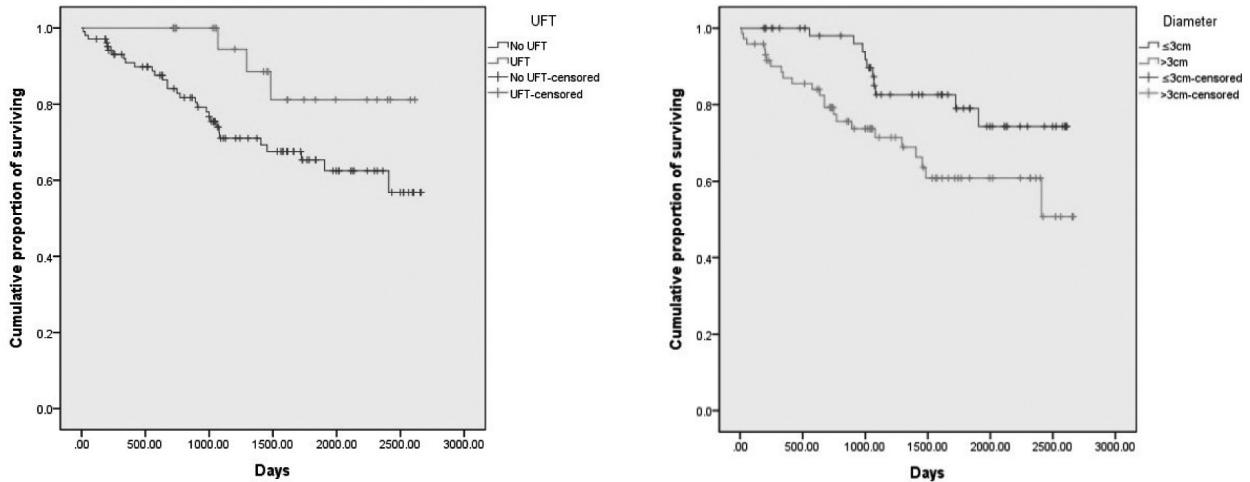


Fig. 2. (A) Survival of Patients with Stage pIB NSCLC, Who Received or Did Not Receive UFT Therapy, $p=0.046$; (B) Survival of Patients with Stage pIB NSCLC, According to Tumor Diameter, $p=0.018$

Table 2. Clinicopathological Risk Factors: Univariate Analysis

Risk factor	<i>p</i> value
Gender	0.502
Operation (VATS/Open) *	0.364
Cell type	0.819
Tumor diameter > 3 cm	0.018
Differential grade	0.343
Angiolymphatic invasion	0.860
Visceral pleural invasion	0.254
Perineural invasion	0.06
UFT	0.046

*VATS: Video-assisted thoracoscopic surgery;

Open: Open thoracotomy

invasion. Tumor diameters exceeding 3 cm were associated with poor overall survival ($p=0.018$; Figure 2B). Other clinicopathological factors, including gender, age, the method of operation, pathological cell type, differential grade, angiolymphatic invasion, and visceral pleural invasion, did not significantly alter the prognosis (Table 2). In multivariate analysis (Table 3), tumor diameter >3 cm (odds ratio=3.496; 95% confidence interval [CI], 1.49-8.202; $p=0.004$)

and use of UFT (odds ratio=0.0180; 95% CI, 0.049-0.660; $p=0.010$) were predictive of overall survival.

We further analyzed the surgical results of pIB patients who were treated with and without UFT. Fifty-five patients had tumor diameters ≤ 3 cm and visceral pleural invasion. The overall survival of the UFT and Non-UFT groups in this subgroup was not significantly different ($p=0.559$). In addition, we analyzed the overall survival of 75 patients whose tumor diameter was greater than 3 cm. In all, 16 patients received UFT for postoperative chemotherapy and the others did not. The 5-year survival of the UFT and Non-UFT groups in this subgroup was 78.4% and 55.4%, respectively. Overall survival was significantly different ($p=0.041$, Figure 3). The survival of patients with tumor diameters >3 cm who received UFT was not inferior to that of patients with tumor diameters ≤ 3 cm ($p=0.855$, Figure 4A). On the other hand, the survival of patients with tumor diameters >3 cm who did not receive UFT was worse than that of patients with tumor diameters of ≤ 3 cm

Table 3. Multivariate Analysis

Factors	Sig	Exp(B)	Exp(B) 95.0% CI	
			Lower limit	Upper limit
Age	0.704	0.993	0.956	1.031
Gender	0.520	0.753	0.318	1.786
Cell type	0.344			
Adenocarcinoma	0.169	0.471	0.161	1.378
Non-adenocarcinoma	0.963	1.039	0.205	5.266
Diameter	0.004	3.496	1.490	8.202
Angiolymphatic invasion	0.444	1.424	0.576	3.517
Visceral pleural invasion	0.328	0.680	0.315	1.472
UFT	0.010	0.180	0.049	0.660
VATS/Open	0.061	0.302	0.086	1.059

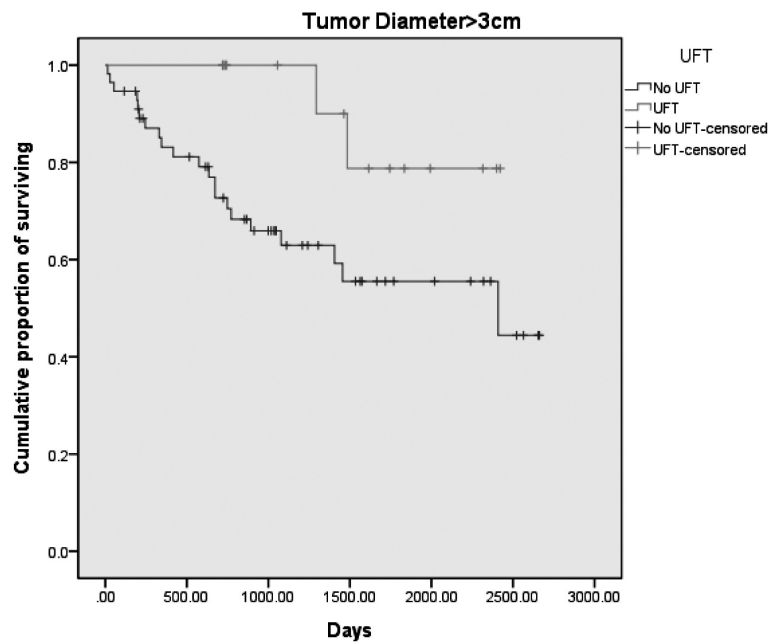


Fig. 3. Survival Curve of Patients with Tumor Diameters of >3 cm with and without UFT ($p=0.041$) - above, use “Tumor Diameter >3 cm”, use “survivors” instead of “surviving”

($p=0.010$, Figure 4B) .

Discussion

In UFT therapy, tegafur and uracil are administered at a fixed molar ratio of 1:4. In the

body, tegafur is converted into 5-fluorouracil (5FU), the active antineoplastic metabolite. 5-FU decreases the biosynthesis of pyrimidine nucleotides by inhibiting thymidylate synthase, which catalyzes the rate-limiting step in DNA synthesis. This results in the “thymineless

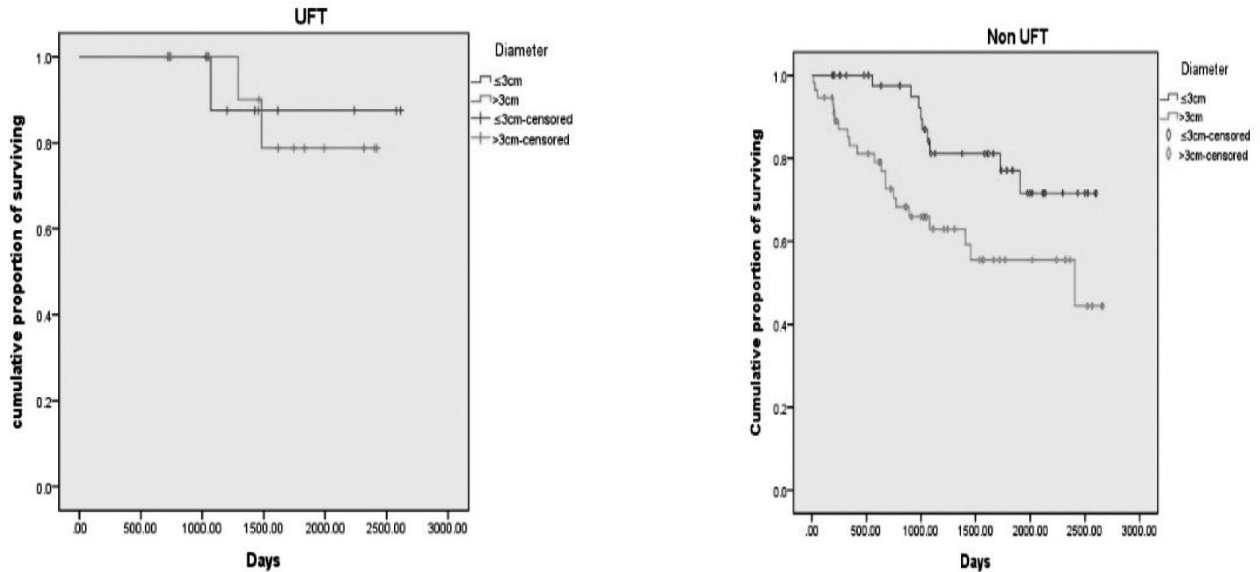


Fig. 4. (A) Survival Curve of Patients with Tumor Diameters >3 cm and Who Received UFT and Those With Tumor Diameters ≤ 3 cm ($p=0.855$); (B) Survival Curve of Patients with Tumor Diameters >3 cm and Who Did Not Receive UFT and Those with Tumor Diameters ≤ 3 cm ($p=0.010$)

death” of rapidly growing cells [15]. The combination of these 2 drugs results in a higher concentration of 5FU in the tumor cells than that obtained by the administration of tegafur alone, because uracil slows the breakdown of 5FU. UFT does not exert potent direct antitumor effects on advanced malignant tumors, as the response rate in advanced and recurrent NSCLC is estimated to be only 7% [16]. However, in the postoperative setting, residual lesions that require control are micrometastases and not bulky tumors. Although the direct antitumor effects of UFT are relatively low, this therapy can be administered for a long time because of its mild toxicity, which results in the control of micrometastases, thereby improving survival [17]. This concept is supported by in vivo experiments using murine metastasis models of breast cancer [18] and lung cancer [19-20] that demonstrated that UFT suppresses the development of micrometastases.

Keto H *et al* showed postoperative adjuvant

UFT therapy increased the 5-year survival of patients with stage IB adenocarcinoma by 11% [8]. However, all patients were classified using the AJCC 6th TNM classification. Patients with AJCC 6th stage pIB disease could be further divided into 3 subgroups according to the AJCC 7th classification. The first group was T2aN0M0 (pIB), including patients whose tumor diameter was less than 3 cm, but who had visceral pleural invasion with a tumor diameter greater than 3 cm. The second group was T2bN0M0 (pIIA). These patients had a tumor 5 to 7 cm in diameter. The third group was T3N0M0 (pIIB), and these patients had a tumor greater than 7 cm in diameter. We wanted to clarify the actual survival benefit of UFT treatment based on the AJCC 7th TNM classification. Propensity score matching is being used increasingly to reduce the impact of treatment selection bias in the estimation of causal treatment effects in observational studies [21]. Therefore, we used propensity score matching to estimate the treatment

effect of UFT on patients with AJCC 7th stage pIB disease.

In previous studies, the 5-year survival rate of patients with stage pIB disease was approximately 50-66% [22-23]. In our control group, the 5-year survival rate was 62.5%, similar to previous studies. Furthermore, we confirmed that UFT therapy confers a survival benefit to patients with AJCC 7th stage pIB disease (odds ratio=0.0180; 95% CI, 0.049-0.660; $p=0.010$). Although a tumor diameter exceeding 3 cm is associated with poor survival, patients with tumor diameters of this size who completed 2 years of UFT treatment had similar overall survival to patients with smaller tumor diameters. We also analyzed patients with tumor diameters of >3 cm, and found that UFT treatment provided a significant survival benefit to this patient group, as well ($p=0.041$). However, we did not identify a significant survival benefit of UFT treatment for patients with tumor diameters of ≤ 3 cm and visceral pleural invasion ($p=0.559$). The lack of a survival benefit may be due to the small number of patients, and thus, we may enroll additional patients in the future to confirm whether UFT treatment confers a survival benefit to these patients. Due to the small number of patients with perineural invasion, we did not clarify its role on the overall survival of patients with stage pIB lung cancer, and larger studies are needed to address this issue. In future studies, combinations of clinical and molecular biological analyses may help to identify the patient populations that might benefit most from adjuvant UFT chemotherapy.

Limitations of this study include its retrospective nature and the small number of cases. Patient compliance is usually a problem in trials of adjuvant chemotherapy. In this study, the primary adverse reactions were anorexia and

nausea; thus, some patients lost their motivation to continue treatment. However, with the help of the oncology case manager, we persuaded these patients to continue UFT therapy without interruption.

Conclusion

In conclusion, UFT treatment was proven to prolong the overall survival of patients with newly diagnosed stage pIB NSCLC in our study. In addition, patients with a tumor diameter >3 cm had poor overall survival, but were able to obtain a survival benefit after completing 2 years of UFT treatment.

References

1. American Joint Committee on Cancer (AJCC) cancer staging handbook. In: Edge SB, Byrd DR, Compton CC, Fritz AG, Greene FL, Trotti A 3rd, eds. AJCC cancer staging manual. 7th ed. Chicago: Springer, 2010: 299-323.
2. Non-small Cell Lung Cancer Collaborative Group. Chemotherapy in non-small cell lung cancer: a meta-analysis using updated data on individual patients from 52 randomised clinical trials. *BMJ* 1995; 311: 899-909.
3. Arriagada R, Dunant A, Pignon JP, *et al.* Long-term results of the international adjuvant lung cancer trial evaluating adjuvant cisplatin-based chemotherapy in resected lung cancer *J Clin Oncol* 2010; 28: 35-42.
4. Pignon JP, Tribodet H, Scagliotti GV, *et al.* Lung adjuvant cisplatin evaluation: a pooled analysis by the LACE Collaborative Group. *J Clin Oncol* 2008; 26: 3552-9.
5. Ichinose Y, Yano T, Asoh H, *et al.* UFT plus cisplatin with concurrent radiotherapy for locally advanced non-small-cell lung cancer. *Oncology (Huntingt)* 1999; 13: Suppl 3: 98-101.
6. Schiller JH, Harrington D, Belani CP, *et al.* Comparison of four chemotherapy regimens for advanced non-small-cell lung cancer. *N Engl J Med* 2002; 346: 92-8.
7. Wada H, Hitomi S, Teramatsu T. Adjuvant chemotherapy after complete resection in non-small-cell lung cancer. *J Clin Oncol* 1996; 14: 1048-54.

8. Kato H, Ichinose Y, Ohta M, *et al.* A randomized trial of adjuvant chemotherapy with uracil-tegafur for adenocarcinoma of the lung. *N Engl J Med* 2004; 350: 1713-21.
9. Travis WD, Brambilla WD, Rami-Porta R, *et al.* Visceral pleural invasion: pathologic criteria and use of elastic stains. Proposal for the 7th edition of the TNM classification for lung cancer. *J Thorac Oncol* 2008; 3: 1384-90.
10. Shimizu K, Yoshida J, Nagai K, *et al.* Visceral pleural invasion is an invasive and aggressive indicator of non-small cell lung cancer *J Thorac Cardiovasc Surg* 2005; 130: 160-5.
11. Katoa T, Ishikawaa K, Aragakia M, *et al.* Angiolymphatic invasion exerts a strong impact on surgical outcomes for stage I lung adenocarcinoma, but not non-adenocarcinoma. *Lung Cancer* 2012; 77: 394-400.
12. Arame A, Mordant P, Cazes A, *et al.* Characteristics and prognostic value of lymphatic and blood vascular microinvasion in lung cancer. *Ann Thorac Surg* 2012; 94: 1673-9.
13. Schuchert MJ, Schumacher L, Kilic A, *et al.* Impact of angiolymphatic and pleural invasion on surgical outcomes for stage I non-small cell lung cancer. *Ann Thorac Surg* 2011; 91: 1059-65.
14. Thoemmes FJ, Kim ES. A systematic review of propensity score methods in the social sciences. *Multivariate behavioral research* 2011; 46: 90-118.
15. Tanaka F, Fukuse T, Wada H, *et al.* The history, mechanism and clinical use of oral 5-fluorouracil derivative chemotherapeutic agents. *Curr Pharm Biotechnol* 2000; 1: 137-64.
16. Taguchi T. Clinical application of biochemical modulation in cancer chemotherapy: Biochemical modulation for 5-FU. *Oncology* 1997; 54: 12-8.
17. Hamada C, Tanaka F, Ohta M, *et al.* Meta-analysis of postoperative adjuvant chemotherapy with tegafur-uracil in non-small-cell lung cancer. *J Clin Oncol* 2005; 23: 4999-5006.
18. Kurebayashi J, Nakatsuka M, Fujioka A, *et al.* Postsurgical oral administration of uracil and tegafur inhibits progression of micrometastasis of human breast cancer cells in nude mice. *Clin Cancer Res* 1997; 3: 653-9.
19. Miyahara R, Nakagawa T, Ishikawa S, *et al.* UFT inhibits lung metastases in spontaneous metastasis model of lung cancer. *Thorac Cardiovasc Surg* 2005; 53: 118-21.
20. Ishikura H, Kondo K, Miyoshi T, *et al.* Suppression of mediastinal metastasis by uracil-tegafur or cis-diammine-dichloroplatinum (II) using a lymphogenous metastatic model in a human lung cancer cell line. *Clin Cancer Res* 2001; 7: 4202-8.
21. Austin PC. Propensity-score matching in the cardiovascular surgery literature from 2004 to 2006: a systematic review and suggestions for improvement. *J Thorac Cardiovasc Surg* 2007; 134: 1128-35.
22. Mountain CF. Revisions in the international system for staging lung cancer. *Chest* 1997; 111: 1710-7.
23. Rami-Porta R, Crowley JJ, Goldstraw P. The revised TMN staging system for lung cancer. *Ann Thorac Cardiovasc Surg* 2009; 15(1): 4-9.
24. Suehisa H, Toyooka S, Hotta K, *et al.* Epidermal growth factor receptor mutation status and adjuvant chemotherapy with uracil-tegafur for adenocarcinoma of the lung. *J Clin Oncol* 2007; 25: 3952-7.

友復（UFT）對於 Stage IB 非小細胞肺癌病患術後的生存益處評估

吳青峰 傅瑞英* 王志偉** 劉永恆 謝明儒
吳青陽 吳怡成 劉會平***

目的：對於 Stage IB 的病患使用友復膠囊作為術後追加的化學治療在台灣以及日本都被廣泛的討論及使用，本篇論文所要討論的就是對於第七版的 AJCC 分期的 IB 病患，使用友復膠囊對於病患生存的益處評估。

方法：我們回溯性的分析 220 位原本在第六版的 AJCC 分期裡 IB 的病患重新依據第七版的 AJCC 分期條件及利用傾向分數（propensity score）1:4 作為分類的方式選出 130 位病患分成兩組：術後使用友復膠囊的病患 26 位，沒有使用友復膠囊的病患 104 位，對於這整群的 IB 病患做預後危險因子分析：包括年紀、性別、手術方式、細胞種類、臟器肋膜的侵犯，以及血管淋巴管侵犯。

結果：根據本文的統計結果，腫瘤大小小於 3 公分跟接受友復（UFT）治療的非小細胞肺癌 IB 病患有較好的存活率。在多重變數分析中，腫瘤大於 3 公分為負向存活指標，（勝算比 odds ratio=3.496; 95% confidence interval, 1.49-8.20），有服用友復的 IB 病患則有較好的存活率（odds ratio=0.180; 95% confidence interval, 0.049-0.660），如果大於 3 公分的病患接受過友復膠囊治療，存活率也較無接受治療的病患好（ $p=0.041$ ）。

結論：總結而言，對於 IB 病患術後服用友復（UFT）的確能增加病患的生存率，且對於大於 3 公分的 IB 病患也能增加術後的存活時間。（*胸腔醫學 2015; 30: 191-200*）

關鍵詞：非小細胞肺癌，分期 IB，友復膠囊，化療

林口長庚紀念醫院 胸腔外科，* 林口長庚紀念醫院 胸腔內科

** 林口長庚紀念醫院 病理科，*** 南京明基醫學中心（已轉任北京新里程醫院）

索取抽印本請聯絡：吳青陽醫師，林口長庚紀念醫院 胸腔外科，333 桃園市龜山區復興街 5 號

Increased Risk of Active Tuberculosis in Diabetic Patients: A Nationwide Population-Based Study

Wen-Wei Shen, Hen-I Lin*, Wei-Chou Chen**

Background: Although several studies have shown a positive correlation between diabetes mellitus (DM) and active tuberculosis (TB), a majority of these studies were conducted with a case-control design or a limited number study subjects. Using a nationwide, population-based database in Taiwan, we conducted a study to examine the relationship between DM and TB.

Methods: We designed a population-based cohort study using the Taiwan National Health Insurance database. After excluding patients who had TB infections diagnosed in the most recent 3 years, we were able to include 47,353 patients with type 2 DM as the study group and 910,577 non-diabetic patients as the control group.

Results: The rate of TB infection during the 2005-2009 follow-up was significantly higher in patients with type 2 DM than in the control group (2.87% vs 0.72%, $P < 0.0001$). The cumulative incidence increased with age among both the diabetic and non-diabetic patients. Risk ratio analysis revealed that diabetic patients had a higher risk than non-diabetic patients in all age groups, especially diabetic males aged < 40 years. Overall, the crude hazard ratio (HR) was 4.019 and the fully adjusted HR (age, gender, hypertension, malignancy, dyslipidemia, chronic obstructive pulmonary disease, liver disease, stroke, nephropathy, pneumoconiosis, and autoimmune diseases) was significant at 1.597 ($P < 0.0001$).

Conclusion: In this national population-based study, we found that DM itself would independently and significantly increase the risk of TB. (*Thorac Med* 2015; 30: 201-209)

Key words: age, diabetes mellitus, risk, tuberculosis

Introduction

Despite recent progress in global control efforts, tuberculosis (TB) is still a major public health issue. In 2009, there were an estimated 9.4 million new cases of TB throughout the

world [1]. Taiwan was no exception: there were 14,625 new cases of TB (63.2 per 100,000 population) and 762 mortalities (3.3 per 100,000 population) in 2008 [2]. To achieve better control of TB, early detection and treatment of patients with TB is essential to avoid further

Department of Social Work, Cardinal Tien Hospital, Fu Jen Catholic University College of Medicine, New Taipei City, Taiwan; *Internal Medicine, Cardinal Tien Hospital, Fu Jen Catholic University College of Medicine, New Taipei City, Taiwan; **Department of Surgery, Cardinal Tien Hospital, Fu Jen Catholic University College of Medicine, New Taipei City, Taiwan

Address reprint requests to: Dr. Wei-Chou Chen, Department of Surgery, Cardinal Tien Hospital, Fu Jen Catholic University College of Medicine, No. 362, Zhongzheng Rd., Xindian Dist., New Taipei City 231, Taiwan

dissemination of *Mycobacterium tuberculosis*. Therefore, we should pay more attention to persons at risk of getting TB, such as those with human immunodeficiency virus infection, those receiving chemotherapy or using steroid, and those with diabetes mellitus (DM). Several studies demonstrated an association between DM and TB, and suggested that TB in diabetic patients would become a challenging public health issue [3-8]. In addition, the global prevalence of DM was estimated to have been 2.8% in 2000, and was expected to increase to 4.4% in 2030. Therefore, the number of patients with DM could increase to 366 million in 2030 [9]. It is possible that as the number of patients with DM increases, the merging of the epidemics of DM and TB could develop thereafter [10-12].

Although several studies showed a positive association between DM and TB, a majority of those studies were conducted as case-control investigations or had a small study population [13-22]. Other limitations were restricting the study cohort to male diabetic patients [19] and defining DM by self-report [19-20]. Furthermore, there were some confounders among the observational studies that affected the estimation of the risk of TB in diabetic patients. In a recent meta-analysis of 13 observational studies including a total of 1,786,212 participants, the relative risk of TB among diabetic patients was estimated at 3.11, with a 95% CI of 2.27-4.26 [23]. However, most studies selected for that meta-analysis were obtained from Western countries, and the TB incidence of the research region varied from 3 to 306 per 100,000 person-years [23].

As in many countries, DM is a serious health issue in Taiwan, and the prevalence and incidence of TB remains high. Using Taiwan's nationwide National Health Insurance (NHI)

database, we conducted a population-based cohort study to estimate the hazard rates (HR) and relative risks of TB in a nationally representative diabetic cohort, according to sex and various age stratifications.

Materials and Methods

Setting

The NHI in Taiwan offers comprehensive medical care coverage to all Taiwan residents. More than 96% of residents in Taiwan have been covered by this program since 1996. Taiwan's Longitudinal Health Insurance Database 2005 (LHID2005) contains the entire claims file for each of 1,000,000 beneficiaries who were sampled randomly from the National Health Insurance Research Database (NHIRD) in 2005, representing approximately 5% of all enrollees in Taiwan. There were no statistically significant differences in sex or age between the sample group and all control enrollees, or between the sample subgroup and all enrollees. We defined TB using ICD-9-CM (International Classification of Diseases, ninth revision, clinical modification) codes (010-018).

Study population

After searching the LHID2005 for the source population for 2000-2004, we identified any hospitalized patients with DM as a discharge diagnosis (ICD-9-CM code 250) and used outpatient claims to identify any visit involving DM (ICD-9-CM code 250 and A code A181). Patients were included in this study if they had at least 1 hospital admission with an ICD-9-CM code 250, or 3 or more outpatient visits with an ICD-9-CM code 250 or A code A181 within 365 days. The definition of DM was validated in a recent study that sampled

9000 patients [24]. In our cohort, 48,566 subjects were identified as having type 2 diabetes. Those individuals who had TB infection diagnosed within the most recent 3 years were excluded, leaving a total of 47,353 subjects with type 2 diabetes comprising the study group.

Control group

Patients with HIV infection (n=77), organ transplant (n=29), type 2 DM (n=48566) and type 1 DM (n=256) were all excluded, leaving a total of 916,350 subjects. After excluding those individuals diagnosed with TB infection within the most recent 3 years, a total of 910,577 subjects were included in the control group.

Statistical analysis

SAS statistical software, version 9.1 was used for statistical analysis, and a $P<0.05$ was defined as statistically significant. To identify the association between DM and TB, several possible risk factors including age, gender, hypertension, malignancy, dyslipidemia, chronic obstructive pulmonary disease, liver disease, stroke, nephropathy, pneumoconiosis, and autoimmune diseases were adjusted in the analysis.

Results

The rate of TB infection during the 2005-2009 follow-up was significantly higher in patients with type 2 DM than in the control group (2.87% vs 0.72%, $P<0.0001$). However, the patients with type 2 DM were significantly older than the control subjects. Other clinical risk factors were also analyzed, and we noted that patients with underlying diseases, such as malignancy, pneumoconiosis, silicosis, stroke, hypertension, chronic obstructive pulmonary disease, nephropathy, liver diseases, autoim-

mune disease, ischemic heart disease, peripheral arterial disease, obesity, and dyslipidemia, were more likely to have TB than patients without these diseases ($P<0.0001$) (Table 1).

The 4-year cumulative incidence markedly increased with age among both the diabetic and non-diabetic patients. Risk ratio analysis showed that diabetic patients had a higher risk than non-diabetic patients in each age group, and in both genders. The highest age-specific risk ratio was observed in diabetic males aged <40 years (Table 2).

The crude HR for the likelihood of developing TB infection among the 2 cohorts during the 4-year follow-up period was 4.019. Demographic-adjusted (age and gender-corrected) HR was 1.724. Fully adjusted HR (age, gender, HTN, malignancy, dyslipidemia, chronic obstructive pulmonary disease, liver disease, stroke, nephropathy, pneumoconiosis, and autoimmune disorder) remained significant at 1.597 ($P<0.0001$). The log-rank test indicated that diabetic patients had significantly lower 4-year TB-free rates than control group patients ($P<0.001$) (Table 3). The results of Kaplan-Meier survival analysis are presented in Figure 1.

Discussion

In this population-based investigation of DM and the subsequent active TB risk, we found that the incidence of active TB in diabetic and non-diabetic patients increased with age, consistent with previous reports [12,25-26]. Our results also indicated that the incidence of TB in DM patients was significantly higher than that of age-matched and sex-matched control subjects, after adjustment of various confounding factors. The highest age-specific risk ratio

Table 1. Characteristics of the Study Subjects

Variable	Control group n=916350	Diabetic group n=47353	P value
General characteristics			
Age (years)			<0.0001
<40	572,611	4058	
40-54	206,351	15,322	
55-69	84,972	18,538	
>70	46,643	9435	
Mean age (\pm standard deviation)	33.3 (19.8)	57.5 (13.2)	<0.0001
Gender			0.5273
Male	449,605	23,452	
Female	460,972	23,901	
Clinical risk factors			
Malignancy	13,131	1834	<0.0001
Pneumoconiosis	890	212	<0.0001
Silicosis	33	9	<0.0001
Stroke	15,820	5273	<0.0001
Hypertension	80,772	23,883	<0.0001
Chronic obstructive pulmonary disease	64,549	7743	<0.0001
Nephropathy	10,974	3657	<0.0001
Liver disease	48,767	11,194	<0.0001
Autoimmune disease	15,130	1460	<0.0001
Ischemic heart disease	25,903	8518	<0.0001
Peripheral arterial disease	7519	3223	<0.0001
Obesity	1738	495	<0.0001
Dyslipidemia	36,059	14,871	<0.0001
Tuberculosis	6575	1358	<0.0001

was found in diabetic patients aged <40 years.

The overall risk of active TB in our diabetic population was still increased after adjustment of several confounding factors. Other large-scale cohort and case control reports had consistent results [13-20]. In South Korea, Kim *et al* found the risk ratio of TB in diabetic patients versus non-diabetic controls was 3.47 (95% CI 2.98-4.03) in a 3-year study (adjusted for age) [27]. In the UK, Jick *et al* found that the ad-

justed odds ratio (adjusted for age, and sex) of TB was 3.8 for diabetic patients, compared with non-diabetic patients, using the General Practice Research Database involving over 2 million patients [16]. In a recent meta-analysis, Jeon *et al* reviewed 13 observational studies and reported that the relative risk of TB in diabetic patients was 3.11 (95% CI, 2.27-4.26) [27]. We had similar findings regarding the strong correlation between DM and TB, but the adjusted

Table 2. Rates (per 100,000) and Risk Ratio of 4-year Cumulative Incidence of Tuberculosis (TB) from 2005 to 2009 in Diabetic and Non-diabetic Patients According to Age and Sex

Variable	Cumulative incidence by age				
	All age	<40	40-54	55-69	>70
Diabetic patients					
No* of TB	1358	64	299	518	477
No of diabetic patients	47,353	4058	15,322	18538	9435
Rate in diabetic patients	28,67.8	1577.1	1951.4	2794.3	5055.6
Nondiabetic patients					
No of TB	6575	1772	1415	1313	2075
No of nondiabetic patients	910,577	572,611	206,351	84972	46643
Rate in nondiabetic patients	722.1	309.5	685.7	1545.2	4448.7
Risk ratio	4.0	5.1	2.8	1.8	1.1
Diabetic males					
No of TB	853	49	206	304	294
No of diabetic males	23,452	2355	8421	8255	4421
Rate in diabetic males	36,37.2	2080.7	2446.3	3682.6	6650.1
Nondiabetic males					
No of TB	3969	889	791	837	1452
No of nondiabetic males	449,605	283,327	100,917	40991	24370
Rate in nondiabetic males	882.8	313.8	783.8	2041.9	5958.1
Risk ratio	4.1	6.6	3.1	1.8	1.1
Diabetic females					
No of TB	505	15	93	214	183
No of diabetic females	23,901	1703	6901	10283	5014
Rate in diabetic females	2112.9	880.8	1347.6	2081.1	3649.8
Nondiabetic females					
No of TB	2606	883	624	476	623
No of nondiabetic females	460,972	289,284	105,434	43981	22273
Rate in nondiabetic females	565.3	305.2	591.8	1082.3	2797.1
Risk ratio	3.7	2.9	2.3	1.9	1.3

*No: number

odds ratio was only 1.75 (95% CI, 1.64-1.86), which was lower than that of previous findings [16,23,28]. There may be several reasons for the difference. First, in contrast to previous reports involving mixed type 1 and 2 DM [13-20], we excluded patients with type 1 DM, so the confounding of a mixture with type 1 DM was

minimal in the present work. Second, this study adjusted many clinical risk factors to minimize possible confounding, and therefore a pure association between DM and TB could be demonstrated. Third, the study subjects were enrolled from the NHI database, which is highly representative, and therefore there was only a small

Table 3. Mutually Adjusted Hazard Ratio (HR) for Tuberculosis (TB) Derived from Diabetic Patients from 2005 to 2009

Variables	Developing TB		
	HR	95% CI	<i>p</i> value
Unadjusted HR	4.019	3.79-4.26	<0.0001
Demographic-adjusted HR*	1.724	1.62-1.83	<0.0001
Fully adjusted HR ⁺	1.597	1.50-1.70	<0.0001

Abbreviations: HR, hazard ratio; CI, confidence interval

*Adjusted for age, and gender

⁺Adjusted for age, gender, hypertension, malignancy, dyslipidemia, chronic obstructive pulmonary diseases, liver disease, stroke, nephropathy, pneumoconiosis, and autoimmune diseases.

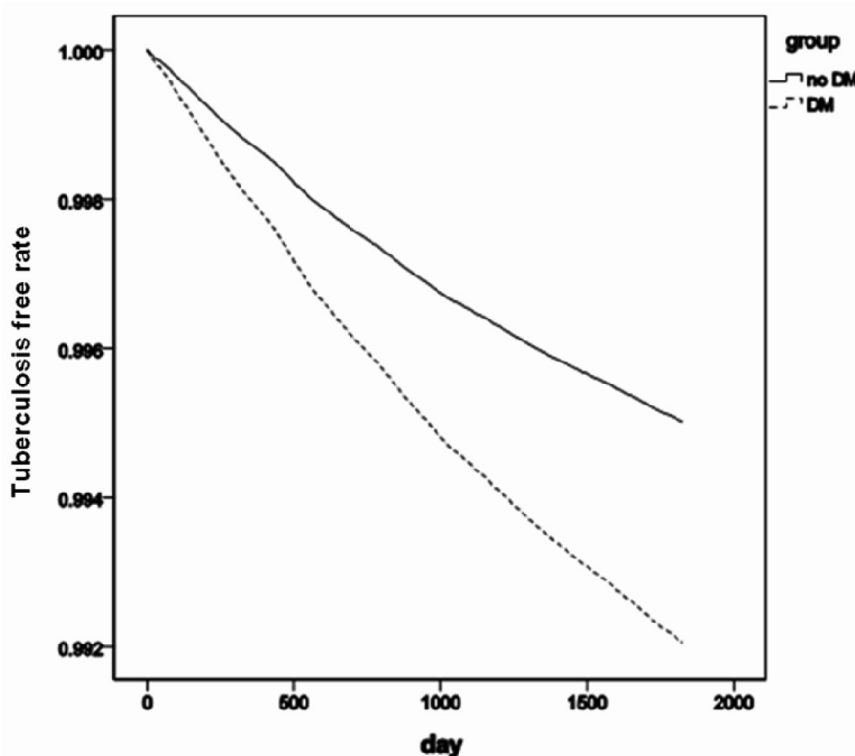


Fig. 1. A plot of tuberculosis-free rate curves based on the Cox model analysis for patients with diabetes mellitus and a comparison cohort after adjustment for age, gender, hypertension, malignancy, dyslipidemia, chronic obstructive pulmonary diseases, liver disease, stroke, nephropathy, pneumoconiosis, and autoimmune diseases.

chance of recall and selection bias. In addition, the possibility of non-response and lost to follow-up of cohort subjects was limited. Overall, our study, based on an extensive nationwide population-based database, can be regarded as

more convincing.

In the present report, the incidence of TB was highest among elderly patients aged >70 years in both groups. This is consistent with findings in previous reports [25-26], that the

incidence of TB is rising among the elderly. As the elderly population increases worldwide, greater awareness in disease recognition and prompt diagnosis and treatment of elderly patients are urgently needed.

We observed the highest risk ratio among the youngest subjects, aged <40 years (Table 2), irrespective of sex, and the effect of age decreased with increasing age. In diabetic men aged >70 years, the risk of TB was almost the same as that of the control subjects. Although the effect of age can be confirmed only after adjustment of other possible risk factors, we found a trend in this study -- that the young diabetic group had the highest risk ratio of TB. Thus, our finding still indicates that we should pay more attention to preventing the development of TB among younger diabetic patients, who are at a higher risk for TB than other age groups. However, further case-control studies are warranted to confirm such a relationship.

There are some limitations in this investigation. First, the duration and treatment regimens of diabetes and other socioeconomic characteristics were not evaluated in the present work; these factors may have affected this analysis. Second, it was difficult to assess whether the strong correlation between DM and TB was due to frequent surveillance of TB among diabetic patients. Third, there may have been a mix of undiagnosed DM patients who have not visited a hospital in the control group.

In conclusion, this national population-based study in Taiwan confirmed the significant effect of DM on active TB.

References

1. Global tuberculosis control report 2010. Available at: http://www.who.int/tb/publications/global_report/2010/gtbr10_main.pdf.
2. Center for Disease Control for Taiwan. Statistics of communicable diseases and surveillance report, Republic of China, 2009. Available at: <http://www.cdc.gov.tw/public/Data/9123117221971.pdf>.
3. Dooley KE, Chaisson RE. Tuberculosis and diabetes mellitus: convergence of two epidemics. *Lancet Infect Dis* 2009; 9: 737-46.
4. Jeon CY, Murray MB. Diabetes mellitus increases the risk of active tuberculosis: a systemic review of 13 observational studies. *PLoS Med* 2008; 5: e152.
5. Alisjahbana B, van Crevel R, Sahiratmadja E, *et al.* Diabetes mellitus is strongly associated with tuberculosis in Indonesia. *Int J Tuberc Lung Dis* 2006; 10: 696-700.
6. Restrepo BI, Fisher-Hoch SP, Crespo JG, *et al.* Nuevo Santander Tuberculosis Trackers: Type 2 diabetes and tuberculosis in a dynamic bi-national border population. *Epidemiol Infect* 2007; 135: 483-91.
7. Shetty N, Shemko M, Vaz M, *et al.* An epidemiological evaluation of risk factors for tuberculosis in South India: a matched case control study. *Int J Tuberc Lung Dis* 2006; 10: 80-6.
8. Pablos-Mendez A, Blustein J, Knirsch C. The role of diabetes mellitus in the higher prevalence of tuberculosis among Hispanics. *Am J Public Health* 1997; 87: 574-9.
9. Wild S, Roglic G, Green A, *et al.* Global prevalence of diabetes: estimates for the year 2000 and projections for 2030. *Diabetes Care* 2004; 27: 1047-53.
10. Restrepo BI. Convergence of the tuberculosis and diabetes epidemics: renewal of old acquaintances. *Clin Infect Dis* 2007; 45: 436-8.
11. Stevenson CR, Forouhi NG, Roglic G, *et al.* DM and tuberculosis: the impact of the DM epidemic on tuberculosis incidence. *BMC Public Health* 2007; 7: 234.
12. Dixon B. Diabetes and tuberculosis: an unhealthy partnership. *Lancet Infect Dis* 2007; 7: 444.
13. Perez A, Brown HS 3rd, Restrepo BI. Association between tuberculosis and diabetes in the Mexican border and non-border regions of Texas. *Am J Trop Med Hyg* 2006; 74: 135-8.
14. Pablos-Mendez A, Blustein J, Knirsch CA. The role of diabetes mellitus in the higher prevalence of tuberculosis among Hispanics. *Am J Public Health* 1997; 87: 574-9.
15. Brassard P, Kenzouh A, Suissa S. Antirheumatic drugs and the risk of tuberculosis. *Clin Infect Dis* 2006; 43:

- 717-22.
16. Jick SS, Liberman ES, Rahman MU, *et al.* Glucocorticoid use, other associated factors, and the risk of tuberculosis. *Arthritis Rheum* 2006; 55: 19-26.
17. Mori MA, Leonardson G, Welty TK. The benefits of isoniazid chemoprophylaxis and risk factors for tuberculosis among Oglala Sioux Indians. *Arch Intern Med* 1992; 152: 547-50.
18. Buskin SE, Gale JL, Weiss NS, *et al.* Tuberculosis risk factors in adults in King Country, Washington, 1998 through 1990. *Am J Public Health* 1994; 84: 1750-6.
19. Rosenman KD, Hall N. Occupational risk factors for developing tuberculosis. *Am J Ind Med* 1996; 30: 148-54.
20. Coker R, McKee M, Atun R, *et al.* Risk factors for pulmonary tuberculosis in Russia: case-control study. *BMJ* 2006; 332: 85-7.
21. John G, Shankar V, Abraham AM, *et al.* Risk factors for post-transplant tuberculosis. *Kidney Int* 2001; 60: 1148-53.
22. Chen CH, Lian JD, Cheng CH, *et al.* Mycobacterium tuberculosis infection following renal transplantation in Taiwan. *Transpl Infect Dis* 2006; 8: 148-56.
23. Jeon CH, Murray MB. Diabetes mellitus increases the risk of active tuberculosis: a systematic review of 13 observational studies. *PLoS Med* 2008; 5: e152.
24. Lin CC, Lai MS, Syu CY, *et al.* Accuracy of diabetes diagnosis in health insurance claims data in Taiwan. *J Formos Med Assoc* 2005; 104: 157-63.
25. Stead WW, Lofgren JP. Does the risk of tuberculosis increase in old age? *J Infect Dis* 1983; 147: 951-5.
26. Davies PD. Tuberculosis in the elderly. *J Antimicrob Chemother* 1994; 34: 93-100.
27. Kim SJ, Hong YP, Lew WJ, *et al.* Incidence of pulmonary tuberculosis among diabetics. *Tuber Lung Dis* 1995; 76: 29-33.

糖尿病患者有較高活動性結核病的風險— 以全國人口為對象之研究

沈文偉 林恆毅* 陳衛洲**

背景：雖然許多的研究都顯示出糖尿病和活動性結核病的正相關性，但是其中大多數的研究都是進行於病例對照研究法或侷限於研究對象的數目。這次我們利用臺灣全國性的資料庫的優勢，針對糖尿病和結核病的關係進行本次研究。

方法：我們使用臺灣國家健康保險資料庫設計此一以全國人口為基礎的世代追蹤研究。排除了最近三年內才診斷感染結核病的人數，研究組共有 47,353 位是糖尿病患者，相對於 910,577 位非糖尿病患者作為控制組。

結果：在西元 2005 至 2009 年間的追蹤內，患有第二型糖尿病的患者，得到結核病感染的機率是有意義的高於控制組 (2.87% vs 0.72%, $P<0.0001$)。不論是否有糖尿病，累計發生率都是隨著年紀增加。危險比值 (risk ratio) 分析顯示在所有年齡組別中，糖尿病患者的風險都是比非糖尿病患者高，尤其是小於四十歲的男性糖尿病患者。總結來說，粗估危險比 (crude hazard ratio, HR) 是 4.019，完全校正危險比 (fully adjusted HR) (年齡、性別、高血壓、癌症、血脂異常、慢性阻塞性肺疾、肝臟疾病、中風、腎臟病、塵肺症及自體免疫疾病) 仍然是有意義的 1.597 ($P<0.0001$)。

結論：根據此次以全國人口為對象的研究，糖尿病本身就是增加結核病感染的風險，而且具有統計上的意義。(胸腔醫學 2015; 30: 201-209)

關鍵詞：年齡，糖尿病，風險，結核病

天主教輔仁大學醫學院耕莘醫院 社會服務室，*天主教輔仁大學醫學院耕莘醫院 內科部

**天主教輔仁大學醫學院耕莘醫院 外科部

索取抽印本請聯絡：陳衛洲醫師，天主教輔仁大學醫學院耕莘醫院 外科部，新北市新店區中正路 362 號

Double Primary Lung Cancer with Contralateral Spontaneous Pneumothorax – A Case Report

Bo-Nian Huang, Wei-Li Huang*, Yi-Jen Chen, Ming-Shian Lin, Shih-Yu Lee

Patients with lung cancer may present with more than one primary lesion arising in the lung at the same time and then be classified as having synchronous multiple primary lung cancer (MPLC). We described an 80-year-old man who presented with a chronic cough and respiratory distress. A roentgenogram of the chest showed the presence of a tumor at the right upper lobe (RUL) and right lower lobe (RLL), accompanied by left pneumothorax. The findings on a computed tomography of the chest showed a tracheal tumor and tumors at the RUL and RLL. Histological examination was carried out, and revealed that the tracheal tumor and the RUL tumor were squamous cell carcinoma, while the RLL tumor was small cell carcinoma. (*Thorac Med* 2015; 30: 210-216)

Key words: double primary, lung cancer, pneumothorax

Introduction

Patients with lung cancer may present with more than one primary lesion arising independently in the lung at the same time, and these patients are then classified as having synchronous multiple primary lung cancer (MPLC). In these circumstances, an infectious process, the presence of a benign nodule and/or the occurrence of metastasis from an extrapulmonary site must then be excluded.

Spontaneous pneumothorax secondary to a tracheal tumor is an unusual occurrence. It is generally attributed to a rupture of the subpleural blebs or emphysematous bullae [1].

This event can also complicate primary or secondary lung tumors and may occur in advanced carcinoma of the lung, due to extension of the disease to the pleura followed by rupture of the membrane. Spontaneous pneumothorax associated with primary pulmonary neoplasm or lung metastasis is very rare, and the estimated rate of joint occurrence is between 0.03% and 0.05% for primary lung cancer cases [2-3]. Reported here is the case of a patient with squamous cell carcinoma and small cell carcinoma of the lung who presented with the symptoms of spontaneous pneumothorax. A brief review of the literature is presented.

Division of Pulmonary Medicine, Department of Internal Medicine, Ditmanson Medical Foundation Chia-Yi Christian Hospital; *Division of Thoracic Surgery, Department of Surgery, Ditmanson Medical Foundation Chia-Yi Christian Hospital

Address reprint requests to: Dr. Shih-Yu Lee, Division of Pulmonary Medicine, Department of Internal Medicine, Ditmanson Medical Foundation Chia-Yi Christian Hospital, 539 Jhongsiao Road, Chia-Yi City, Taiwan

Case Report

An 80-year-old man presented with a history of hypertension and an old cerebrovascular accident. He came to the outpatient department at Chia-Yi Christian Hospital on November 12, 2013 because of a cough with blood-tinged sputum that had been present for weeks. He had been a heavy smoker previously and had quit for a number of years. Physical examination revealed mild rales and wheezing sounds in the bilateral lungs. Findings on a roentgenogram of the chest, which had been taken at an outside hospital four days previously, revealed a lesion in the right lung (Figure 1). Computed tomography (CT) of the chest was arranged, and showed the presence of, first, a 1.9 cm soft tissue abnormality in the right tracheal wall, second, a spiculated soft tissue lesion in the right upper lobe (RUL) (1.9 cm) and, third, a spiculated soft tissue lesion in the right lower lobe (RLL) (2.3 cm) (Figure 2).



Fig. 1. Chest X-ray shows a tumor at the right lower lobe.

The patient returned one week later for the chest CT report and was found to be suffering from severe dyspnea, respiratory distress and stridor. He was then transferred to the emergency room because of progressive respiratory distress. Physical examination revealed tachycardia and tympanic percussion with decreased breathing sounds at the left lower chest. Routine investigations revealed Hb: 9.1%, blood urea: 38.5 mg/dl, and creatinine: 1.8 mg/dl. Liver function and sugar, etc., were normal. Direct smear examination of the sputum was negative for acid-fast bacilli as well as the presence of malignant cells. Findings from a roentgenogram of the chest that was carried out at the emergency room indicated pneumothorax affecting the left lung (Figure 3). As a result of this finding, a tube thoracostomy was performed.

Fiberoptic bronchoscopy was carried out, and this revealed a huge mid-tracheal tumor that almost totally occluded the lumen (Figure 4). Bronchoscopic removal of the tumor together with bronchoscopic laser abrasion was performed. Histological examination of the bronchoscopic biopsy specimen indicated squamous cell carcinoma. Video-assisted thoracic surgery (VATS) wedge resection at the RUL and RLL was also performed. Histological examination of the VATS specimen showed squamous cell carcinoma affecting the RUL and small cell carcinoma affecting the RLL. The postoperative treatment strategy, which involved both chemotherapy and radiotherapy, was based on the presence of small cell carcinoma of the RLL.

Discussion

Patients with lung cancer may present with more than one primary lesion arising in the lung at the same time, but the patient must ful-

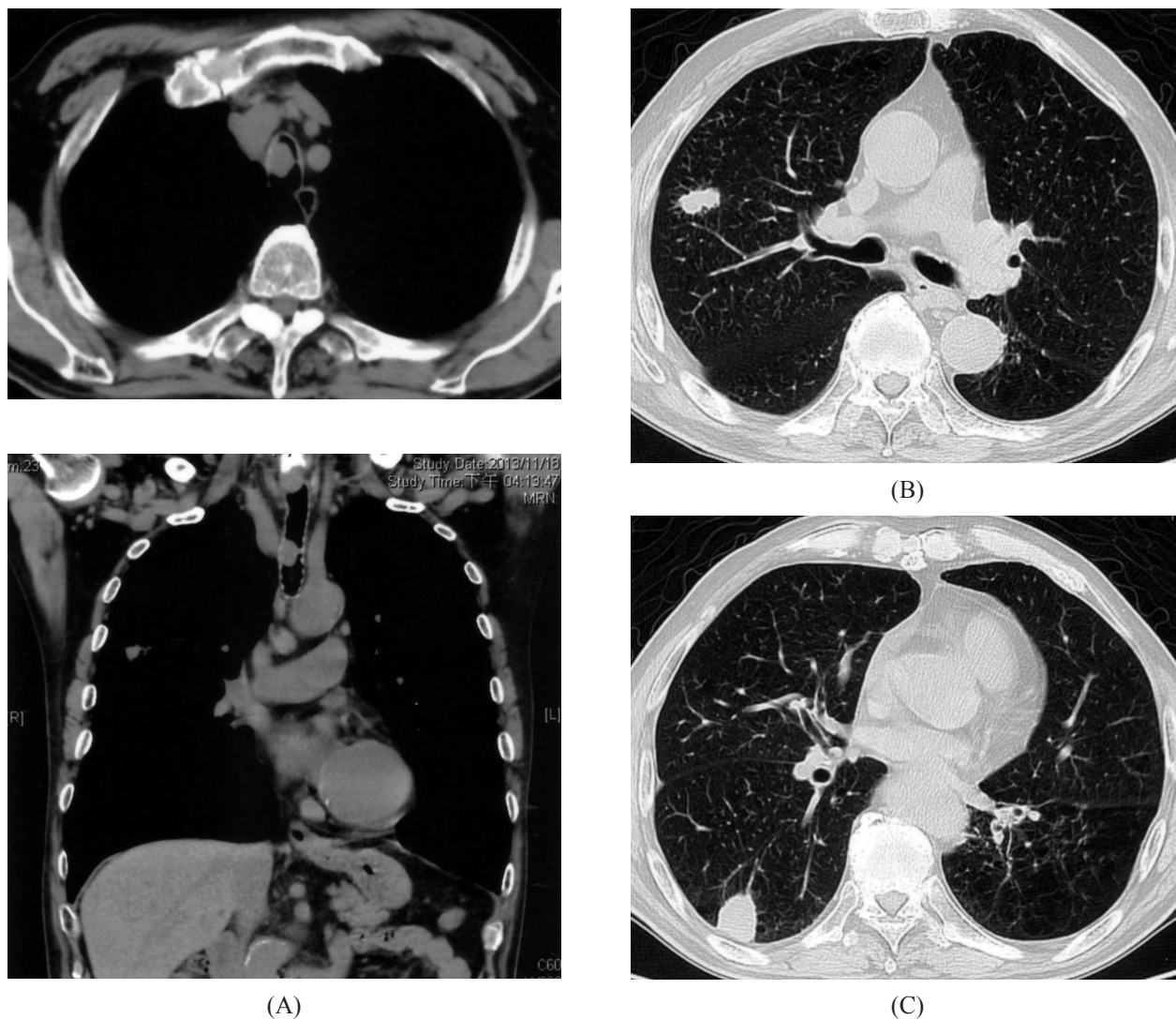


Fig. 2. Chest computed tomography reveals the following. A) a 1.9 cm soft tissue density in the right tracheal wall. B) a spiculated soft tissue lesion in the right upper lobe (1.9 cm). C) a spiculated soft tissue lesion in the right lower lobe (2.3 cm).

fill strict criteria to be classified as having synchronous MPLC. Both lesions must have arisen independently in the lung and both must be malignant. The diagnosis of synchronous MPLC requires tissue from multiple lung tumors. Furthermore, the presence of an infectious process, the occurrence of a benign nodule and/or metastatic spread from an extrapulmonary site must be excluded. Histologically identical lesions within the same lobe are considered to be “sep-

arate tumor nodules”.

The staging of a patient presenting with synchronous MPLC is complex and needs to be meticulous if potentially curative resection is being contemplated. Both fluorodeoxyglucose positron emission tomography (FDG-PET) and magnetic resonance imaging (MRI) of the brain should be performed to evaluate the possibility of a presence of extra-thoracic metastatic events within the lungs.



Fig. 3. Chest X-ray shows a left pneumothorax and the presence of lesions at the right upper lobe and the right lower lobe.

After the imaging study and the operation (bronchoscopic removal and laser abrasion of the tracheal tumor together with VATS wedge resection in the RUL and RLL), the staging of this patient was classified as synchronous MPLC with tracheal squamous cell carcinoma, RUL squamous cell carcinoma, pT1bN0M0, stage IB, and RLL small cell carcinoma, pT2aN0M0, stage IB, limited stage.

Once the diagnosis of synchronous primary lung cancers has been established, the patient should be assessed for an individualized treatment strategy. The benefit of using chemotherapy and radiotherapy in patients with MPLC is still not definitive, since there are no randomized trials to use as guidelines. Cell morphology and highest stage of the tumor appear to be the best predictors of prognosis in patients with synchronous MPLC, so a treatment strategy involving chemotherapy and radiotherapy that

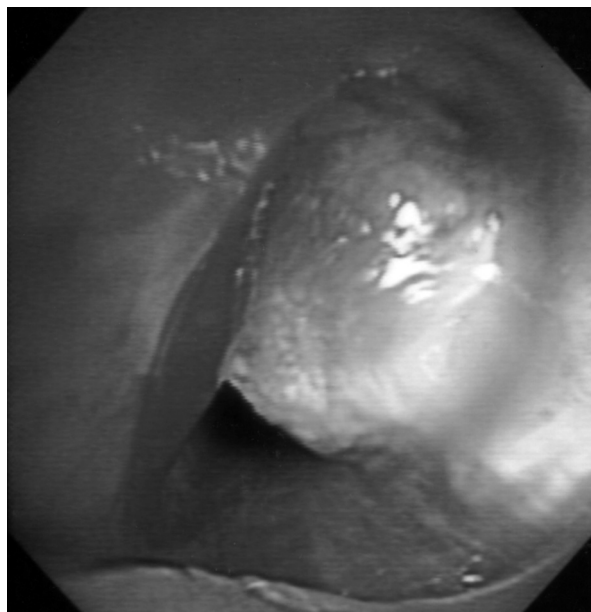


Fig. 4. Fiberoptic bronchoscopy revealed a huge mid-tracheal tumor that has almost totally occluded the lumen.

was based on RLL small cell carcinoma was instituted for our patient.

Spontaneous pneumothorax is classified as primary or secondary pneumothorax. Primary spontaneous pneumothorax most commonly afflicts the young and healthy who do not have a known lung disease, and this usually occurs when the patient is at rest [6]. The secondary type is defined as a pneumothorax that occurs as a complication of underlying lung disease. The most commonly associated diseases are chronic obstructive pulmonary disease, cystic fibrosis, primary or metastatic lung malignancy and necrotizing pneumonia.

Both primary and metastatic lung malignancies have been associated with secondary spontaneous pneumothorax. Heimlich and Rubin [9] and Citron [10] reported several cases in which a primary bronchial carcinoma was associated with spontaneous pneumothorax.

Spontaneous pneumothorax secondary to bronchogenic carcinoma is an unusual occurrence [11-12]. Only 2% of all cases of spontaneous pneumothorax have been found to be coexistent with malignant lung diseases, more commonly primary lung cancer than metastatic disease [13]. Pulmonary malignancy should be suspected if an older individual with cancer develops spontaneous pneumothorax, especially if the latter is associated with a nonexpanding lung.

Dines *et al* [4], have proposed four pathogenic processes for spontaneous pneumothorax in patients with bronchogenic and other malignancies of the lung. The first mechanism involves direct pleural invasion by a neoplasm, and in this circumstance, the pneumothorax may be a result of tumor necrosis and/or rupture of the necrotic neoplastic tissue in the pleural cavity [2]. The second mechanism, which is considered to occur with sarcoma, is the presence of a bronchopleural fistula that is created by an actual rupture of necrotic tumor tissue into a bronchus and the pleural space [3]. The third mechanism is that of cancer with a related check valve mechanism; this is a condition in which a tumor of the lung may obstruct the bronchioles and lead to over-inflation of the affected lung, followed by rupture of the lung [14]. The fourth proposed mechanism is not related directly to bronchogenic carcinoma. The population of patients with bronchogenic carcinoma is largely composed of cigarette smokers, who often have chronic obstructive lung disease. In this state, the bullae may rupture following disturbance of the lung architecture by the bronchial cancer [15].

Two of the above mechanisms fit the circumstances of the our patient and are likely related to his pneumothorax. First, chronic bronchitis or emphysema bullae may have been

present in his lungs, and these bullae may have ruptured following the disturbance of the lung architecture by the bronchial cancer. Second, the presence of overinflated alveoli or bullae, which were caused by the check-valve mechanism as a result of the huge mid-tracheal tumor obstruction, may have resulted in rupture.

Conclusion

Multiple primary lung cancer is a relatively uncommon entity. Once the diagnosis of synchronous primary lung cancers has been established, the patient should be assessed to create an individualized treatment strategy. The benefit of the use of chemotherapy and radiotherapy in patients with MPLC is still not definitive, since there are no randomized trials to use as guidelines. Cell morphology and the highest stage of the tumor appear to be the best predictors of prognosis in patients with synchronous MPLC.

Spontaneous pneumothorax may develop in the presence of a carcinoma of the lung as a result of rupture of a subpleural bleb in an area of obstructive emphysema, as well as invasion of the pleura by the malignancy. Spontaneous pneumothorax in association with lung cancer is rarely seen. Pulmonary malignancy should always be considered as a possible cause if an individual is of cancer age or is a heavy smoker, and then develops spontaneous pneumothorax, especially if the latter is associated with a non-expanding lung.

References

1. Bauman MH, Noppen M. Pneumothorax. *Respirology* 2004; 9: 157-64.
2. Tsukamoto T, Satoh T, Yamada K, *et al.* Primary lung cancer presenting as spontaneous pneumothorax. *Nihon*

- Kyobu Shikkan Gakkai Zasshi 1995; 33(9): 936-9.
3. Steinhäuslin CA, Cuttat JF. Spontaneous pneumothorax. A complication of lung cancer. *Ann Thorac Surg* 2005; 79: 716.
 4. Dines DE, Cortese DA, Brennan MD, *et al.* Malignant pulmonary neoplasms predisposing to spontaneous pneumothorax. *Mayo Clin Proc* 1973; 48: 541-4.
 5. Tanvetyanon T, Finley DJ, Fabian T, *et al.* Prognostic factors for survival after complete resections of synchronous lung cancers in multiple lobes: pooled analysis based on individual patient data. *Ann Oncol* 2013; 24: 889.
 6. Bense L, Wiman LG, Hedenstierna G. Onset of symptoms in spontaneous pneumothorax: correlations to physical activity. *Eur J Respir Dis* 1987; 71: 181.
 7. Sahn SA, Heffner JE. Spontaneous pneumothorax. *N Engl J Med* 2000; 342: 868.
 8. Noppen M, De Keukeleire T. Pneumothorax. *Respiration* 2008; 76: 121.
 9. Heimlich J, Rubin M. Spontaneous pneumothorax as a presenting feature of primary carcinoma of the lung. *Chest* 1955; 27: 457-64.
 10. Citron KM. Spontaneous pneumothorax complicating bronchial carcinoma. *Tubercle* 1959; 40: 384-6.
 11. Galbis CJM, Mafé MJJ, Baschwitz GB, *et al.* Spontaneous pneumothorax as the first sign of pulmonary carcinoma. *Arch Bronconeumol* 2001; 37(9): 397-400.
 12. O'Connor BM, Ziegler P, Spaulding MB. Spontaneous pneumothorax in small cell lung cancer. *Chest* 1992; 102(2): 628-9.
 13. Pohl D, Herse B, Criée CP, *et al.* Spontaneous pneumothorax as the initial symptom of bronchial cancer. *Pneumologie* 1993; 47(2): 69-72.
 14. Minami H, Sakai S, Watanabe A, *et al.* Check-valve mechanism as a cause of bilateral spontaneous pneumothorax complicating bronchioloalveolar cell carcinoma. *Chest* 1991; 100(3): 853-5.
 15. Okada D, Koizumi K, Haraguchi S, *et al.* Pneumothorax manifesting primary lung cancer. *J Thorac Cardiovasc Surg.* 2002; 50(3): 133-6.

兩個同時發現的原發性肺癌合併對側自發性氣胸

黃柏年 黃維立* 陳奕仁 林明憲 李世瑜

同時期發現兩個原發性肺癌並不常見。兩處的病灶必須是互相獨立且必須是惡性的。我們報告一位八十歲男性因長期咳嗽及呼吸困難而住院；其影像學顯示腫瘤位於氣管，右上肺葉及右下肺葉並合併左側氣胸。氣管內及右上肺葉腫瘤的病理切片為鱗狀上皮癌；右下肺葉腫瘤的病理切片為小細胞癌。氣胸發生前的電腦斷層發現左側肺氣腫且無腫瘤侵犯。(*胸腔醫學* 2015; 30: 210-216)

關鍵詞：氣胸，同時期原發的肺癌

Pneumonia and Bacteremia Due to Community-Acquired *Staphylococcus aureus* in a Healthy Adult Carrying the Panton-Valentine Leukocidin Gene – A Case Report

Chia-Wei Kuo, Shu-Chen Kuo*, Jeng-Yuan Hsu, Pin-Kuei Fu**

Community-acquired methicillin-resistant *Staphylococcus aureus* (CA-MRSA) differs from nosocomial MRSA in that the former often carries genes for virulence factors such as Panton-Valentine leukocidin (PVL), which produce toxins and cause infections in previously healthy individuals. Pneumonia caused by CA-MRSA that harbors the PVL toxin gene is often characterized by high fever, sepsis, respiratory failure, and high mortality. We report a young adult who suffered from CA-MRSA-associated pneumonia and bacteremia. The CA-MRSA isolate was a staphylococcal cassette chromosome *mec* (SCC*mec*) type V strain and carried the PVL gene. The young man presented with high fever and multi-lobar pneumonia, and subsequently developed pneumatoceles. All symptoms and pneumonic consolidations resolved after completion of the treatment course. (*Thorac Med* 2015; 30: 217-223)

Key words: community-acquired methicillin-resistant *Staphylococcus aureus* (CA-MRSA), Panton-Valentine leukocidin (PVL), pneumonia, pneumatocele

Introduction

Methicillin-resistant *Staphylococcus aureus* (MRSA) has been a major cause of nosocomial infections since the 1960s. However, the epidemiology of MRSA infection throughout the world has changed over the past 2 decades [1-2]. Community-acquired MRSA (CA-MRSA) is different from nosocomial MRSA due to the former's ability to infect children or young

adults without risk factors for MRSA acquisition, including players of team sports, military personnel and inmates in correction facilities [3-7]. CA-MRSA can be more virulent than nosocomial MRSA strains, and part of its virulence is due to the production of Panton-Valentine leukocidin (PVL), a harmful cytotoxin of CA-MRSA [1] that destroys bacterium-engulfing immune cells and respiratory tissue [1]. PVL is associated with necrotizing pneumonia,

Division of Chest Medicine, Department of Internal Medicine, Taichung Veterans General Hospital, Taichung, Taiwan; *National Institute of Infectious Diseases and Vaccinology, National Health Research Institutes, Miaoli County, Taiwan; **Division of Critical Care & Respiratory Therapy, Department of Internal Medicine, Taichung Veterans General Hospital, Taichung, Taiwan

Address reprint requests to: Dr. Pin-Kuei Fu, Division of Critical Care & Respiratory Therapy, Department of Internal Medicine, Taichung Veterans General Hospital, Taichung, Taiwan, 1650 Taiwan Boulevard Sect. 4, Taichung, Taiwan

skin and soft tissue infection, sepsis, and a high mortality rate [6-8]. The present case is that of a young Taiwanese adolescent male who was diagnosed with CA-MRSA pneumonia and bacteremia. The CA-MRSA carried the genes of staphylococcal cassette chromosome *mec* (SC-*Cmec*) type V and PVL toxin. Chest radiograph and CT scan disclosed pneumatoceles formation. After adequate treatment, the pneumonia resolved, and no lasting deleterious effect was noted in the lungs.

Case Report

A 17-year-old Taiwanese male, who was previously in apparently good health without any medical or surgical history and was without a smoking or alcohol-drinking history, presented with symptoms of fever and cough with gray-colored sputum, which had been occasionally blood-tinged since April 19, 2013. He reported experiencing an influenza-like illness and persistent high fever up to 39°C with cold sweating, right chest pain and shortness of breath since April 24, 2013. There was no skin eruptions, myalgia, arthralgia, or consciousness disturbance. Because of symptoms progression, he went to a local community hospital for help on April 24. Physical examination showed that his body temperature was 38.4°C, heart rate was 110 beats/minute, respiratory rate was 25 breaths/minute, and blood pressure was 117/65 mmHg; SpO₂ was 93% in room air, no accessory muscle was used, and chest auscultation showed bilateral rhonchi. Chest radiograph showed multiple patches diffusely infiltrating the bilateral lung fields. Laboratory data showed that WBC was 12440/ul, C-reactive protein (CRP) was 17.64 mg/dl, and the influenza A and B rapid test was negative. He was

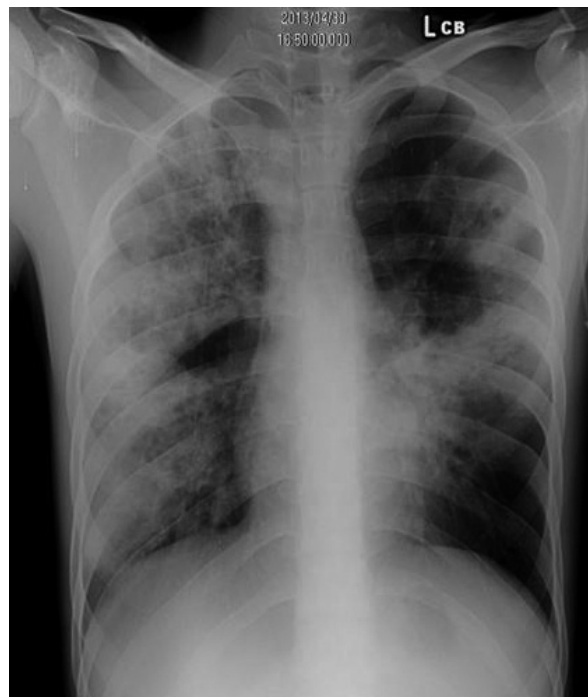


Fig. 1A. Chest radiograph on April 30, 2013 shows multilobar alveolar infiltrates and small cavities in the left upper lung field.

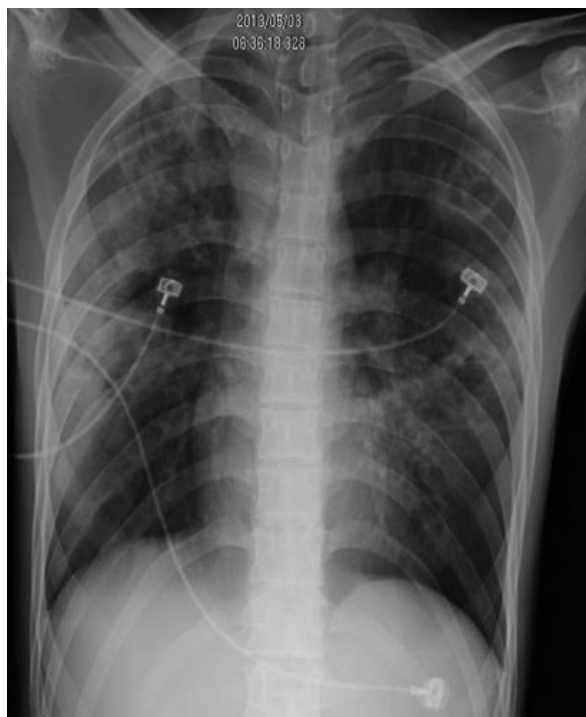


Fig. 1B. Chest radiography on May 3, 2013 shows improving alveolar infiltrates; however, multiple cavitory lesions were observed in the patches.

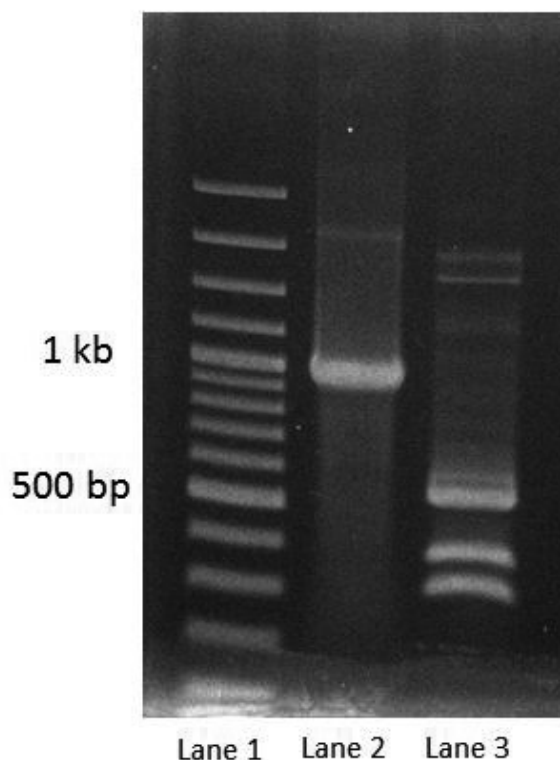


Fig. 2. The polymerase chain reaction (PCR) result of the MRSA isolate was positive for the PVL gene (Lane 2). SCCmec type V was identified by multiplex PCR (Lane 3). Lane 1 was the molecular weight marker.

treated with piperacillin/tazobactam and amikacin (April 24 to 25), azithromycin (April 24 to 26), imipenem/cilastatin and vancomycin (April 25 to 30), and oseltamivir (April 25 to 29) for severe pneumonia. On April 28, 2013, sputum and blood cultures both yielded MRSA, which was sensitive to vancomycin, clindamycin, and sulfamethoxazole/trimethoprim. However, he still had progressive dyspnea and worsening of the consolidation on the follow-up chest radiograph (Figure 1A). Therefore, he was transferred to our Intensive Care Unit (ICU) due to progressive hypoxemia on April 30, 2013.

On admission to the ICU, the patient was well oriented. His body temperature was 37.6°C, pulse rate was 98 beats/minute, blood

pressure was 97/53 mmHg, and respiratory rate was 26 breaths/minute. Chest auscultation showed rhonchi in the bilateral lower lung fields. Laboratory tests revealed a white blood cell count (WBC) of 20,800/ μ L with 91% neutrophils, and an elevated CRP level of 12.07 mg/dl (normal range <0.3 mg/dl). Arterial blood gas analysis using a non-invasive positive pressure ventilator (Bipap) revealed pH: 7.459, PaO₂: 77 mmHg, PaCO₂: 35.8 mmHg, and HCO₃⁻: 24.8 mmol/L. Chest radiograph showed multiple patches of consolidation in the right upper, right lower, and left upper lung field (Figure 1A). Titers of atypical pneumonia pathogens such as *Mycoplasma*, *Legionella pneumophila* and *Chlamydia trachomatis* were within normal range. Acid-fast staining of sputum was also negative. We sent the patient's blood sample to the Institute of Infectious Diseases and Vaccinology of the National Health Research Institutes (NHRI) in Taiwan; the gene sequencing results identified the presence of the PVL gene, and typing of CA-MRSA identified the SC-Cmec type V strain (Figure 2). Linezolid was prescribed for 1 day on April 30, 2013. After antibiotics review by an infectious diseases specialist, vancomycin and clindamycin were both prescribed beginning May 1, 2013. The patient's clinical condition gradually improved and the follow-up sputum and blood culture were negative. However, a subsequent chest radiograph on May 3, 2013 showed multiple cavities in the infiltrating patches (Figure 1B). A chest CT was arranged which revealed multiple pneumatoceles (Figure 3). He was discharged in stable condition on May 8, 2013 and continued to receive oral linezolid for 1 week after discharge. No other antibiotic was prescribed. Follow-up chest radiograph on May 20, 2013 showed resolution of the pneumonic patches

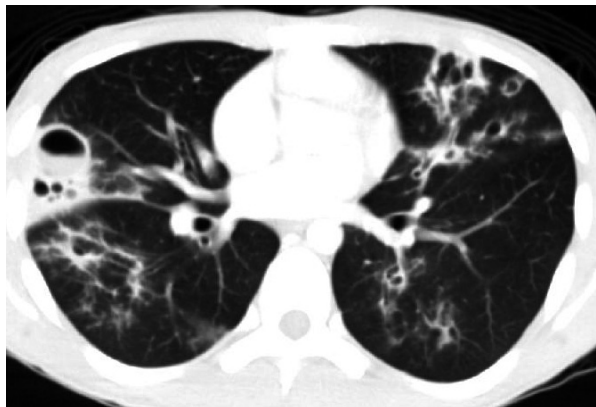


Fig. 3. Chest CT on May 6, 2013 shows multiple thin-walled, air-filled cysts, suggesting pneumatocoeles.



Fig. 4. Chest radiography on May 20, 2013 shows resolution of the pneumonic patches.

and pneumatocoeles (Figure 4).

Discussion

We reported the case of a young adult who

suffered from pneumonia and bacteremia caused by a CA-MRSA strain that was confirmed to be SCCmec type V with a positive PVL gene. The patient had received vancomycin from April 25 to April 30, 2013 for pneumonia. However, due to progression of symptoms, he was transferred to our ICU on April 30. After receiving a combination of vancomycin and clindamycin, the patient gradually improved. The initial chest radiographs showed multilobar alveolar infiltrates; CT showed multiple pneumatocoeles, suggesting necrotizing pneumonia. Symptoms and radiographic consolidations resolved after the patient had completed the treatment course.

MRSA has been considered a healthcare-associated pathogen since the 1960s, due to its close relationship with healthcare risk factors such as the presence of an invasive device at admission, history of MRSA infection or colonization, history of surgery or hospitalization, dialysis, and residence in a long-term care facility for over 12 months before the infection. However, since the 1990s, MRSA has also been found to cause infection in patients without risk factors for nosocomial MRSA infection, and has been known as CA-MRSA [1,5]. These strains of MRSA are responsible for infections in previously healthy individuals, and may lead to skin and soft tissue infection, necrotizing pneumonia, and even severe sepsis with high mortality in young adults [6,8-9]. Due to its high respiratory failure and mortality rate, it is important to consider and diagnose CA-MRSA as early as possible so that patients can receive timely treatment [6].

The most common findings on chest radiograph were multi-lobar infiltrations with/without cavitation formation [1,8-9]. In our case, the chest radiograph and chest CT scan revealed several thin-walled cysts compatible

with pneumatoceles. Pneumatocele formation usually occurs in the presence of pathogens, including *Staphylococcus aureus*, *Streptococcus pneumoniae*, *Haemophilus influenzae*, *Escherichia coli*, *Serratia marcescens*, *Klebsiella pneumoniae* and *Mycobacterium tuberculosis* [10-14]. *Staphylococcus aureus* is the most common pathogenic cause of acute pneumonia leading to pneumatoceles [10-11,13,15-16]. In most circumstances, pneumatoceles are asymptomatic, requiring only effective antibiotics to treat the underlying pneumonia [10-11]. The natural course of a pneumatocele is characterized by slow resolution. Adequate treatment requires close observation and follow-up in the early stage of the infection until resolution of the pneumatocele is achieved [10-11]. Invasive approaches should be reserved for patients who develop complications, such as tension pneumatocele, bronchopleural fistula, or an infected pneumatocele [10-11,15].

In our case, the CA-MRSA strain was characterized by identification of genes for SCCmec type V and PVL. Most strains of CA-MRSA carry the SCCmec type IV and type V genes [6-9,17-23], whereas most nosocomial MRSA strains carry SCCmec types I, II, and III [6-9,19,23]. PVL has been identified frequently in CA-MRSA, but rarely in nosocomial strains [8]. The production of PVL, a powerful cytolytic toxin that destroys bacterium-engulfing innate immune cells, has been reported to be associated with severity of pneumonia in some studies [19]. Pneumonia caused by the CA-MRSA strain, which harbors the PVL gene, is characterized by high fever, hemoptysis, sepsis, respiratory failure, and high mortality [6-8,21]. However, PVL may not be the only toxin contributing to the clinical toxicity [7].

Vancomycin was previously recommended

as the first choice of antibiotics for CA-MRSA pneumonia and bacteremia [1,6,19]. However, vancomycin has many limitations in the treatment of MRSA infection, such as a narrow therapeutic index, nephrotoxic potential at high doses, a gradual increase of minimum inhibitory concentrations (MICs), and slow bactericidal activity and clinical response [1,4,6,9,21]. In addition, vancomycin does not have the ability to stop the production of PVL [6]. Therefore, clindamycin, which exhibits good tissue penetration in abscesses and in the lung parenchyma, should be combined with vancomycin to inhibit PVL toxin synthesis [8,21]. Linezolid has been reported to inhibit the production of PVL cytotoxin [6,21,24]. However, the optimal treatment for CA-MRSA pneumonia has not been established. In this case, due to progression of symptoms after receiving several kinds of antibiotics, including vancomycin, in a previous hospital admission, he was transferred to our ICU. With maintenance of vancomycin, combined with clindamycin, the patient gradually recovered. This suggests that combining bactericidal and toxin-inhibiting agents is a better treatment strategy for pneumonia and bacteremia due to a CA-MRSA strain that carries the PVL toxin.

In conclusion, CA-MRSA pneumonia should be suspected in previously healthy individuals with a rapidly progressive course with severe pneumonia and sepsis. Pulmonary pneumatoceles may develop and require interventions in case of complications. Aggressive treatment with effective antibiotics can improve outcomes.

References

1. Karampela I, Poulakou G, Dimopoulos G. Community acquired methicillin resistant *Staphylococcus aureus*

- pneumonia: an update for the emergency and intensive care physician. *Minerva Anestesiol* 2012; 78(8): 930-40.
2. Vardakas KZ, Matthaiou DK, Falagas ME. Comparison of community-acquired pneumonia due to methicillin-resistant and methicillin-susceptible *Staphylococcus aureus* producing the Panton-Valentine leukocidin. *Int J Tuberc Lung Dis* 2009; 13(12): 1476-85.
 3. Millar BC, Loughrey A, Elborn JS, *et al.* Proposed definitions of community-associated methicillin-resistant *Staphylococcus aureus* (CA-MRSA). *J Hosp Infect* 2007; 67(2): 109-13.
 4. Defres S, Marwick C, Nathwani D. MRSA as a cause of lung infection including airway infection, community-acquired pneumonia and hospital-acquired pneumonia. *Eur Respir J* 2009; 34(6): 1470-6.
 5. Nathwani D, Morgan M, Masterton RG, *et al.* Guidelines for UK practice for the diagnosis and management of methicillin-resistant *Staphylococcus aureus* (MRSA) infections presenting in the community. *J Antimicrob Chemother* 2008; 61(5): 976-94.
 6. Shilo N, Quach C. Pulmonary infections and community associated methicillin resistant *Staphylococcus aureus*: a dangerous mix? *Paediatr Respir Rev* 2011; 12(3): 182-9.
 7. DeLeo FR, Otto M, Kreiswirth BN, *et al.* Community-associated methicillin-resistant *Staphylococcus aureus*. *Lancet* 2010; 375(9725): 1557-68.
 8. Hidron AI, Low CE, Honig EG, *et al.* Emergence of community-acquired methicillin-resistant *Staphylococcus aureus* strain USA300 as a cause of necrotizing community-onset pneumonia. *Lancet Infect Dis* 2009; 9(6): 384-92.
 9. Rubinstein E, Kollef MH, Nathwani D. Pneumonia caused by methicillin-resistant *Staphylococcus aureus*. *Clin Infect Dis* 2008; 46 Suppl 5: S378-85.
 10. Kim SH, Chung YT, Lee KD, *et al.* Infected pneumatocele following anaerobic pneumonia in adult. *Korean J Intern Med* 2005; 20(4): 343-5.
 11. McGarry T, Giosa R, Rohman M, *et al.* Pneumatocele formation in adult pneumonia. *Chest* 1987; 92(4): 717-20.
 12. Nandwani S, Pande A, Saluja M. A case of *Staphylococcus toxic shock syndrome* presenting with multiple pneumatoceles in the chest. *Indian J Chest Dis Allied Sci* 2013; 55(1): 45-7.
 13. Imamoglu M, Cay A, Kosucu P, *et al.* Pneumatoceles in postpneumonic empyema: an algorithmic approach. *J Pediatr Surg* 2005; 40(7): 1111-7.
 14. Liao WH, Lin SH, Wu TT. Pneumatocele formation in adult pulmonary tuberculosis during antituberculous chemotherapy: a case report. *Cases J* 2009; 2: 8570.
 15. Hunt JP, Buechter KJ, Fakhry SM. *Acinetobacter calcoaceticus* pneumonia and the formation of pneumatoceles. *J Trauma* 2000; 48(5): 964-70.
 16. Colling J, Allaouchiche B, Floccard B, *et al.* Pneumatocele formation in adult *Escherichia coli* pneumonia revealed by pneumothorax. *J Infect* 2005; 51(3): e109-11.
 17. Nakou A, Woodhead M, Torres A. MRSA as a cause of community-acquired pneumonia. *Eur Respir J* 2009; 34(5): 1013-4.
 18. Tacconelli E, De Angelis G. Pneumonia due to methicillin-resistant *Staphylococcus aureus*: clinical features, diagnosis and management. *Curr Opin Pulm Med* 2009; 15(3): 218-22.
 19. Gould IM, David MZ, Esposito S, *et al.* New insights into methicillin-resistant *Staphylococcus aureus* (MRSA) pathogenesis, treatment and resistance. *Int J Antimicrob Agents* 2012; 39(2): 96-104.
 20. Boyle-Vavra S, Ereshefsky B, Wang CC, *et al.* Successful multiresistant community-associated methicillin-resistant *Staphylococcus aureus* lineage from Taipei, Taiwan, that carries either the novel *Staphylococcal* chromosome cassette *mec* (SCCmec) type VT or SCCmec type IV. *J Clin Microbiol* 2005; 43(9): 4719-30.
 21. Lobo LJ, Reed KD, Wunderink RG. Expanded clinical presentation of community-acquired methicillin-resistant *Staphylococcus aureus* pneumonia. *Chest* 2010; 138(1): 130-6.
 22. Mandell LA, Wunderink R. Methicillin-resistant *Staphylococcus aureus* and community-acquired pneumonia: an evolving relationship. *Clin Infect Dis* 2012; 54(8): 1134-6.
 23. Vardakas KZ, Matthaiou DK, Falagas ME. Incidence, characteristics and outcomes of patients with severe community acquired-MRSA pneumonia. *Eur Respir J* 2009; 34(5): 1148-58.
 24. Soavi L, Signorini L, Stellini R, *et al.* Linezolid and clindamycin improve the outcome of severe, necrotizing pneumonia due to community-acquired methicillin-resistant *Staphylococcus aureus* (CA-MRSA). *Infez Med* 2011; 19(1): 42-4.

有 PVL 毒素之社區型 methicillin 抗藥性金黃色葡萄球菌在健康成年人引起的肺炎與菌血症病例報告

郭家維 郭書辰* 許正園 傅彬貴**

社區型抗藥性金黃色葡萄球菌 (CA-MRSA) 感染所致的社區型肺炎與院內感染型肺炎最大的不同處在於，前者多半感染於過去健康狀態良好的宿主，而且金黃色葡萄球菌上帶有 Pantan-Valentine leukocidin (PVL) 的毒素。被帶有 PVL 毒素的抗藥性金黃色葡萄球菌感染的社區型肺炎，常見的表現為高燒、敗血症及呼吸衰竭，因此有較高的死亡率。本病例報告在闡述一位台灣健康年輕男性得到抗藥性金黃色葡萄球菌導致的社區型肺炎和菌血症，經檢查分析發現此 CA-MRSA 菌株為 staphylococcal cassette chromosome *mec* (*Sccmec*) type V 菌株並帶有 PVL 基因，且在影像學方面表現出多葉性肺炎而後進展成 pneumatoceles。在經過完整的抗生素包括 vancomycin 及 clindamycin 治療後，患者的症狀以及影像學上的病灶便消失。(胸腔醫學 2015; 30: 217-223)

關鍵詞：社區型抗藥性金黃色葡萄球菌，Pantan-Valentine leukocidin (PVL)，肺炎，Pneumatocele

Proper Diagnostic Differentiation of Atypical Adenomatous Hyperplasia and Pulmonary Adenocarcinoma

Kevin S. Lai*, Sey-En Lin**, Ming-Syong Zeng*, Kai-Ling Lee*,
Shih-Hsin Hsiao*, Chi-Li Chung*,***

Atypical adenomatous hyperplasia (AAH) is a precursor of lung adenocarcinoma. Pure AAH lesions often manifest as ground glass opacities on computed tomography (CT) scans, and are usually less than 5 mm in diameter. The histological diagnosis of AAH is often made with small biopsies, which raises doubts about the true nature of the whole lung lesion. We reported 4 patients presenting with a solitary pulmonary nodule greater than 5 mm in diameter and with an initial diagnosis of AAH based on CT-guided lung biopsies. Three of the patients who later received surgical resection or lung re-biopsy were ultimately diagnosed as having pulmonary adenocarcinoma. Further gene analyses revealed that all 3 patients with adenocarcinoma harbored epidermal growth factor receptor (*EGFR*) mutations. Differentiation between AAH and adenocarcinoma is clinically important, particularly with small biopsy specimens or when radiological images highlight the possibility of a more advanced disease status. (*Thorac Med* 2015; 30: 224-231)

Key words: atypical adenomatous hyperplasia, pulmonary adenocarcinoma epidermal growth factor receptor

Introduction

Atypical adenomatous hyperplasia (AAH) is defined as atypical bronchioloalveolar cuboidal or columnar cells that proliferate along the alveolar walls [1-2], and is considered to be a precursor of adenocarcinoma. AAH typically appears as solitary or multifocal small ground glass opacities (GGOs) on computed tomography (CT) scans and is usually less than 5 mm

in diameter [3]. In an attempt to understand the multistep process of tumorigenesis of adenocarcinoma, various studies have described the frequencies of AAH in adenocarcinoma [4-5], while others have investigated the presence of epidermal growth factor receptor (EGFR) gene mutations in AAH [7-8].

We reviewed the results of consecutive patients that underwent CT-guided core biopsy for lung lesions between January 2006 and Decem-

*Division of Pulmonary Medicine, Department of Internal Medicine; **Department of Pathology, Taipei Medical University Hospital, Taipei, Taiwan; ***School of Respiratory Therapy, College of Medicine, Taipei Medical University, Taipei, Taiwan

Address reprint requests to: Dr. Shih-Hsin Hsiao, Division of Pulmonary Medicine, Department of Internal Medicine, Taipei Medical University Hospital, No. 252, Wu-Hsing Street, Taipei 11031, Taiwan

Table 1. Clinical Characteristics of 4 Patients with Initial Diagnosis of AAH

Case	Sex	Age (Years)	Smoking	Location	Lesion size on chest CT (mm)
1	M	37	yes	RLL	88
2	M	72	yes	RLL	18
3	F	71	no	RUL	17
4	F	78	no	RML	9

Abbreviations: AAH = atypical adenomatous hyperplasia; CT = computed tomography; M = male; F = female; RLL = right lower lobe, RUL = right upper lobe, RML = right middle lobe.

Table 2. Pathological Results of 4 Patients with Initial Diagnosis of AAH Based on Small Biopsy Specimens

Case	Initial diagnosis	Final diagnosis	TNM	Stage	EGFR mutation
1	AAH	Adenocarcinoma	pT4N2M0	IIIB	exon 21 (L858R)
2	AAH	Adenocarcinoma	cT1aN3M0	IIIB	exon 19 deletion
3	AAH	Adenocarcinoma	pT4N1M1a	IV	exon 19 deletion
4	AAH	*	-	-	-

AAH: atypical adenomatous hyperplasia, EGFR: epidermal growth factor receptor

*Patient hesitant to accept other interventions; however, no significant change in lesion size was noted on serial chest radiographs for 18 months.

ber 2011 and found that 4 (1.2%) out of 321 CT-guided lung biopsies revealed AAH. The lesion size ranged from 9 to 88 mm in diameter (Table 1). Three out of these 4 cases were eventually proved to be invasive adenocarcinoma. EGFR gene testing demonstrated that all 3 patients with adenocarcinoma harbored EGFR mutations, including exon 19 in 1 patient and exon 21 in 2 others (Table 2).

Case Report

Case 1

A 37-year-old male smoker presented with intermittent dyspnea for 1 year, and productive cough for 1 month. The chest CT (Figure 1A) revealed a lobar consolidation with heterogeneous density in the right lower lobe (RLL). The CT-guided lung biopsy showed focal areas of atypical epithelial cell proliferation along the alveolar wall with fibrous thickening. The atypical cells revealed hyperchromatic nuclei

without conspicuous coarse chromatin, nucleoli or increased mitoses, which was suggestive of AAH (Figure 1B). Subsequent surgical intervention proved this to be lung adenocarcinoma (Figure 1C), pathological stage IIIB (pT4N2M0).

Case 2

A 72-year-old male smoker was admitted for spinal vertebral compression surgery in January 2011 and was referred for the incidental findings on his thoracic imaging. An irregular nodule measuring up to 18 mm in diameter (Figure 1D) was localized in the RLL on the chest CT, along with the presence of mediastinal lymphadenopathy. CT-guided core biopsy of the RLL nodule provided the diagnosis of AAH (Figure 1E). The patient declined the surgical intervention we suggested. Progressive enlargement of mediastinal lymphadenopathy was detected on a chest CT taken 8 months later, although with no increase in the size of the

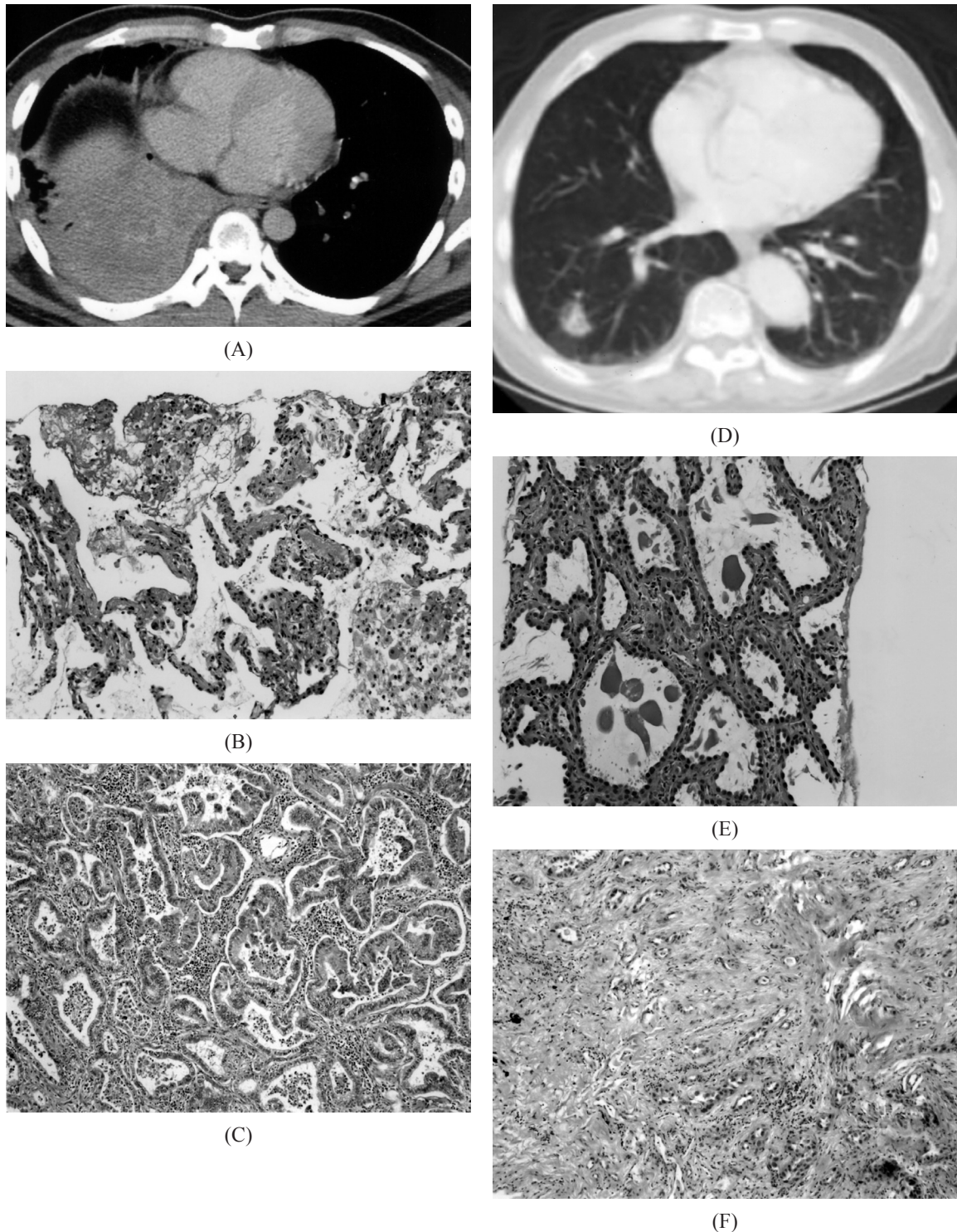


Fig. 1. Case 1: (A) Chest CT showed a lobar consolidation with heterogeneous densities in the right lower lobe. (B) CT-guided biopsy revealed atypical adenomatous hyperplasia (AAH) along the alveolar walls (H&E, 100X). (C) Excisional biopsy demonstrated primary pulmonary adenocarcinoma (H&E, 100X). Case 2: (D) Chest CT showed a part-solid ground glass nodule in the right lower lobe. (E) CT-guided biopsy revealed AAH (H&E, 100X) and (F) Re-biopsy of the nodule confirmed the diagnosis of a primary well-differentiated adenocarcinoma (H&E, 100X).

lung nodule. Re-biopsy of the nodule confirmed the diagnosis of a primary well-differentiated adenocarcinoma, acinar type (Figure 1F). The clinical staging was cT1aN3M0, stage IIIB.

Case 3

A 71-year-old non-smoking female underwent a partial mastectomy with axillary lymph node dissection and radiotherapy for her right breast cancer in 2002. She was regularly followed uneventfully until 2009, when an ill-defined density was identified at the right upper lung (RUL) on the chest radiograph, and was later confirmed in the chest CT to be a 17 mm nodule (Figure 2A). The CT-guided core biopsy of the lesion revealed AAH with relatively uniform proliferation of low columnar epithelial cells lining the alveolar walls with no obvious cytological atypia (Figure 2B). The patient declined further interventions until 2011, when she agreed to re-biopsy of the enlarging lung nodule, which revealed neoplastic cells arranged in an irregular glandular pattern infiltrating the desmoplastic stroma (Figure 2C). The patient underwent a wedge resection of the RUL. Hers was a case of primary lung adenocarcinoma with pleural seeding, pT4N1M1a, stage IV.

Case 4

A 78-year-old non-smoking female had a chest radiograph taken in September 2010 that revealed a right lung lesion. The chest CT identified a 9 mm lung nodule in the right middle lobe (Figure 2D). CT-guided biopsy of this lesion disclosed AAH (Figure 2E). The patient hesitated to accept further surgical intervention. She received serial chest radiographs for 18 months, and no significant growth of the lesion was seen.

Discussion

We reported 4 patients with a solitary pulmonary nodule greater than 5 mm in diameter that was initially diagnosed as AAH by small biopsies. Three of the 4 patients that underwent further interventions were ultimately proved to have lung adenocarcinoma with EGFR mutations. It is widely accepted that AAH is a precancerous lesion that develops into lung adenocarcinoma. For example, a clinicopathological study by Nakahara *et al.* reported an AAH incidence up to 23.2% in 508 surgically resected cases of lung cancer [4]. Moreover, Chapman *et al.*, found AAH lesions in about 30% of lung adenocarcinoma patients [5]. AAH may exist as a single or multiple lesions; the latter is associated with a high frequency of lung adenocarcinoma or with an increased risk of developing into metachronous lung cancer [4]. In line with the results of the previous study [4], AAH was found to exist concomitantly with primary adenocarcinoma in our case 1. However, we cannot determine that adenocarcinoma was initially present in cases 2 and 3, or whether these AAH lesions served as precursors and subsequently progressed to malignancy. Nevertheless, our cases highlight the postulated multistep progression of carcinogenesis through AAH to adenocarcinoma. Our series demonstrated the importance of careful interpretation of histological diagnoses of AAH based on small biopsy samples, particularly when radiological findings depict lung lesion(s) greater than 5 mm and the presence of solid components within the GGOs on chest CT.

Given the known relationship between EGFR mutation and a subset of adenocarcinoma, residual tumor specimens from surgery were submitted for EGFR mutational testing.

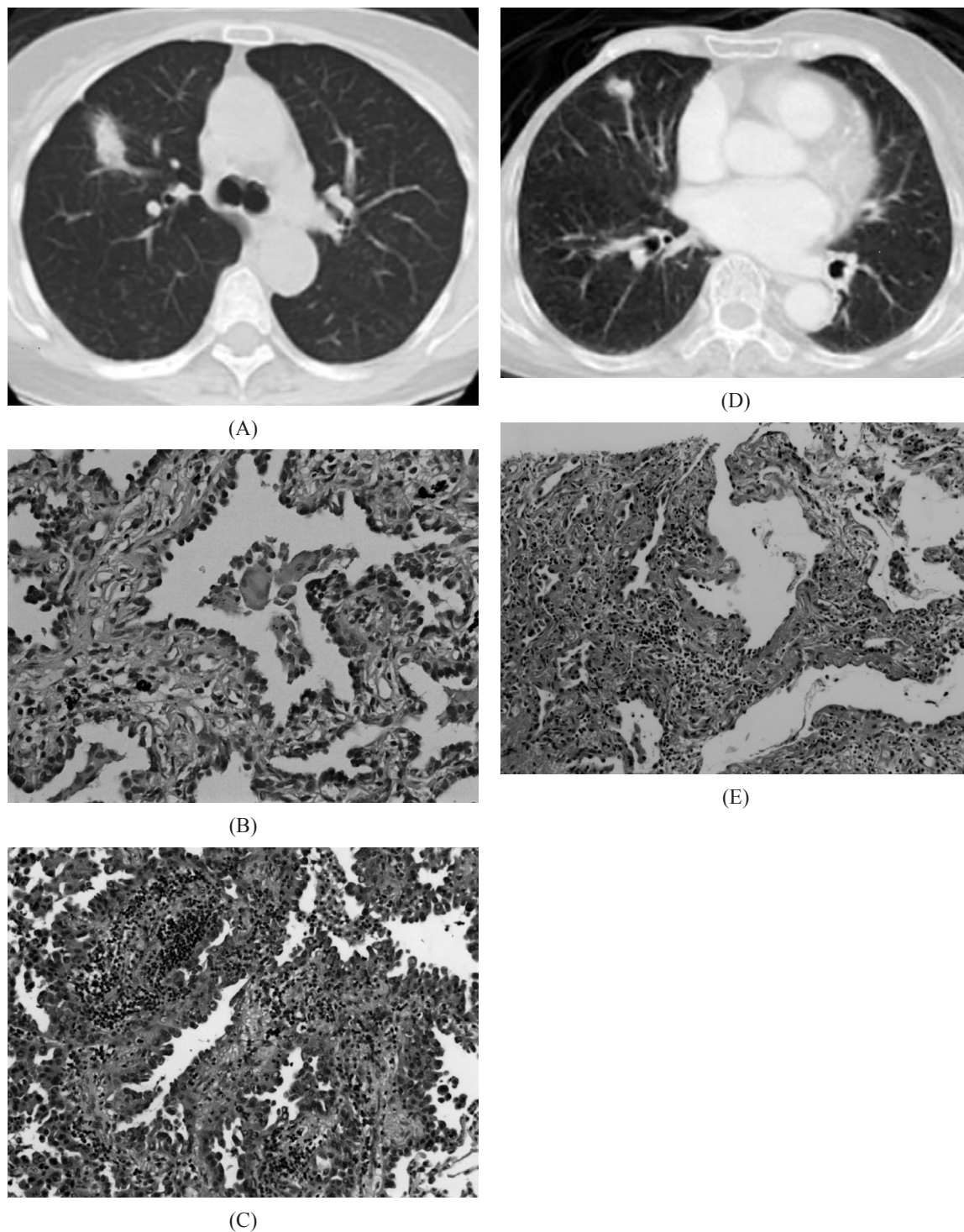


Fig. 2. Case 3: (A) Chest CT showed a lung nodule with a spiculated margin in the right upper lobe. (B) CT-guided biopsy revealed atypical adenomatous hyperplasia (AAH) (H&E, 200X). (C) Re-biopsy of the lung nodule revealed primary pulmonary adenocarcinoma (H&E, 100X). Case 4: (D) The chest CT showed a round nodule in the right lower lobe (H&E, 100X). (E) CT-guided biopsy revealed AAH.

All 3 cases of adenocarcinoma had EGFR gene mutations. Case 1 had an exon 21 point mutation, and cases 2 and 3, an exon 19 deletion (Table 2). EGFR mutation was not initially assessed in the AAH lesions of our cases due to the small biopsy specimens. It would be interesting to see if these genetic alterations were detectable in the AAH specimens, since they might possibly act as driver oncogenes.

McIntire *et al.* examined gene dysregulation and found an increase in EGFR copy number in AAH, similar to that of bronchioloalveolar carcinoma (BAC) (now referred to as adenocarcinoma in situ), but less than that of adenocarcinoma [6]. This evidence of EGFR amplification in AAH represents an early morphological distinction between normal epithelium and potential pre-invasive cells. In fact, EGFR mutations in AAH have been reported previously. Sakuma *et al.* detected EGFR mutations in up to 32% of 54 AAH cases [7], whereas Yoshida *et al.*, reported only a 3% prevalence of EGFR mutations in AAH [8]. The discrepancies might be due to the different detection methods used. In another study of primary lung cancer associated with AAH foci, Sartori and colleagues detected identical EGFR mutations among AAH foci and concomitant adenocarcinoma in 3 out of 4 cases. These findings may support the key role of EGFR mutation in initiating carcinogenesis and that AAH is a precursor lesion of lung adenocarcinoma [9].

Clinical management for AAH is yet to be determined [4]. Based on previous studies [6-9] and our own observations, we proposed that EGFR mutation testing in biopsied AAH foci may have clinical implications. Although negative testing does not rule out the potential of malignancy in AAH, positive testing may indicate (1) a high likelihood of progression to ade-

nocarcinoma; (2) that the biopsied lesion might be in the proximity of the malignancy and unlikely a pure AAH lesion; and (3) that further surgical resection is mandatory for diagnosis of the whole lesion.

Conclusion

These cases are a reminder to clinicians that tissue strips from small lung biopsies could represent either the true nature of the lesion or a focus peripheral to an undetected malignancy, such as adenocarcinoma. We suggest patients with a diagnosis of AAH based on small samples need further interventions to reach a conclusive diagnosis. Our cases also support the possibility of an AAH-adenocarcinoma sequence in the development of lung cancer and that EGFR mutation testing may provide an alternative perspective on the realm of a biopsied AAH lesion.

References

1. Travis WD, Brambilla E, Nogouchi M, *et al.* International Association for the Study of Lung Cancer/American Thoracic Society/European Respiratory Society international multidisciplinary classification of lung adenocarcinoma. *J Thorac Oncol* 2011; 6: 244-85.
2. Kerr K. Morphology and genetics of pre-invasive pulmonary disease. *Curr Diagn Pathol* 2004; 10: 259-68.
3. Park C, Goo J, Lee H, *et al.* CT findings of atypical adenomatous hyperplasia in the lung. *Korean J Radiol* 2006; 7: 80-6.
4. Nakahara R, Yokose T, Nagai K, *et al.* Atypical adenomatous hyperplasia of the lung: a clinicopathological study of 118 cases including cases with multiple atypical adenomatous hyperplasia. *Thorax* 2001; 56: 302-5.
5. Chapman A, Kerr K. The association between atypical adenomatous hyperplasia and primary lung cancer. *Br J Cancer* 2000; 83: 632-6.
6. McIntire M, Santagata S, Ligon K, *et al.* Epidermal gro-

- wth factor receptor gene amplification in atypical adenomatous hyperplasia of the lung. *Am J Transl Res* 2010; 2(3): 309-15.
7. Sakuma Y, Matsukuma S, Yoshihara M, *et al.* Distinctive evaluation of non-mucinous and mucinous subtypes of bronchioloalveolar carcinomas in EGFR and K-ras gene-mutation analyses for Japanese lung adenocarcinomas: confirmation of the correlations with histological subtypes and gene mutations. *Am J Clin Pathol* 2008; 128: 100-8.
8. Yoshida Y, Shibata T, Kokubu A, *et al.* K-ras oncogene activation in atypical alveolar hyperplasia and bronchioloalveolar carcinoma of the lung. *Lung Cancer* 2005; 50: 1-8.
9. Sartori G, Cavazza A, Bertolini F, *et al.* A subset of lung adenocarcinoma and atypical adenomatous hyperplasia-associated foci are genotypically related. *Am J Clin Pathol* 2008; 129: 202-10.

異形腺瘤性增生與肺腺癌的迷思

黎書亮* 林賜恩** 曾明雄* 李凱靈* 蕭世欣* 鍾啟禮*,***

異形腺瘤性增生 (atypical adenomatous hyperplasia, 簡稱 AAH) 為肺腺癌的癌前病變。真正的 AAH 在電腦斷層影像中多呈現小於 5 mm 的毛玻璃狀病灶。如使用小的肺切片檢體診斷出 AAH 時, 需懷疑是否代表肺病灶的全部性質。我們提出 4 個病例, 其肺結節皆大於 5 mm, 經電腦斷層導引切片初步診斷為 AAH, 其中 3 個個案接受手術切除, 最終診斷為具有表皮細胞生長因子接受器 (epidermal growth factor receptor) 基因突變的肺腺癌。在只有小切片檢體可供病理診斷或影像高度懷疑為肺惡性腫瘤時, 仔細鑑別 AAH 或肺腺癌是非常重要的。(胸腔醫學 2015; 30: 224-231)

關鍵詞: 異形腺瘤性增生, 肺腺癌, 表皮細胞生長因子接受器

* 台北醫學大學附設醫院 內科部 胸腔內科, ** 台北醫學大學附設醫院 病理科

*** 台北醫學大學醫學院 呼吸治療學系

索取抽印本請聯絡: 蕭世欣醫師, 台北醫學大學附設醫院 內科部 胸腔內科, 台北市信義區吳興街 252 號

Chest Wall Extramedullary Plasmacytoma with Myelomatous Pleural Effusion

Kuo-Liang Huang*, **, Wen-Lin Su**, ***, Shao-Ting Chou*, Chih-kung Lin****, Wann-Cherng Perng**

Plasmacytoma primarily involves the bone marrow, but can also be present in many other organs. Pleural effusion in patients with multiple myeloma is not common, and has many etiologies, including congestive heart failure, nephrotic syndrome, infection, chronic renal failure, pulmonary embolism, and even secondary malignancy. Myelomatous pleural effusions in patients with extramedullary plasmacytoma are extremely rare. We presented a case of extramedullary plasmacytoma of the chest wall presenting with myelomatous pleural effusion. The myelomatous pleural effusion was diagnosed by cytology of the pleural effusion and pleural biopsy. (*Thorac Med* 2015; 30: 232-238)

Key words: extramedullary plasmacytoma, myelomatous pleural effusion, chest wall

Introduction

Plasmacytoma presents as the over-proliferation of a single clone of plasma cells, producing a monoclonal immunoglobulin. These abnormal plasma cells are usually present in the bone marrow and often lead to skeletal destruction with osteolytic lesion, osteopenia, and even pathologic fracture. Approximately 7% of patients with multiple myeloma present with extramedullary plasmacytoma [1], and another 6% of patients will develop extramedullary plas-

macytoma later in the course of multiple myeloma [2]. Approximately 80% of patients with extramedullary plasmacytoma have upper respiratory tract involvement, producing epistaxis, nasal discharge, or nasal obstruction [3-4]. Other sites, including the gastrointestinal tract [5], liver [6], lymph nodes [7], testes [8], skin, and central nervous system, are less commonly involved [9]. Primary plasmacytoma of the lung often presents as a pulmonary nodule or hilar mass with or without hemoptysis [10]. Pleural effusion of any etiology may present in 6% of

*Division of Pulmonary and Critical Care Medicine, Department of Internal Medicine, Kaohsiung Armed Forces General Hospital, Kaohsiung, Taiwan, ROC; **Division of Pulmonary and Critical Care Medicine, Department of Internal Medicine, Tri-Service General Hospital, National Defense Medical Center, Taipei, Taiwan; ***Division of Pulmonary and Critical Care Medicine, Department of Internal Medicine, Taipei Tzu Chi Hospital, Buddhist Tzu Chi Medical Foundation; ****Department of Pathology, Tri-Service General Hospital and National Defense Medical Center, Taipei, Taiwan

Address reprint requests to: Dr. Wen-Lin Su, Division of Pulmonary and Critical Care Medicine, Department of Internal Medicine, Taipei Tzu Chi Hospital, Buddhist Tzu Chi Medical Foundation, No. 289, Jianguo Rd., Xindian Dist., New Taipei City 23142, Taiwan, Republic of China

patients with myeloma during the course of the disease [11]. However, myelomatous pleural effusion (MPE) is rarely reported. Here, we present a rare case of extramedullary plasmacytoma of the chest wall with pleural involvement, and massive MPE. We used the immunohistochemical stain method to reach a definite diagnosis of MPE.

Case Report

A 61-year-old male had a history of hypertension with regular medical control for more than 20 years, but otherwise, there was nothing of particular note in his personal or family history. He was sent to our hospital due to progressive shortness of breath for 2 weeks. When he arrived, his vital signs were blood pressure: 143/81 mmHg, heart rate: 120/min, respiratory rate: 25/min, body temperature: 36.6°C, and oxygen saturation: 90%. Physical examination showed decreased breathing sounds with dullness on percussion at the right basal part of the lung. Chest X-ray (CXR) showed massive pleural effusion at the right chest (Figure 1). There was no punched out lesion of bone in the series images, including skull films. Due to acute hypoxemic respiratory failure, the patient received immediate bi-level positive airway pressure (BiPAP) ventilator support. A complete blood count (CBC) revealed a white blood cell (WBC) count of 11780/uL (69.3% neutrophils, 18.8% lymphocytes, 7.3% monocytes, 4.2% eosinophils and 0.4% basophils), hemoglobin of 6.4 g/dL, and a platelet count of 2.7×10^5 /uL. Blood biochemistry tests showed blood urea nitrogen (BUN) of 158 mg/dL, creatinine 8.8 mg/dL, sodium 134 mmol/L, potassium 6.1 mmol/L, aspartate aminotransferase (AST) 42U/L, alanine aminotransferase (ALT) 20U/L, lactate

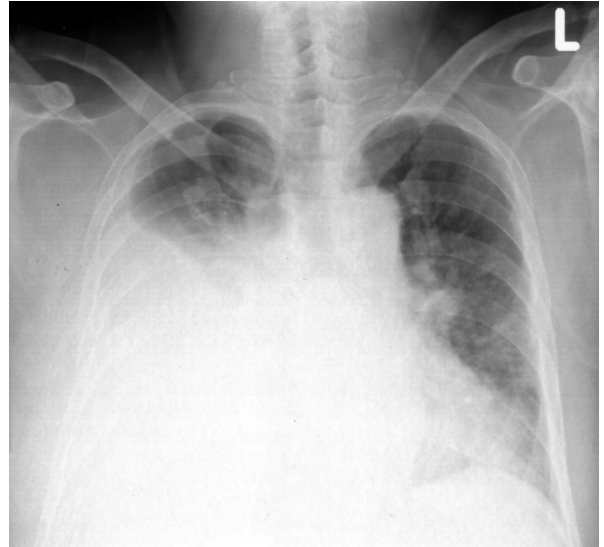


Fig. 1. A standing chest radiograph showing massive pleural effusion at the right side.

dehydrogenase (LDH) 1483 U/L, albumin 3 g/dL, total protein 5 g/dL, glucose 170 mg/dL, β_2 microglobulin 11.86×5 mg/L (1~2.4), C-reactive protein (CRP) 2.6 mg/dL, serum total calcium 9.1 mg/dL, uric acid 22.1 mg/dL, thyroid stimulating hormone (TSH) 0.55 uIU/ml, carbohydrate antigen 19-9 (CA19-9) 150 U/ml, carcinoembryonic antigen (CEA) 2.7 ng/ml, and squamous cell carcinoma antigen (SCC) of 1.7 ng/ml. Serum protein electrophoresis showed IgG 596 mg/dL (751~1560), IgM 43 mg/dL (46~304), IgA 62 mg/dL (82~453), IgD 48 IU/ml (0~90), IgE 29.2 IU/ml (0~165), kappa 1100 mg/dL (629~1350), and lambda 206 mg/dL (313~723). Electrophoresis of urine showed kappa of 743 mg/dL (0~1.85) and lambda of 9.32 mg/dL (0~5).

Acute kidney injury with hyperkalemia, a uremic state and oliguria developed, so the patient underwent hemodialysis. The following CXR showed persistent massive pleural effusion at the right part of the lung. Chest CT (Figure 2) showed pleural wall thickening at the

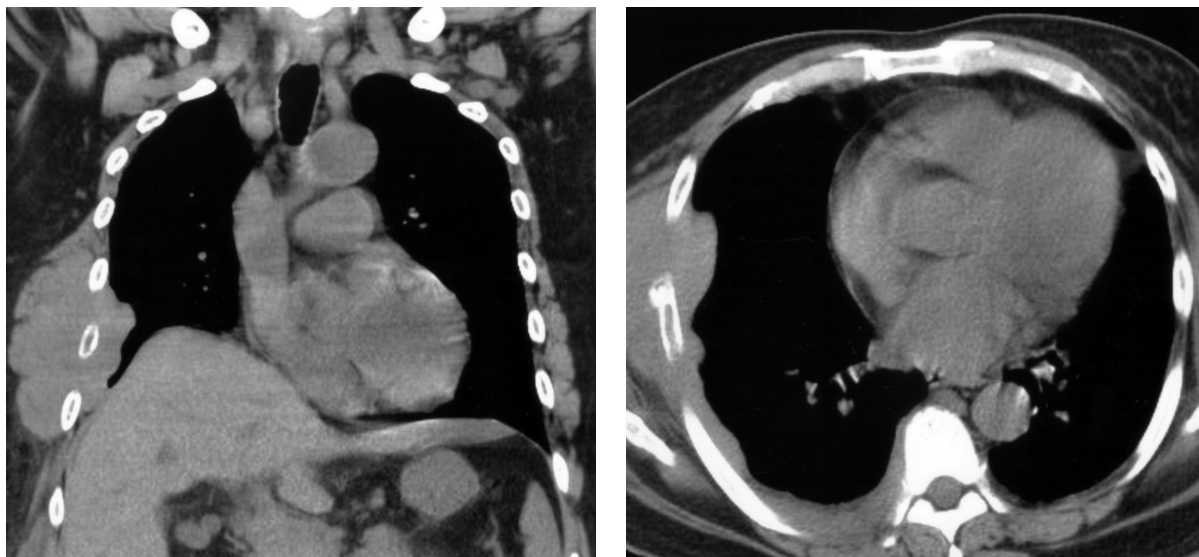


Fig. 2. Computed tomography of the chest showing pleural wall thickening at the right lower hemithorax and a focal mass with encasement of the right 6-7th ribs. No lymphadenopathy in the mediastinum, bilateral hilar region, and axillary fossas was found.

right lower hemithorax, favoring a focal mass with encasement of the right 6-7th ribs, but with no significant lymphadenopathy in the mediastinum, both hilar regions and axillary fossas. There was no evidence of pulmonary embolism. Echocardiography showed left ventricle dilation, and the ejection fraction of the left ventricle was estimated to be 76%. A thoracentesis was performed and about 1 L of pleural fluid was drained from the right side. The analysis of pleural effusion showed glucose of 89 mg/dL, total protein of 3.8 g/dL and LDH of 1435 U/L, so exudative pleural effusion was indicated. The pleural effusion contained WBC: 14700 (100% of mononuclear cells), and the Rivalta test was positive. No acid-resistant bacilli, bacteria, or fungus were detected in the pleural fluid. The cytological examination revealed many abnormal eccentric and hyperchromatic cells, so malignant pleural effusion was diagnosed. Since the immunocytochemistry stain of these cells showed positive for CD138, a plasma or mesothelial origin had to be considered. With the

confirmation of malignant pleural effusion, a pleural biopsy was done. The pathology showed a picture of discohesive, medium- to large-sized tumor cells infiltrating the muscle and fibrous tissue, with hyperchromatic nuclei and a focal plasmacytoid pattern (Figure 3). The histopathological findings and immunohistochemical stain results were compatible with plasmacytoma. After explaining the findings of plasmacytoma with malignant pleural effusion to the family, both the patient and family refused bone marrow aspiration and biopsy to confirm multiple myeloma. The patient later expired due to acute renal failure, progressive pneumonia with hypoxic respiratory failure, and septic shock.

Discussion

Plasmacytoma is a bone marrow disease, but it can present with variable clinical symptoms and signs, and can also involve different extramedullary sites. Pleural effusion can be a clinical presentation of patients with myeloma. Ac-

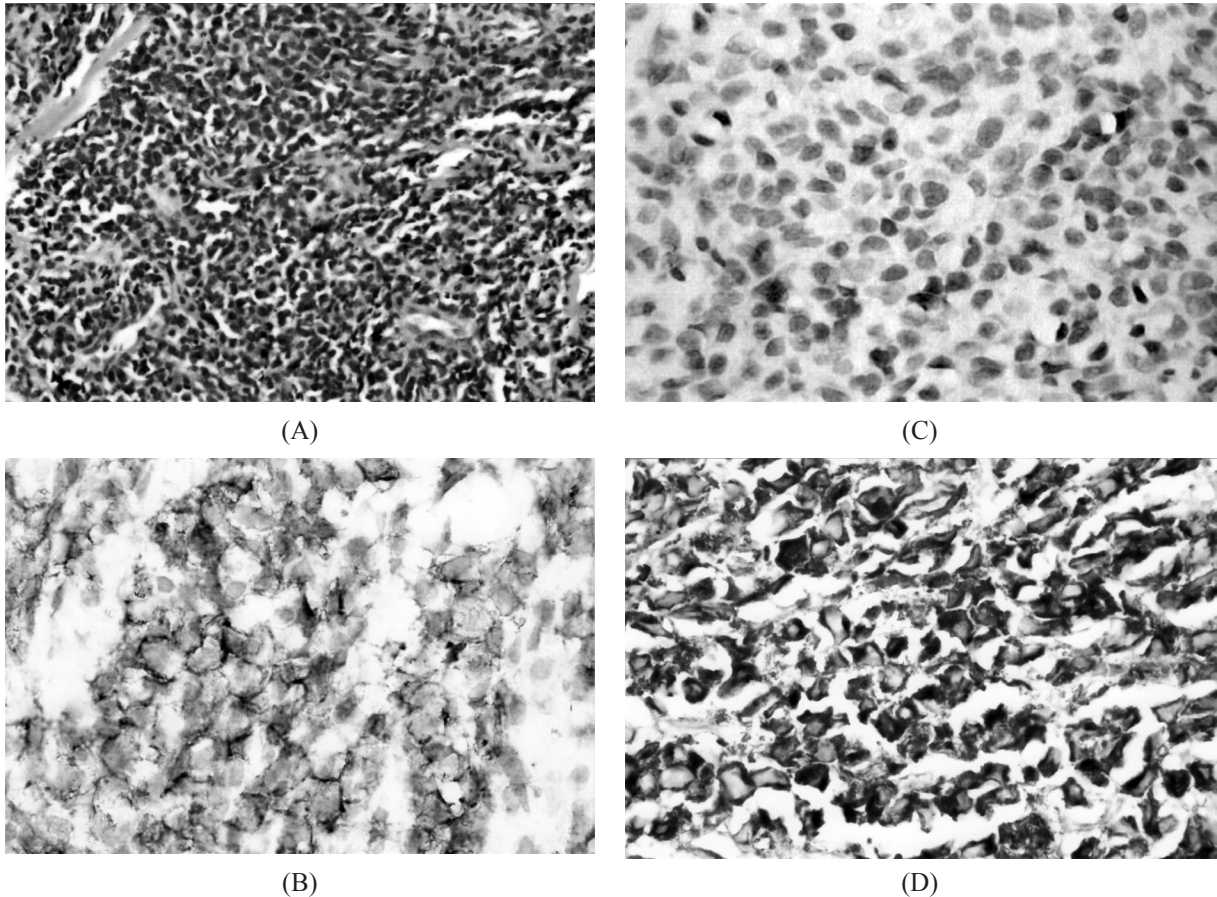


Fig. 3. (A) Discohesive medium-to-large size tumor cells infiltrating the muscle and fibrous tissue with hyperchromatic nuclei and a focal plasmacytoid pattern. (B) CD 138 stain showed positive; (C) lambda stain showed negative; (D) kappa stain showed monoclonality.

cording to a previous review, pleural effusion caused by any etiology would be present in 6% of patients with myeloma during the course of the disease [11]. However, MPE has rarely been reported. Pleural effusion in patients with myeloma is often caused by heart failure, chronic renal failure, infection, nephrotic syndrome, and even pulmonary embolism [12]. Some reports also showed secondary neoplasms were present in patients with myeloma; these patients also had malignant pleural effusion [13]. Therefore, pleural effusion in patients with myeloma requires a series of examinations, and MPE should be considered.

MPE is rare and occurs in less than 1% of patients with myeloma [14]; it was found mostly in patients with IgG myeloma, which is the most common type of myeloma [15]. Two reviews indicated that MPE has equal gender distribution, was hemorrhagic, more commonly involved the left site, and had a poor prognosis [15-16]. The pathogenesis of MPE is not well understood, but several possible mechanisms have been proposed. These include: 1. direct extension to the pleura, 2. tumor deposits on the pleura, and 3. lymphatic obstruction [11]. The diagnostic criteria of MPE include: 1. detection of atypical plasma cells in the pleural fluid;

2. demonstration of a monoclonal protein on pleural fluid electrophoresis; and 3. histological confirmation using pleural biopsy specimens or autopsy [17]. Our patient did not undergo electrophoresis of the pleural effusion, but the results of his other examinations met criteria 1 and 3, so MPE was diagnosed.

Even though diagnostic criteria have been proposed, the diagnosis of MPE is still a challenge. Malignant plasma cells have a variable morphology and a low number in pleural effusion, so a definite diagnosis may be missed. In addition, during sample processing, degeneration and change in morphology both lead to difficulties in recognition. Pleural biopsy may be helpful, but is not always diagnostic. Flow cytometry could be used to supplement the diagnosis, but it might not be diagnostic due to poor specimen quality. Abnormal cytogenetic karyotype in the pleural effusion can present unequivocal evidence to support the diagnosis, but this is a low diagnostic rate. In our reported case, the diagnosis relied mostly on abnormal plasma cells and monoclonal protein present in the pleural effusion. We used immunohistochemical staining, which offered a good method to reach a definite diagnosis of MPE.

MPE is a poor prognostic factor despite aggressive treatment. Some literature has shown that the median survival time of these patients is about 4 months. Many treatments have been proposed, including a combination of systemic chemotherapy and intra-pleural injection of adriamycin or interferon. However, the majority of these patients have had a transient response and recurrence. Further research into the development and use of novel therapies and agents is needed.

The pleural effusion in patients with multiple myeloma can be induced by a variety of

factors, some of which are treatable. A series of examinations of the pleural effusion in patients with multiple myeloma is important, especially diagnostic thoracentesis with a careful cytological examination and protein electrophoresis. Other studies, including pleural biopsy, flow cytometry, and cytogenetics, could be considered if available.

References

1. Varettoni M, Corso A, Pica G, *et al.* Incidence, presenting features and outcome of extramedullary disease in multiple myeloma: a longitudinal study on 1003 consecutive patients. *Ann Oncol* 2010; 21: 325.
2. Bladé J, Fernández de Larrea C, Rosiñol L, *et al.* Soft-tissue plasmacytomas in multiple myeloma: incidence, mechanisms of extramedullary spread, and treatment approach. *J Clin Oncol* 2011; 29: 3805.
3. Shirley MH, Sayeed S, Barnes I, *et al.* Incidence of haematological malignancies by ethnic group in England, 2001-7. *Br J Haematol* 2013; 163: 465.
4. Huang SY, Yao M, Tang JL, *et al.* Epidemiology of multiple myeloma in Taiwan: increasing incidence for the past 25 years and higher prevalence of extramedullary myeloma in patients younger than 55 years. *Cancer* 2007; 110: 896.
5. Lynch HT, Sanger WG, Pirruccello S, *et al.* Familial multiple myeloma: a family study and review of the literature. *J Natl Cancer Inst* 2001; 93: 1479.
6. Lynch HT, Watson P, Tarantolo S, *et al.* Phenotypic heterogeneity in multiple myeloma families. *J Clin Oncol* 2005; 23: 685.
7. Lynch HT, Ferrara K, Barlogie B, *et al.* Familial myeloma. *N Engl J Med* 2008; 359: 152.
8. Jain M, Ascensao J, Schechter GP. Familial myeloma and monoclonal gammopathy: a report of eight African American families. *Am J Hematol* 2009; 84: 34.
9. Landgren O, Kristinsson SY, Goldin LR, *et al.* Risk of plasma cell and lymphoproliferative disorders among 14621 first-degree relatives of 4458 patients with monoclonal gammopathy of undetermined significance in Sweden. *Blood* 2009; 114: 791.
10. Vachon CM, Kyle RA, Therneau TM, *et al.* Increased risk

- of monoclonal gammopathy in first-degree relatives of patients with multiple myeloma or monoclonal gammopathy of undetermined significance. *Blood* 2009; 114: 785.
11. Kintzer JS, Rosenow EC, Kyle RA. Thoracic and pulmonary abnormalities in multiple myeloma: A review of 958 cases. *Arch Intern Med* 1978; 138: 727-30.
12. Hughes JC, Votaw ML. Pleural effusion in multiple myeloma. *Cancer* 1979; 44: 1150-4.
13. Law I, Blom J. Second malignancies in patients with multiple myeloma. *Oncology* 1977; 34: 20-4.
14. Kamble R, Wilson CS, Fassas A, *et al.* Malignant pleural effusion of multiple myeloma: Prognostic factors and outcome. *Leuk Lymphoma* 2005; 46: 1137-42.
15. Fekih L, Fenniche S, Hassene H, *et al.* Multiple myeloma presenting with multiple thoracic manifestations. *Indian J Chest Dis Allied Sci* 2010; 52: 47-9.
16. Huang TC, Chao TY. Myelomatous pleural effusion. *QJM* 2010; 103: 705-6.
17. Rodriguez JN, Pereira A, Martinez JC, *et al.* Pleural effusion in multiple myeloma. *Chest* 1994; 105: 622-4.

胸壁漿細胞瘤合併大量的骨髓瘤性肋膜積液

黃國良^{*,**} 蘇文麟^{**,***} 周紹庭^{*} 林志恭^{****} 彭萬誠^{**}

漿細胞瘤主要侵犯骨髓，也可以影響許多其他器官。在多發性骨髓瘤患者中發生肋膜積液並不常見；肋膜積液有許多病因，包括充血性心臟衰竭，腎病症候群，感染，慢性腎衰竭，肺栓塞，甚至是續發性惡性腫瘤所造成。在多發性骨髓瘤患者發生骨髓瘤性肋膜積液是極其罕見的。我們提出胸壁的漿細胞瘤合併有骨髓瘤性肋膜積液的罕見病例，骨髓瘤性肋膜積液是經由肋膜積液細胞學檢查和肋膜切片檢查診斷，並且做文獻回顧。*(胸腔醫學 2015; 30: 232-238)*

關鍵詞：漿細胞瘤，骨髓瘤性肋膜積液，胸壁

* 國軍高雄總醫院 內科部 胸腔內科，** 三軍總醫院胸腔內科及國防醫學院

*** 佛教慈濟醫療財團法人台北慈濟醫院，**** 三軍總醫院病理部及國防醫學院

索取抽印本請聯絡：蘇文麟醫師，台北慈濟醫院 胸腔內科，23142 新北市新店區建國路 289 號

Post-Traumatic Left Main Bronchus Stenosis: Case Report

Kai-Wei Chang, Yi-Ting Yen, Yau-Lin Tseng, Wu-Wei Lai

Tracheobronchial injury following blunt chest trauma is a rare but potentially lethal injury. Often the diagnosis and treatment are delayed, resulting in attempted surgical repair months or even years after the injury. We described the case of a patient with post-traumatic left main bronchus stenosis. Before the diagnosis, the patient, with left lung white-out, was subjected to a tube thoracostomy, resulting in splenic penetration. Thus, the importance of a “safe triangle” and ultrasound guidance are emphasized for chest drainage. The late injury presenting as a stenosis was successfully managed by sleeve resection and reconstruction of the left main bronchus. (*Thorac Med* 2015; 30: 239-246)

Key words: tracheobronchial injury, tube thoracostomy, splenic penetration

Introduction

Post-traumatic tracheobronchial injuries are an uncommon but life-threatening occurrence [1-2]. The infrequency and occult clinical nature of such injuries often result in a delay in diagnosis [3]. The diagnosis is often made late, when pulmonary collapse and sepsis occur. Prompt excision of the stenosis and surgical repair is of utmost importance. A functional return appears to be roughly inversely proportional to the length of time that the lung was compromised [4-5]. Here, we offer the case of a patient with pigtail malposition with penetration into the abdomen due to unrecognized lung collapse on chest plain film after left main bronchus injury.

Case Report

A 29-year-old previously healthy female was involved in a debris flow in Miaoli. One of her company died at the scene, and she sustained vigorous blunt trauma to the anterior chest wall by a huge stone. She was sent to the hospital there and underwent endotracheal tube intubation for poor oxygenation. Bilateral tube thoracostomy for bilateral pneumothorax was also performed. Thereafter, she gradually recovered and was extubated. Both chest tubes were removed, as well. However, she felt persistent mild dyspnea with stridor, and was therefore transferred to another hospital in Tainan on post-trauma day (PTD) 19.

The initial chest radiograph on PTD 19

Division of Thoracic Surgery, National Cheng Kung University Hospital, Tainan City, Taiwan
Address reprint requests to: Dr. Kai-Wei Chang, Division of Thoracic Surgery, National Cheng Kung University Hospital, No. 138, Sheng-Li Road, Tainan 704, Taiwan

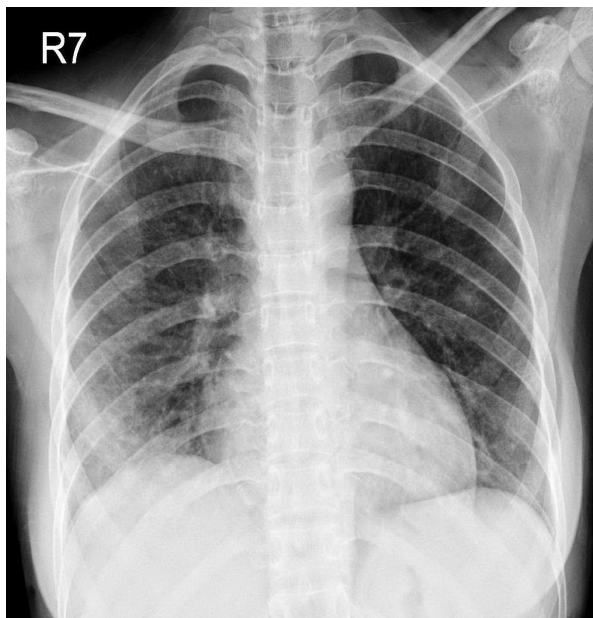


Fig. 1. Initial chest radiograph on PTD 19 revealed an unremarkable lung lesion.

(Figure 1) revealed bilateral clear lung fields, and the position of the heart and the diaphragm were both adequate. Chest computed tomography (CT) on PTD 23 (Figure 2) showed bilateral 1st to 6th rib fracture with bilateral resolving subcutaneous emphysema, and no lung contusion, consolidation, pneumothorax, pleural effusion or mediastinal emphysema was seen. There was also mucous plug-like material in the left main bronchus without distal atelectasis. In the early morning of PTD 32, she had breathing difficulty with saturation decreased below 90% after waking up, but no hypotension or tachycardia was noted. Chest plain film (Figure 3) showed total white-out in the left lung. Under the suspicion of a large amount of pleural effusion or delayed hemothorax, a pigtail was inserted at the left 8th intercostal space, but only a small amount of fresh blood was drained out. She was then transferred to our hospital immediately.



Fig. 2. Chest CT on PTD 23 showed bilateral 1st to 6th rib fracture with bilateral resolving subcutaneous emphysema (white arrow); there was also mucous plug-like material in the left main bronchus (black arrow) without distal atelectasis.

At the ER, her vital signs were stable without obvious tachycardia or desaturation under nasal cannula use. Chest CT (Figure 4,5) was performed, and revealed 1., a soft tissue plug, about 2 cm in length, in the midway of the left main bronchus with left lung total collapse, and 2., the pigtail catheter had penetrated through the spleen. Fearing internal bleeding, she was admitted to the intensive care unit with the pigtail in place. Bronchoscopy showed the fibrotic stricture that caused nearly total obstruction of the left main bronchus at 1cm below the carina.

Under the impression of post-traumatic left main bronchus stenosis, we first tried bronchial stent placement on PTD 37, but even the guide-wire could not pass through the narrowed lumen (Figure 6). On PTD 40, a scheduled left posterolateral thoracotomy with sleeve resection and reconstruction of the left main bronchus (Figure 7) was performed smoothly, and we also removed the pigtail in the operating room under close monitoring. Follow-up bronchoscopy on PTD 47 and 54 (Figure 8) showed a patent left main bronchus.

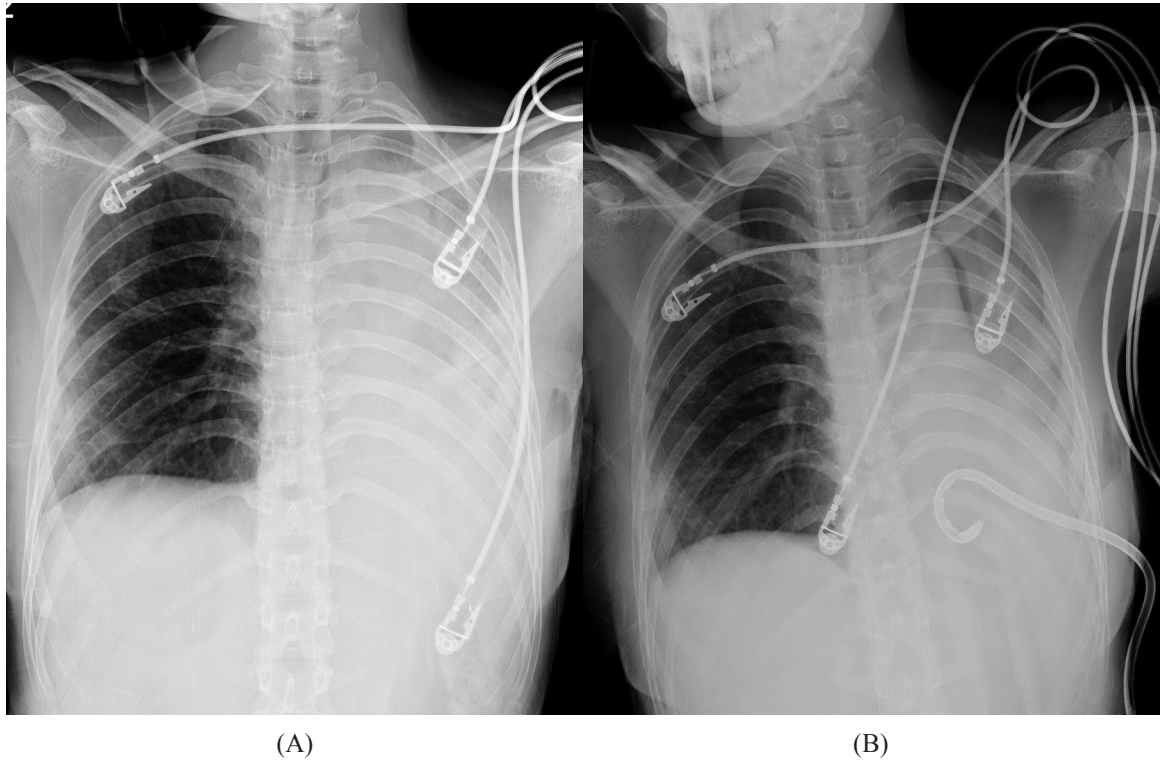


Fig. 3. A. Chest x-ray taken in the morning on PTD 32 due to breathing difficulty with desaturation. B. Chest x-ray taken after pigtail insertion on the same day.

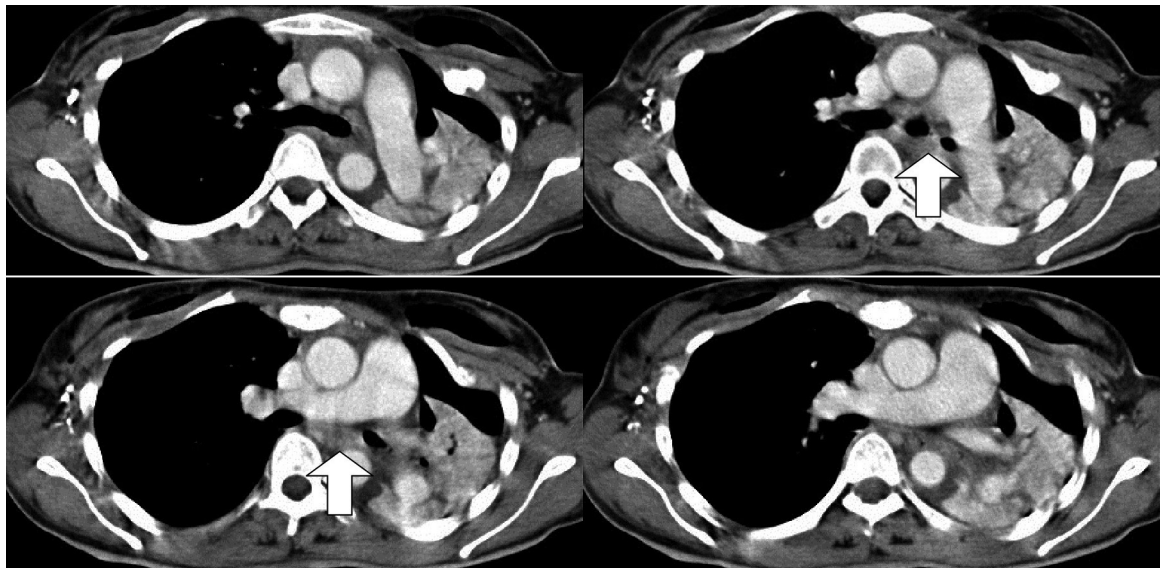


Fig. 4. Serial axial contrast CT scan images on PTD 32 revealed a plug (arrow) about 2 cm in length in the midway — at the middle of the left main bronchus with left lung obstructive pneumonitis and total collapse.

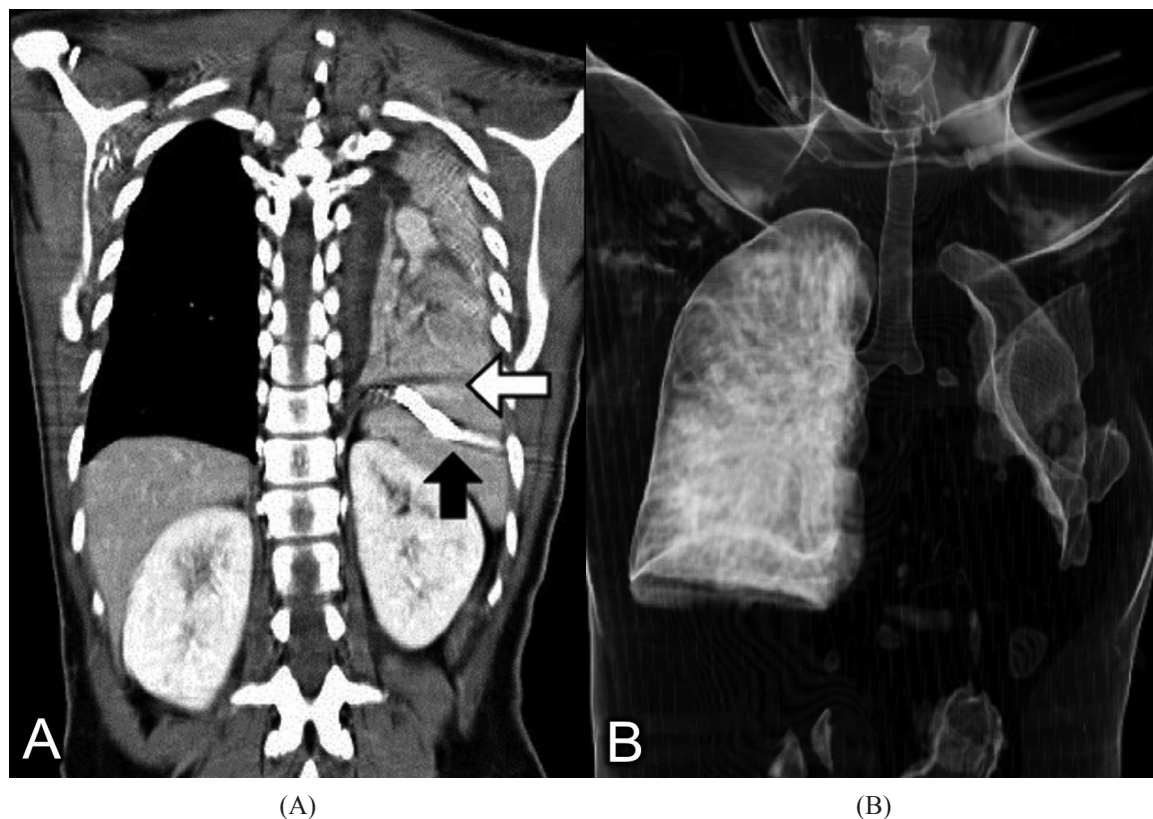


Fig. 5. A. CT scan coronal view revealed the elevated hemidiaphragm (white arrow) due to collapsed lung and the spleen penetrated by the pigtail (black arrow). B. Overt left main bronchus obstruction on CT image reconstruction.



Fig. 6. Bronchoscopy showed left main bronchus stenosis on PTD 37.

Discussion

Tracheobronchial injuries caused by blunt trauma may be unrecognized, and the lumen of the trachea or bronchus could be reduced to only a tiny opening by the time the diagnosis is made [6]. In this case, left main bronchus rupture was not detected initially. Thus, the complete white-out of the left lung noted about 1 month after the trauma was a challenge for differential diagnosis.

Delayed hemothorax is rarely seen (7/167, 4.2%), and was associated with a lower Injury Severity Score, shorter hospital length of stay, and no mortality compared to acute hemothorax in 1 study [7]. In another study [8], 36 cases of

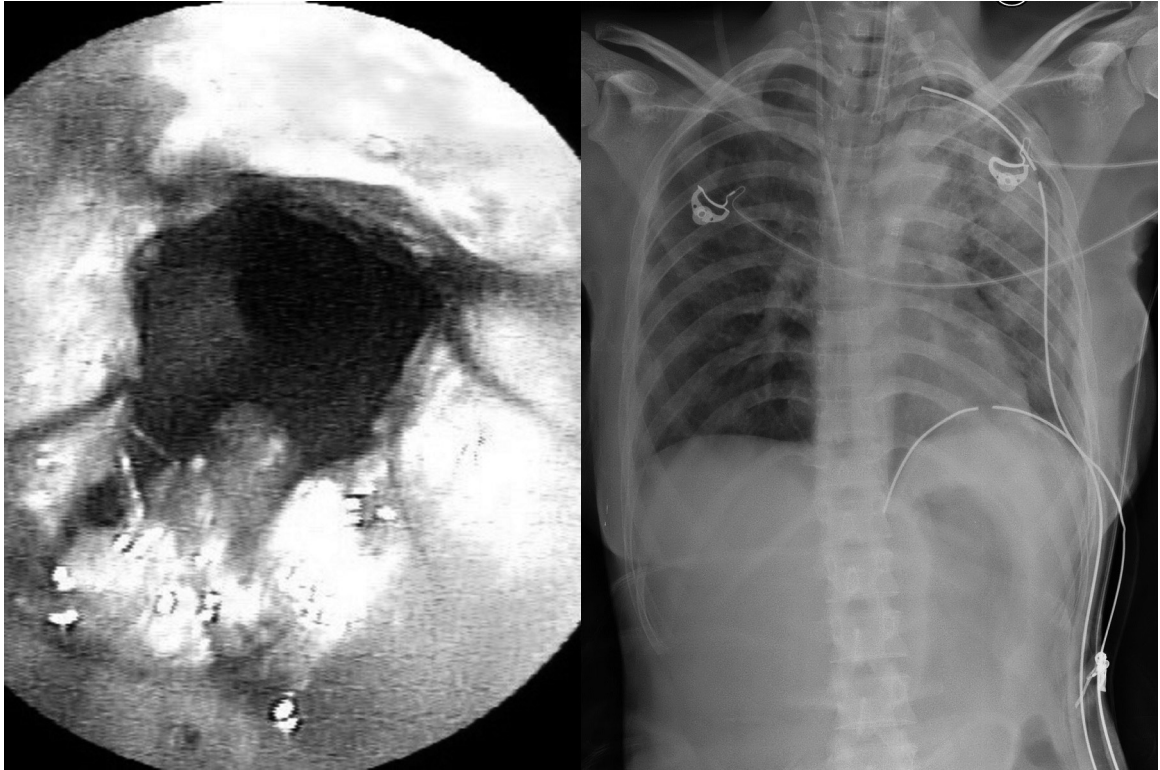


Fig. 7. A. Intra-operative bronchoscopy right after sleeve resection and reconstruction of the left main bronchus on PTD 40. B. Initial postoperative chest plain film.

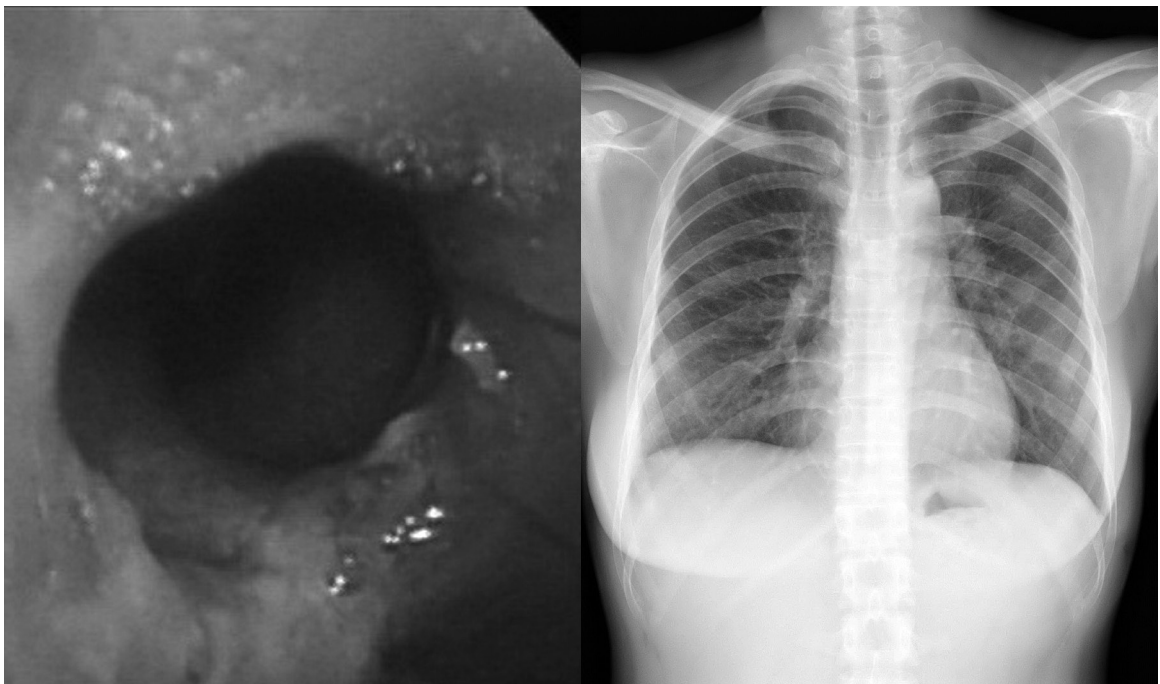


Fig. 8. A. Follow-up bronchoscopy on PTD 54. B. Chest x-ray at final clinic visit on PTD 65 showed the left lung was expanded fully.

hemothorax in 308 patients suffering from blunt thoracic injury at a Level I trauma center were also retrospectively reviewed for a 3-year period. Of the 36 patients, 24 developed immediate hemothorax and 12 met the criteria for delayed hemothorax. These 12 patients had had more than one normal chest radiographs before hemothorax was diagnosed. The delay in presentation of the 12 patients ranged from 18 hours to 6 days, with a mean delay of 3.06 days.

In the chest x-ray taken on PTD 32, when the patient had breathing difficulty and desaturation, showed total white-out in the left lung. At that time, massive hemothorax was suspected and led to misplacing the pigtail in the abdomen. We knew that massive hemothorax can be immediately life-threatening due to 3 mechanisms: accumulation of blood in the thorax resulting in a compression of the heart and great vessels; a severe loss of blood resulting in acute hypovolemia; and hypoxia from the collapsed lung [9]. Distention of neck veins and tracheal deviation toward the contralateral side could also be seen on the chest radiograph. For the above reasons, left lung total collapse was more likely than massive hemothorax in our patient, if the trauma history, interval from the trauma event, vital signs, physical examination findings, and the position of the mediastinum on chest x-ray film were taken into consideration [10].

Malposition of chest drainage would not happen if the diagnosis was correct or tube thoracostomy was never performed below the 6th intercostal space without echo-guided or clear image evidence [11-13]. The British Thoracic Society Standards of Care Committee announced the guidelines for the insertion of a chest drain in 2003, and mentioned that the insertion should be done within the “safe triangle”, bordered by

the anterior border of the latissimus dorsi muscle, the lateral border of the pectoralis major muscle, a line superior to the horizontal level of the nipple, and an apex below the axilla [14]. Fluoroscopy, ultrasonography, and CT scanning can all be used as adjunctive guides to the site of tube placement. Last but not least, air or fluid should be aspirated before insertion. It is recommended that ultrasound be used if initial blind aspiration fails.

We attempted laser treatment and temporary stent placement in the beginning. Open surgical resection and reconstruction are unquestionably the best treatment for benign and malignant airway obstruction if the patient can tolerate it [6], but the results of using endoscopic techniques in the management of benign tracheobronchial stenosis are also good [15-16]. These procedures, including balloon dilatation, Nd: YAG laser, cryotherapy, mechanical dilatation with a rigid bronchoscope, and stent placement, usually offer immediate symptom relief and remain reliable in the longer term after discharge from the hospital [17-18].

The key to surgical success is undoubtedly careful preoperative treatment of infection and inflammation, as well as meticulous mucosal approximation of healthy margins at the anastomosis [19-20]. The same concepts were also emphasized by Grillo [21]. Clean and sharp lines of bronchial transection are important, meaning that jagged and devascularized edges must be avoided. Absorbable sutures should be used to avoid development of suture line granulomas. A pedicled flap of pleura or pericardial fat is then passed around the anastomosis as a buttress and to separate the suture line from nearby vascular structures. Finally, repeated flexible bronchoscopic aspiration may be necessary postoperatively to prevent early atelectasis.

In summary, bronchial stenosis should be considered when lung collapse is noted in the chest plain film after chest blunt trauma, especially in those with a history of dyspnea and stridor. Chest drain insertion should be in the “safe triangle” or under the guidance of ultrasound. Prompt excision of stenosis and meticulous surgical repair can achieve satisfactory results.

References

1. Kiser AC, O'Brien SM, Detterbeck FC. Blunt tracheobronchial injuries: treatment and outcomes. *Ann Thorac Surg* 2001; 71(6): 2059-65.
2. Huh J, Milliken JC, Chen JC. Management of tracheobronchial injuries following blunt and penetrating trauma. *Am Surg* 1997; 63(10): 896-9.
3. Lin MY, Wu MH, Chan CS, *et al.* Bronchial rupture caused by blunt chest injury. *Ann Emerg Med* 1995; 25(3): 412-5.
4. Deslauriers J, Beaulieu M, Archambault G, *et al.* Diagnosis and long-term follow-up of major bronchial disruptions due to nonpenetrating trauma. *Ann Thorac Surg* 1982; 33(1): 32-9.
5. Hwang JJ, Kim YJ, Cho HM, *et al.* Traumatic tracheobronchial injury: delayed diagnosis and treatment outcome. *Korean J Thorac Cardiovasc Surg* 2013; 46(3): 197-201.
6. Shields TW. General thoracic surgery. 7th ed. Philadelphia: Wolters Kluwer Health/Lippincott Williams & Wilkins 2009; 967-80.
7. Sharma OP, Hagler S, Oswanski MF. Prevalence of delayed hemothorax in blunt thoracic trauma. *Am Surg* 2005; 71(6): 481-6.
8. Simon BJ, Chu Q, Emhoff TA, *et al.* Delayed hemothorax after blunt thoracic trauma: an uncommon entity with significant morbidity. *J Trauma* 1998; 45(4): 673-6.
9. Keough V, Pudelek B. Blunt chest trauma: review of selected pulmonary injuries focusing on pulmonary contusion. *AACN Clin Issues* 2001; 12(2): 270-81.
10. Shaftan GW. The initial evaluation of the multiple trauma patient. *World J Surg* 1983; 7(1): 19-25.
11. Rauch RF, Korobkin M, Silverman PM, *et al.* CT detection of iatrogenic percutaneous splenic injury. *J Comput Assist Tomogr* 1983; 7(6): 1018-21.
12. Khan S, Yousuf MI, Bisharat M, *et al.* Iatrogenic splenic injury in percutaneous procedures. *Ulster Med J* 2008; 77(2): 131-2.
13. Sethuraman KN, Duong D, Mehta S, *et al.* Complications of tube thoracostomy placement in the emergency department. *J Emerg Med* 2011; 40(1): 14-20.
14. Laws D, Neville E, Duffy J. Pleural Diseases Group SoCCBTS. BTS guidelines for the insertion of a chest drain. *Thorax* 2003; 58 Suppl 2: ii53-9.
15. Chhajed PN, Malouf MA, Glanville AR. Bronchoscopic dilatation in the management of benign (non-transplant) tracheobronchial stenosis. *Intern Med J* 2001; 31(9): 512-6.
16. Sheski FD, Mathur PN. Long-term results of fiberoptic bronchoscopic balloon dilation in the management of benign tracheobronchial stenosis. *Chest* 1998; 114(3): 796-800.
17. Husain SA, Finch D, Ahmed M, *et al.* Long-term follow-up of ultraflex metallic stents in benign and malignant central airway obstruction. *Ann Thorac Surg* 2007; 83(4): 1251-6.
18. Eisner MD, Gordon RL, Webb WR, *et al.* Pulmonary function improves after expandable metal stent placement for benign airway obstruction. *Chest* 1999; 115(4): 1006-11.
19. Palade E, Passlick B. Surgery of traumatic tracheal and tracheobronchial injuries. *Chirurg* 2011; 82(2): 141-7.
20. Thompson DA, Rowlands BJ, Walker WE, *et al.* Urgent thoracotomy for pulmonary or tracheobronchial injury. *J Trauma* 1988; 28(3): 276-80.
21. Grillo HC. Surgery of the trachea and bronchi. Hamilton, Ont.; Lewiston, NY: BC Decker, 2004; 619-29.

創傷後左主支氣管狹窄－病例報告

張凱惟 顏亦廷 曾堯麟 賴吾為

胸部鈍傷後引起的氣管支氣管損傷是一種罕見但潛在的致命傷害。診斷和治療時常被延遲，而導致在受傷後幾個月或甚至幾年後才進行修復手術。我們描述一個創傷後左主支氣管狹窄的病例。然而在確定診斷之前，患者因左肺整片變白而接受胸管置入術，進而導致脾臟穿刺傷。藉此再次強調「安全三角區域」和超音波導引在胸腔引流中的重要性。而此病人在創傷晚期以支氣管狹窄呈現，則成功地藉由左主支氣管袖狀切除及重建來處理。*(胸腔醫學 2015; 30: 239-246)*

關鍵詞：氣管支氣管損傷，胸管置入術，脾臟穿刺傷

Ventriculoperitoneal Shunt Catheter Dislocation Causing Massive Right-Side Pleural Effusion: A Case Report

Yen-Fu Chen, Chih-Wei Chen, Jiunn-Min Shieh, Shian-Chin Ko

Ventriculoperitoneal (VP) shunting is a common method used to treat hydrocephalus; however, it can cause a variety of complications, such as infection, dysfunction, malposition and over-drainage. Pleural effusion is an uncommon complication of VP shunting and is usually associated with diaphragm defects. Refractory massive pleural effusion can cause respiratory failure. Surgical intervention is usually needed to correct the VP shunt-related pleural effusion. Here, we describe the case of a 51-year-old man who presented with respiratory failure due to persistent massive right-sided pleural effusion, caused by dislocation of the distal tip of the VP shunt catheter. After surgical revision of the VP shunt catheter and proper drainage, the pleural effusion was eliminated. (*Thorac Med* 2015; 30: 247-252)

Key words: ventriculoperitoneal (VP) shunt, pleural effusion, respiratory failure

Introduction

Ventriculoperitoneal (VP) shunt is the most commonly used and safest procedure for the management of hydrocephalus [1]. The excess cerebrospinal fluid (CSF) is drained into the peritoneal cavity via the VP shunt catheter to maintain normal intracranial pressure. However, the VP shunt is associated with a variety of complications, including infections, mechanical complications and over-drainage.

These complications have been reported to occur in association with pleural effusion after VP shunt insertion [2-5]. Most of the reported cases were combined with diaphragm defects

and intrathoracic migration of the VP shunt catheter. We report the case of a 51-year-old man with massive right-side pleural effusion and respiratory failure due to VP shunt catheter migration into the subphrenic space just above the liver dome, without intrathoracic migration.

Case Report

A 51-year-old male merchant with a history of type 2 diabetes mellitus and hypertension presented to our emergency department due to left-side facial palsy and limb weakness. Acute stroke was suspected and brain computed tomography (CT) confirmed the diagnosis of right

Division of Chest Medicine, Department of Internal Medicine, Chi Mei Medical Center, Division of Neurosurgery, Department of Surgery, Chi-Mei Medical Center, Tainan City, Taiwan

Address reprint requests to: Dr. Shian-Chin Ko, Division of Chest Medicine, Department of Internal Medicine, Chi Mei Medical Center, No. 901, Zhonghua Rd., Yongkang Dist., Tainan City 710, Taiwan (R.O.C.)

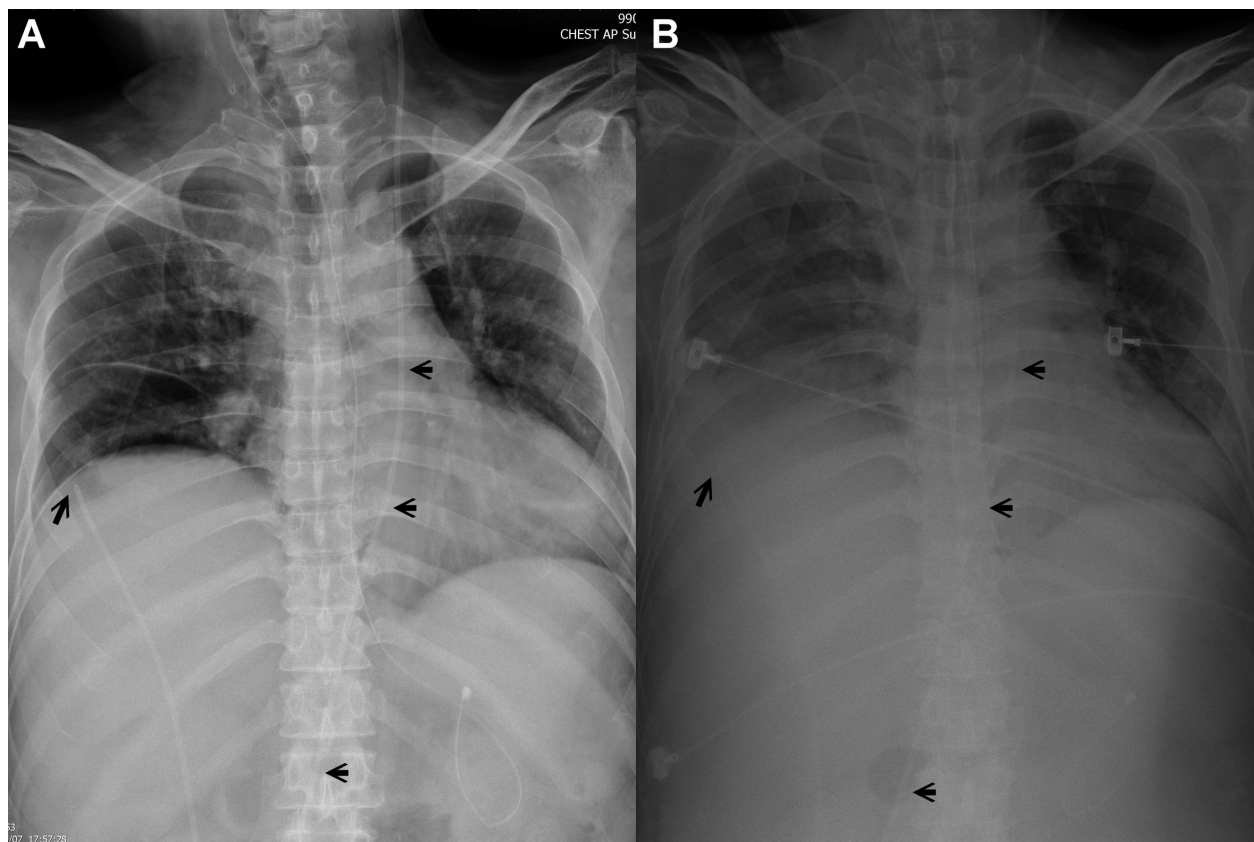


Fig 1. Chest radiography. (A) One and 1 half month after VP shunt insertion. The short arrowheads denote the course of the VP shunt and the long arrowhead the distal tip of the VP shunt. Note that the distal tip of the VP shunt was just beneath the right-side diaphragm. (B) Two days later, right-side pleural effusion appeared and the patient developed dyspnea.

putaminothalamic hemorrhage with rupture into the intraventricular system. Thus, he was admitted to the surgical intensive care unit (SICU) and received emergency surgery to evacuate the intracerebral blood clots. His vital signs stabilized during the postoperative period, but difficult weaning from the ventilator developed. He was then transferred to the respiratory care center (RCC) and was gradually liberated from the ventilator.

However, his consciousness level deteriorated in the general ward and follow-up brain CT revealed significant hydrocephalus. Thus, a VP shunt catheter placement was performed. During the hospital course, his disease was com-

plicated with nosocomial pneumonia caused by carbapenem-resistant *Acinetobacter baumannii*. Respiratory failure recurred and he was reintubated. Dyspnea and abdominal distention were noted. Physical examination showed bilateral wheezes and decreased right-side breathing sounds. Chest radiography showed increased right-side lung infiltration with a blunting costophrenic angle (Figure 1B), compared with the previous chest X-ray (Figure 1A). The tentative diagnosis was pneumonia with parapneumonic effusion. Antibiotics and diuretics were prescribed for infection and suspected fluid overload. However, the right-sided pleural effusion persisted, even with the use of aggressive

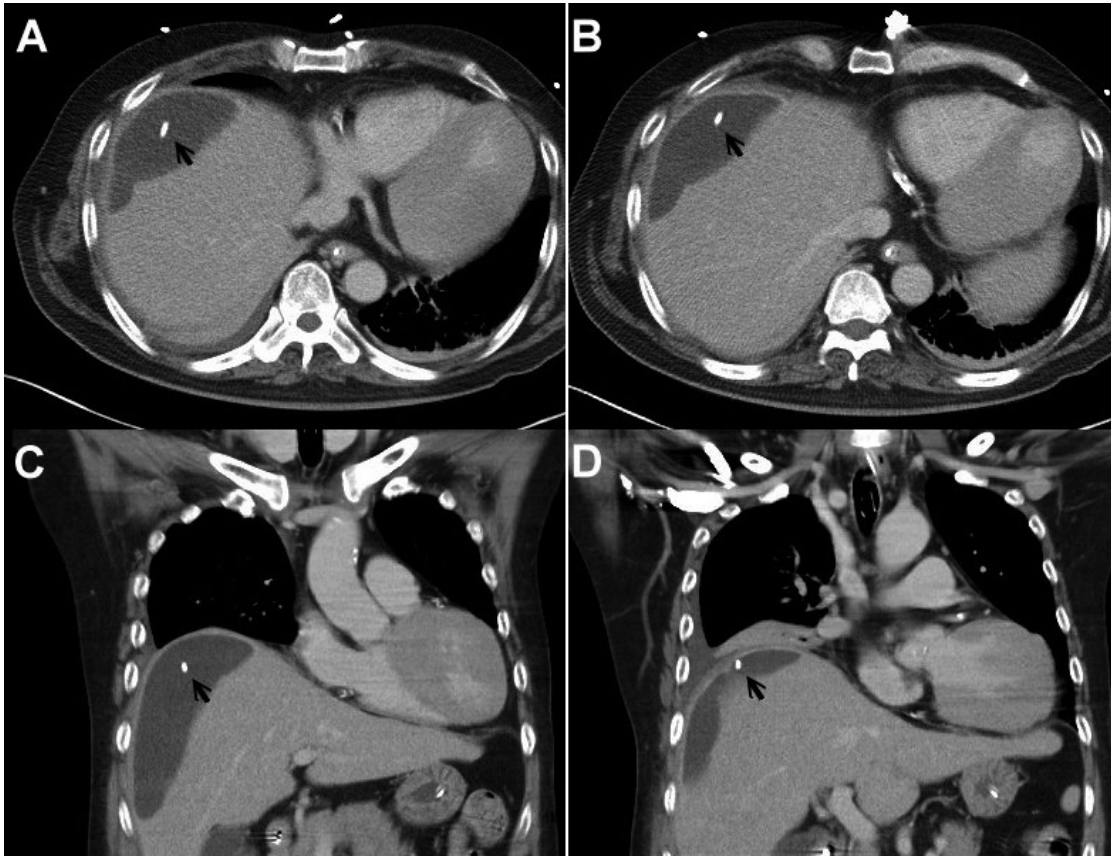


Fig 2. Chest CT scan. (A, B) The transverse sections of the thorax. (C, D) The frontal sections of the thorax. The arrowheads denote the distal tip of the VP shunt. Note that the distal tip of the VP shunt was located between the liver dome and the right-side hemidiaphragm. A cystern of fluid accumulation in the right subphrenic area was also found.

diuretics.

To seek the cause of the persistent pleural effusion, chest CT was performed, and revealed that the distal tip of the VP shunt catheter was located in the right subphrenic area with fluid accumulation around it (Figure 2A and 2B). It was assumed that the right-side pleural effusion was caused by the transdiaphragmatic movement of the accumulated fluid, which resulted from dislocation of the distal tip of the VP shunt catheter. Exploratory mini-laparotomy was then performed. The peritoneal catheter was pulled out and was repositioned on the Douglas pouch. A pig-tail insertion was done for residual pleural effusion drainage, and 680 ml of pleural ef-

fusion, cloudy and transudative in appearance, was drained initially (1050 ml in total). The pleural effusion no longer occurred after shunt revision (Figure 3).

Discussion

VP shunt is the most common modality for the management of hydrocephalus, and complications are not rare. Catheter malfunction developed in about 40% of patients receiving VP shunt within the first year after placement, and the annual malfunction rate is 5% in subsequent years [6]. The major complications of VP shunt include infection, mechanical failure, and over-

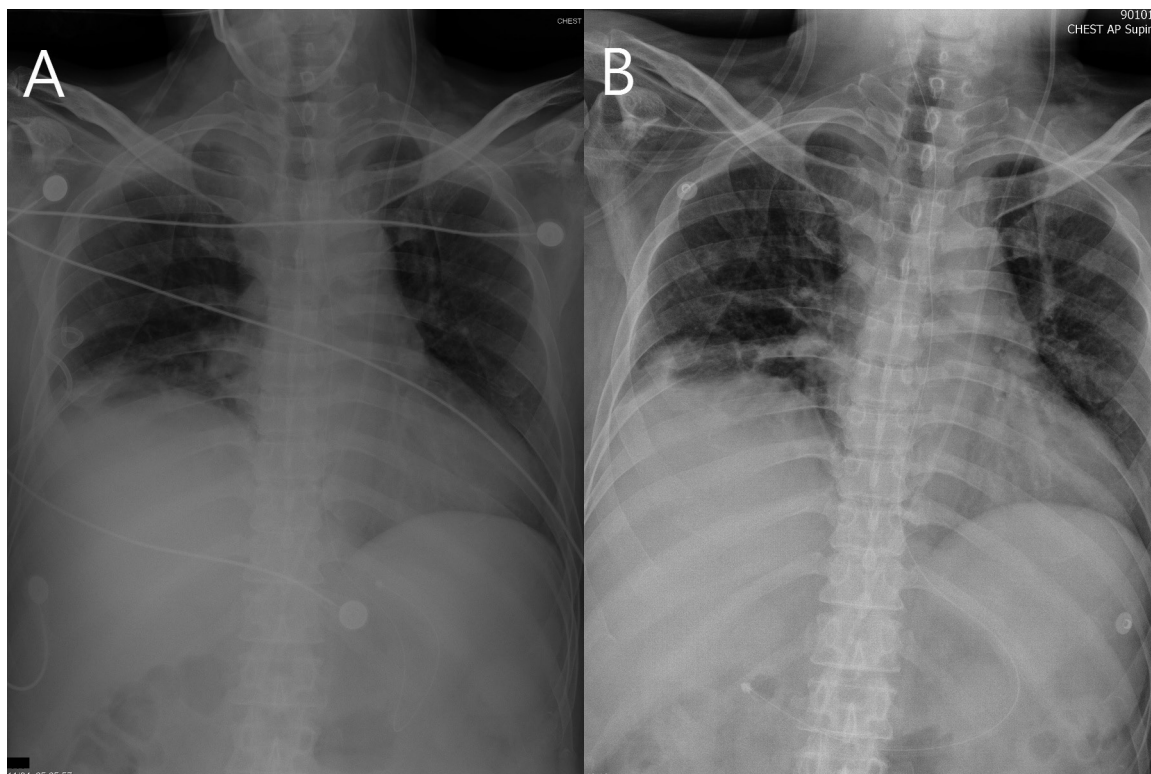


Fig 3. Chest radiography. (A) Pig-tail was inserted for right-side pleural effusion drainage for 1 week. The X-ray was taken before we removed the pig-tail. (B) We removed the pig-tail 1 week later, and no more pleural effusion was noted in the follow-up X-ray.

drainage [7].

Shunt infection usually develops within 1 month, and *Staphylococcus* species is the most common pathogen [8]. The risk factors for shunt infection are multiple revisions, young age, holes in surgical gloves, postoperative leakage, and limited experience of the surgeon [8]. Systemic prophylactic antibiotics within the first 24 hours postoperatively reduce the risk of shunt infection by approximately 50% [9].

Mechanical failure includes obstruction, fracture, and migration. Over 50% of the initial shunt failures result from obstruction at the ventricular catheter. Catheter fracture accounts for about 15% of shunt failures, and catheter migration for 7.5% [7].

Over-drainage of CSF can cause functional

shunt failure, which leads to subnormal intracranial pressure, particularly in the upright position, and is associated with characteristic neurological symptoms such as postural headache and nausea [7].

Pleural effusions associated with VP shunt have been reported sporadically [2-5]. The mechanism is usually congenital diaphragmatic defects. The distal tip of the VP shunt catheter may be displaced into the pleural cavity via the defects [10]. In the present case, the distal tip of the VP shunt was displaced and located in the subphrenic space just above the liver dome. A cistern of CSF accumulation in the subphrenic area was also found by CT scan. Migration of the VP shunt may be caused by vigorous bowel movement. It was assumed that the negative

intrathoracic pressure could draw the accumulated CSF into the pleural space though the diaphragm, as seen in a case of hepatic hydrothorax [11]. After revision of the peritoneal catheter, the CSF accumulation disappeared.

It is difficult to differentiate CSF from other transudates in the pleural effusion using the ordinary biochemistry method. A simple method to distinguish CSF from hepatic ascites by assessing the concentration of β -2 transferrin in the pleural effusion was reported by Smith, *et al* [12]. β -2 transferrin is a carbohydrate-free isoform of transferrin, found almost exclusively in the CSF, making it a specific CSF marker.

Conclusion

We reported a case of refractory massive right-side pleural effusion and respiratory failure caused by VP shunt displacement. When an unexplained pleural effusion develops in a patient with VP shunt, displacement of the shunt catheter should be considered, and surgical shunt revision is mandatory.

References

1. Noetzel MJ, Baker RP. Shunt fluid examination: risks and benefits in the evaluation of shunt malfunction and infection. *J Neurosurg* 1984; 61: 328-32.
2. Doh JW, Bae HG, Lee KS, *et al*. Hydrothorax from intrathoracic migration of a ventriculoperitoneal shunt catheter. *Surg Neurol* 1995; 43: 340-3.
3. Rengachary SS. Transdiaphragmatic ventriculoperitoneal shunting: technical case report. *Neurosurgery* 1997; 41: 695-7.
4. Chuen IM, Smyth MD, Segura B, *et al*. Recurrent pleural effusion without intrathoracic migration of ventriculoperitoneal shunt catheter: a case report. *Pediatr Pulmonol* 2012; 47: 91-5.
5. Miyamoto J, Nijima K. Migration of the distal catheter of ventriculo-peritoneal shunt into the thoracic cavity. *No Shinkei Geka* 2012; 40: 241-5.
6. Stein SC, Guo W. Have we made progress in preventing shunt failure? A critical analysis. *J Neurosurg Pediatr* 2008; 1: 40-7.
7. Chumas P, Tyagi A, Livingston J. Hydrocephalus — what's new? *Arch Dis Child Fetal Neonatal Ed* 2001; 85: F149.
8. Wells DL, Allen JM. Ventriculoperitoneal shunt infections in adult patients. *AACN Adv Crit Care* 2013; 24: 6-12.
9. Ratilal B, Costa J, Sampaio C. Antibiotic prophylaxis for surgical introduction of intracranial ventricular shunts. *J Neurosurg Pediatrics* 2008; 1: 48-56.
10. Huang PM, Chang YL, Yang CY, *et al*. The morphology of diaphragmatic defects in hepatic hydrothorax: thoracoscopic finding. *J Thorac Cardiovasc Surg* 2005 Jul; 130(1): 141-5.
11. Singh A, Bajwa A, Shujaat A. Evidence-based review of the management of hepatic hydrothorax. *Respiration* 2013; 86: 155-73.
12. Smith JC, Cohen E. Beta-2-transferrin to detect cerebrospinal fluid pleural effusion: a case report. *J Med Case Rep* 2009 Mar 13; 3: 6495.

腦室腹膜分流管異位導致大量右側肋膜積液：病例報告

陳彥甫 陳志偉 謝俊民 柯獻欽

腦室腹膜分流術是治療水腦症的一種常用治療方式。腦室腹膜分流術所致肋膜積液是一種少見的併發症，而且過去的病例報告多伴隨著橫隔膜缺損。腦室腹膜分流術所導致的肋膜積液可能會造成呼吸衰竭，必須以手術治療。在此我們描述一位 51 歲男性因腦室腹膜分流管的遠端管尖異位，導致持續性大量肋膜積液，而造成呼吸衰竭。病人在接受腦室腹膜分流管復位手術且適當引流後，才改善此一肋膜積液現象。
(*胸腔醫學* 2015; 30: 247-252)

關鍵詞：腦室腹膜分流管，肋膜積液，呼吸衰竭

Hypereosinophilic Syndrome with Liver Involvement in Advanced Lung Cancer

Shih-Wen Hu, Tzu-Hsiu Tsai, Jin-Yuan Shih

Eosinophilia is a paraneoplastic syndrome of solid cancer, and is present in approximately 3% of patients with lung cancer. Hypereosinophilic syndrome is defined when marked blood ($\geq 1.5 \times 10^3/\mu\text{L}$) and tissue eosinophilia results in a wide variety of organ damage and/or dysfunction. In patients with lung cancer, hypereosinophilic syndrome is extremely rare. Here, we present a case of advanced lung adenocarcinoma with severe blood eosinophilia and associated eosinophilic hepatitis. The marked blood eosinophilia and associated liver dysfunction resolved after disease control with platinum-based cytotoxic chemotherapy, suggesting that this paraneoplastic phenomenon is linked to tumor extent. However, the rapid disease progression and short survival in our case suggests that reactive hypereosinophilic syndrome may be a poor prognostic indicator associated with aggressive tumors. (*Thorac Med* 2015; 30: 253-260)

Key words: eosinophilia, hypereosinophilic syndrome, paraneoplastic syndrome, lung cancer

Introduction

Eosinophilia refers to an increased absolute eosinophil count of more than 500 eosinophils/ μL in the peripheral blood. Eosinophilia is a paraneoplastic syndrome of solid cancer, and is present in approximately 3% of patients with lung cancer [1]. Peripheral blood eosinophilia traditionally was divided into mild ($0.5\text{--}1.5 \times 10^3/\mu\text{L}$), moderate ($1.5\text{--}5.0 \times 10^3/\mu\text{L}$), and severe ($>5.0 \times 10^3/\mu\text{L}$). “Hypereosinophilic syndrome” is defined as when marked blood ($\geq 1.5 \times 10^3/\mu\text{L}$) or tissue eosinophilia results in a wide va-

riety of organ damage and/or dysfunction [2]. Hypereosinophilic syndrome associated with lung cancer is extremely rare. Here, we present the case of a patient with advanced lung adenocarcinoma with reactive hypereosinophilic syndrome and associated liver dysfunction. The clinical course of our case emphasizes the importance of recognizing this rare paraneoplastic syndrome in association with lung cancer, since any delay in effective anti-tumor treatment may result in catastrophic organ dysfunction.

Division of Pulmonary and Critical Care Medicine, Department of Internal Medicine, National Taiwan University Hospital, Taipei, Taiwan

Address reprint requests to: Dr. Tzu-Hsiu Tsai, Division of Pulmonary and Critical Care Medicine, Department of Internal Medicine, National Taiwan University Hospital, Taipei, Taiwan, No. 7 Chung-Shan South Road, Taipei, Taiwan

Case Report

In November 2013, a 59-year-old man was referred to our hospital because of cough, dyspnea, and weight loss of more than 10 kg in 1 month. He was a never-smoker and had no major underlying diseases. An initial chest X-ray revealed a mass at the right-upper-lung field and blunting of the right costophrenic angle (Figure 1). The computed tomography (CT) scan of the chest and upper abdomen showed a spiculated mass (6.1 cm at its greatest dimension) at the right upper lobe (RUL), numerous pleural nodulations along the right major fissure, mild right-sided pleural effusion, and enlarged lymph nodes at the right hilar, pretracheal retrocaval, subcarina, and contralateral prevascular regions (Figure 2A-2C). Pathology of the CT-guided



Fig. 1. A right-upper-lung mass and blunting of the right costophrenic angle were found on chest X-ray.

biopsy of the RUL mass showed histological features consistent with an adenocarcinoma of pulmonary origin. Also, effusion cytology proved the presence of right-sided malignant pleural effusion. After staging work-ups including brain magnetic resonance imaging (MRI) and positron emission tomography (PET) scans, the patient was conclusively diagnosed as having lung adenocarcinoma, stage IV (cT2b-N3M1a). The serum carcinoembryonic antigen (CEA) level was within the normal limit (0.56 ng/mL). The epidermal growth factor receptor gene (*EGFR*) status later turned out to be wild type.

Results of laboratory investigations upon admission on November 24, 2013 included the following: leukocytes, 21270/ μ L (bands, 23.8%; segments, 24.8%; eosinophils, 26.7%; and lymphocytes, 20.9%); aspartate aminotransferase (AST), 67 U/L; alanine aminotransferase (ALT), 110 U/L; and total bilirubin (T-Bil), 0.77 mg/dL. Later, the patient was re-admitted for examination of progressive leukocytosis, eosinophilia, and liver function impairment (Figure 4 and 5). The peaking of the leukocytosis and absolute eosinophil count occurred on December 26, 2013, with the blood test showing 93,360/ μ L leukocytes in the peripheral blood and 58% eosinophils. Hyperbilirubinemia (T-Bil, 3.09 mg/dL) became more evident, though the hepatic transaminase levels were only mildly increased (AST, 42 U/L; ALT, 47 U/L). The stool specimen was negative for leukocytes, protozoa and parasite ova. Serum immunoglobulin E (IgE) was elevated to 538 IU/ml. The peripheral blood smear showed excessive mature eosinophils and leukocytes. The human immunodeficiency virus screening test was negative.

The patient received a first cycle of cytotoxic chemotherapy with pemetrexed (500 mg/

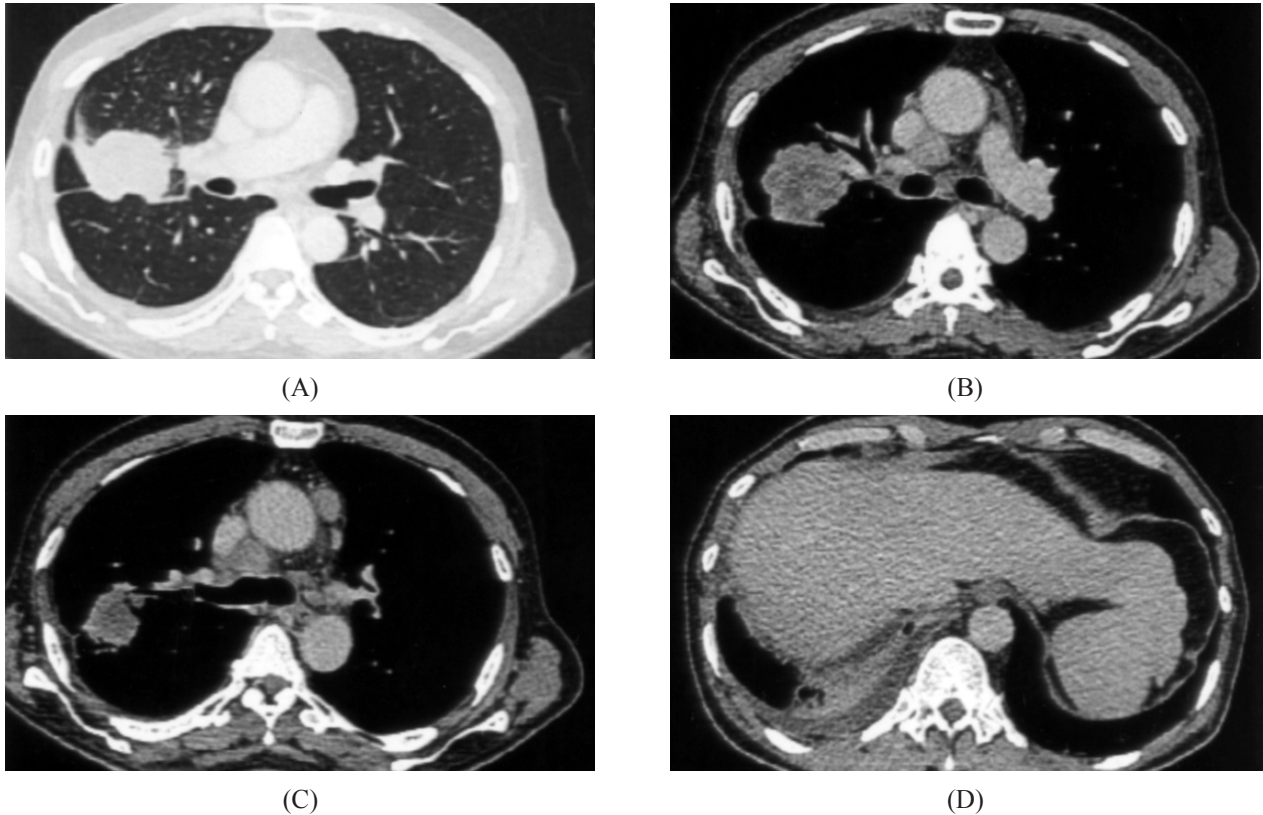


Fig. 2. Computed tomography scan of the chest showing a right-upper-lobe tumor, numerous pleural nodulations, mild right-sided pleural effusion, and enlarged lymph nodes at the right hilar, pretracheal retrocaval, subcarina, and contralateral prevascular regions.

m²) plus cisplatin (75 mg/m²) on December 30, 2013. Laboratory data on January 7, 2014 revealed decreased leukocytosis (leukocyte count, 34120/μL; eosinophils, 90.5%). However, the liver function test showed that the impairment had progressively worsened (T-Bil, 6.79 mg/dL; D-Bil, 3.66 mg/dL; AST, 27 U/L; ALT, 65 U/L; ALP, 411 U/L; and GGT, 648 U/L). As for the abnormal liver function test, the patient reported no use of herbal drugs or other possible offending medications. CT scan of the abdomen revealed no liver lesions. Liver biopsy revealed multiple foci of confluent necrosis, with the portal areas and the necrotic foci showing mixed neutrophilic, eosinophilic and lymphoplasmacytic cell infiltration (Figure 3). Of these, the

eosinophilic infiltration was especially prominent. The bone marrow biopsy on January 20, 2014 showed hypercellular marrow with myeloid hyperplasia and an increase in eosinophil infiltration. No excess blast was seen. As such, reactive hypereosinophilia with liver involvement, probably associated with the underlying lung cancer, was considered the etiology of liver dysfunction in this patient.

The patient received subsequent courses of pemetrexed plus cisplatin on January 24, February 17, March 10, and March 31, 2014, respectively. The serial chest X-rays generally showed no change. During the courses of cytotoxic chemotherapy, resolution of eosinophilic leukocytosis and liver function impairment was

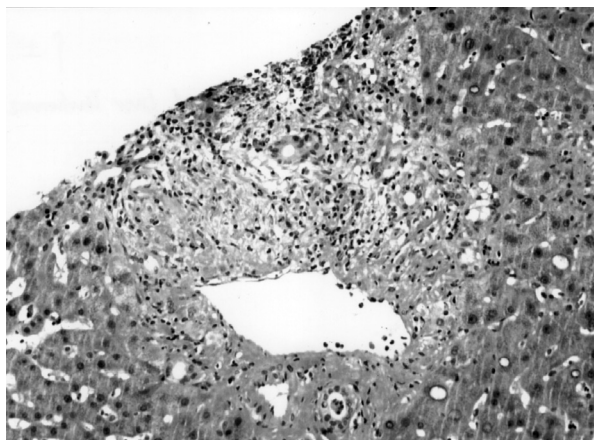


Fig. 3. Liver biopsy revealed multiple foci of confluent necrosis; the portal areas and the necrotic foci both showed mixed neutrophilic, eosinophilic and lymphoplasmic cell infiltration. The eosinophilic infiltration was especially prominent.

observed. The run charts of leukocyte and absolute eosinophil counts, and total bilirubin levels are shown in Figure 4 and Figure 5.

However, follow-up CT scan of the chest

on April 18, 2014 showed disease progression. Laboratory data in the following days showed relapse of eosinophilic leukocytosis, with the leukocyte count increasing from 22,040/ μ L (eosinophil, 16.0%) on April 21 to 68,930/ μ L (eosinophil, 6%) on April 26, 2014. Second-line cytotoxic chemotherapy with weekly docetaxel (35 mg/ m^2) was initiated, but CT scan of the abdomen showed rapid development of multiple hepatic tumors and peritoneal seeding. On May 14, 2014, the patient finally expired due to disease progression and respiratory failure, about 6 months after the diagnosis of lung cancer.

Discussion

Reactive eosinophilia can be caused by allergic diseases, parasitic and fungal infections, medications, and neoplastic diseases [3]. Among the neoplastic disorders, reactive eosinophilia is most commonly seen in some hematologic

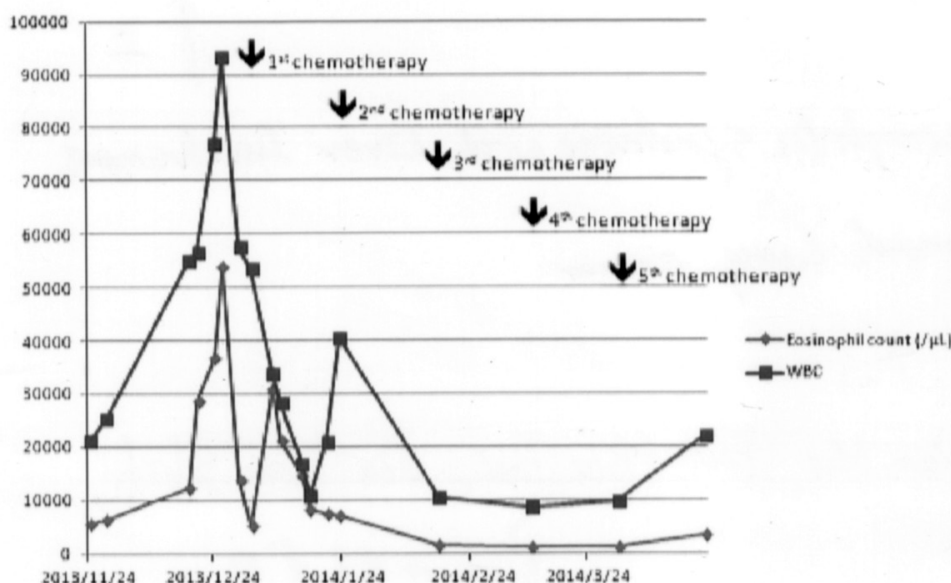


Fig. 4. The run chart of leukocyte and absolute eosinophil counts, showing decreased leukocyte and eosinophil counts with cytotoxic chemotherapy with pemetrexed plus cisplatin.

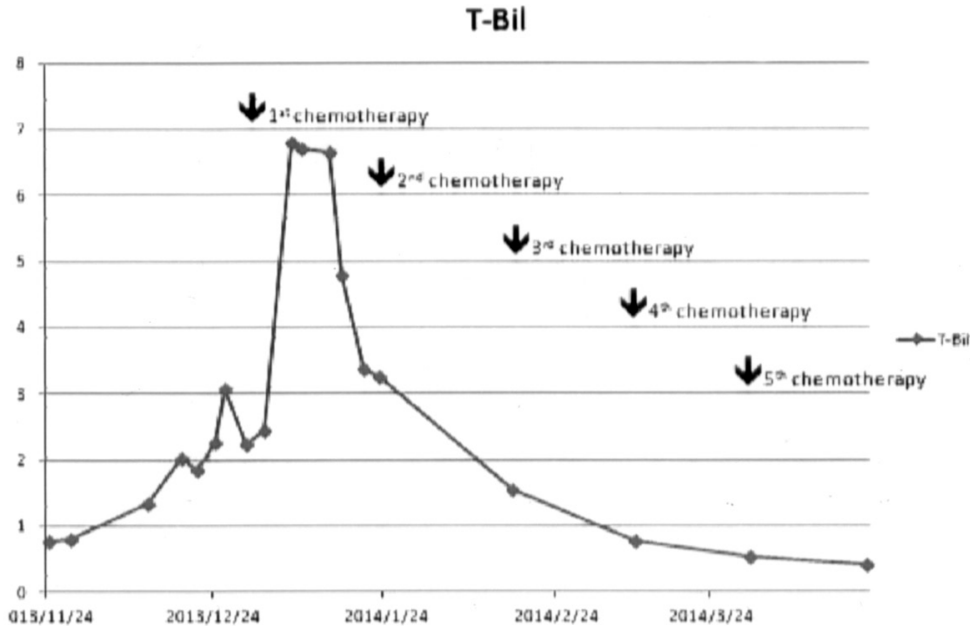


Fig. 5. The run chart of serum total bilirubin, showing that the total bilirubin level increased initially and then decreased to a normal range with cytotoxic chemotherapy with pemetrexed plus cisplatin.

malignancies, such as lymphoma, and myelogenous and lymphocytic leukemia. Eosinophilia is also found in a variety of solid cancers as a rare paraneoplastic syndrome, accounting for ~1% of all cancer patients [1]. It was estimated that eosinophilia is present in approximately 3% of patients with lung cancer. Some reports have demonstrated that blood eosinophilia in lung cancer is associated with the production of eosinophilopoietic cytokines (GM-CSF and IL-5) by the tumor cells [4-5]. However, the functional role of eosinophilia in human cancer remains unclear.

Hypereosinophilic syndrome was first defined by Chusid *et al.* in 1975, and can be divided into variant types, including idiopathic, primary (neoplastic/clonal), and secondary (reactive) forms [2,6]. Hypereosinophilic syndrome is present if all of the following criteria are met: (1) criteria for peripheral blood hypere-

osinophilia; (2) organ damage and/or dysfunction attributed to tissue hypereosinophilia; and (3) exclusion of other disorders or conditions as a major reason for organ damage [2]. Although hypereosinophilic syndrome is extremely rare in lung cancer, the diagnosis of this paraneoplastic phenomenon in association with cancer should be made promptly, with cautious exclusion of other etiologies of eosinophilia. As seen in our patient, timely treatment of lung cancer is the most effective way to avoid the progressive and catastrophic organ dysfunctions associated with hypereosinophilic leukocytosis. However, there may be pitfalls for the differential diagnosis of hypereosinophilic leukocytosis, especially the ruling out of coexisting hematological malignancy as the etiology.

Paraneoplastic leukocytosis associated with a high G-CSF level is not uncommon in lung cancer, and has been associated with a poor

prognosis [7]. However, the clinical significance of reactive eosinophilia associated with lung cancer has not been clearly elucidated. Several studies have indicated that eosinophilia in solid cancer is more commonly found in patients with aggressive tumors, that it frequently reflects extensive disease, and is associated with a poor outcome [8-11]. The rapid disease progression and short survival of our patient support the argument that eosinophilic leukocytosis, especially with hypereosinophilic syndrome, may be considered a poor prognostic indicator in patients with lung cancer.

Some reports indicated that eosinophilia may disappear after tumor removal, and the return of eosinophilia may be an indicator of tumor recurrence [12-13]. In our case, the marked eosinophilia (as well as the associated liver dysfunction) resolved after disease control with platinum-based cytotoxic chemotherapy, but recurred after disease progression. Eosinophilia, if present, can be a marker in the follow-up of lung cancer, either in local disease after curative treatment or in the setting of an advanced stage following palliative therapy. However, clinicians should also be aware of the pitfalls in this context, as noticeable eosinophilia may occur with some delay after cancer progression.

In conclusion, hypereosinophilic syndrome is rarely described in patients with non-small cell lung cancer. In our case, the marked eosinophilia (and related liver dysfunction) resolved after tumor response to treatment, but recurred after disease progression, suggesting that this paraneoplastic phenomenon is linked to tumor extent. It is important to note that prompt diagnosis of hypereosinophilic syndrome in association with lung cancer may result in timely anti-tumor treatment and effectively reduce the risk of catastrophic organ dysfunction in these

patients.

References

1. Jameson J, Longo DL: Chapter 100. Paraneoplastic syndromes: Endocrinologic/hematologic. In: Harrison's Principles of Internal Medicine, 18 edn. New York: NY: McGraw-Hill; 2012.
2. Valent P, Klion AD, Horny HP, *et al.* Contemporary consensus proposal on criteria and classification of eosinophilic disorders and related syndromes. *J Allergy Clin Immunol* 2012; 130(3): 607-12. e9.
3. Rothenberg ME. Eosinophilia. *N Engl J Med* 1998; 338(22): 1592-600.
4. Pandit R, Scholnik A, Wulfekuhler L, *et al.* Non-small-cell lung cancer associated with excessive eosinophilia and secretion of interleukin-5 as a paraneoplastic syndrome. *Am J Hematol* 2007; 82(3): 234-7.
5. Lammel V, Stoeckle C, Padberg B, *et al.* Hypereosinophilia driven by GM-CSF in large-cell carcinoma of the lung. *Lung Cancer (Amsterdam, Netherlands)* 2012; 76(3): 493-5.
6. Chusid MJ, Dale DC, West BC, *et al.* The hypereosinophilic syndrome: analysis of fourteen cases with review of the literature. *Medicine* 1975; 54(1): 1-27.
7. Matsumoto S, Tamai T, Yanagisawa K, *et al.* Lung cancer with eosinophilia in the peripheral blood and the pleural fluid. *Internal Med (Tokyo, Japan)* 1992; 31(4): 525-9.
8. El-Osta H, El-Haddad P, Nabbout N. Lung carcinoma associated with excessive eosinophilia. *J Clin Oncol* 2008; 26(20): 3456-7.
9. Teoh SC, Siow WY, Tan HT. Severe eosinophilia in disseminated gastric carcinoma. *Singap Med J* 2000; 41(5): 232-4.
10. Chang WC, Liaw CC, Wang PN, *et al.* Tumor-associated hypereosinophilia: report of four cases. *Chang Gung Med J* 1996; 19(1): 66-70.
11. Zhu YL, Tong ZH, Jin ML, *et al.* [Lung cancer with marked blood eosinophilia: case report and literature review]. *Zhonghua jie he hu xi za zhi* 2009; 32(5): 369-72.
12. Anagnostopoulos GK, Sakorafas GH, Kostopoulos P, *et al.* Disseminated colon cancer with severe peripheral blood eosinophilia and elevated serum levels of interleukine-2, interleukine-3, interleukine-5, and GM-CSF. *J*

- Surg Oncol 2005; 89(4): 273-5.
13. Walter R, Joller-Jemelka HI, Salomon F. Metastatic squamous cell carcinoma with marked blood eosinophilia and elevated serum interleukin-5 levels. Exp Hematol 2002; 30(1): 1-2.

嗜伊紅性白血球超增多症候群（Hypereosinophilic syndrome）合併肝臟侵犯—晚期肺癌的罕見表現

胡釋文 蔡子修 施金元

嗜伊紅性白血球增多是實質固態癌（solid cancer）的腫瘤附屬症候群之一，大約可見於3%左右的肺癌病人。而嗜伊紅性白血球超增多症候群，則定義為當血中的嗜伊紅性白血球每微升高於1,500顆、合併組織中有嗜伊紅性白血球浸潤並造成器官損傷。在肺癌病患中，同時患有嗜伊紅性白血球超增多症候群是極少見的。我們提出討論的個案為一位新診斷的晚期肺腺癌病患，同時發現有嚴重的血中嗜伊紅性白血球增多、及肝臟內嗜伊紅性白血球浸潤造成的肝功能異常。此病患在接受化學治療後，血中顯著增加的嗜伊紅性白血球及肝功能異常，皆獲得改善，暗示著此種腫瘤附屬症候群與癌症嚴重程度上有著某種關連。此病患後來病況急速惡化亦顯示嗜伊紅性白血球超增多症候群可能反映腫瘤的高度侵襲性，而為不良預後的指標。（*胸腔醫學* 2015; 30: 253-260）

關鍵詞：嗜伊紅性白血球超增多症候群，腫瘤附屬症候群，肺癌